Tran-SET

Transportation Consortium of South-Central States

Solving Emerging Transportation Resiliency, Sustainability, and Economic Challenges through the Use of Innovative Materials and Construction Methods: From Research to Implementation

Effectiveness of Softening Agents for Enhancing Properties of Asphalt Mixes with High RAP Contents

Project No. 20BASU23

Lead University: Arkansas State University

Final Report

August 2021

Disclaimer

The contents of this report reflect the views of the authors, who are responsible for the facts and the accuracy of the information presented herein. This document is disseminated in the interest of information exchange. The report is funded, partially or entirely, by a grant from the U.S. Department of Transportation's University Transportation Centers Program. However, the U.S. Government assumes no liability for the contents or use thereof.

Acknowledgements

The authors gratefully acknowledge the funding support, which was provided by the United States Department of Transportation (USDOT) through the Transportation Consortium of the South- Central States (TranSET). The authors are also thankful to the Arkansas Department of Transportation (ARDOT) and Ergon, Inc. for their assistance in providing test materials for this study. The authors also appreciate all members of the Project Review Panel (PRC) for providing their inputs throughout the duration of this project. Furthermore, the authors would like to thank other industry partners and collaborators including Atlas Asphalt Inc., Delta Asphalt of Arkansas Inc. (AR, Paragould), Ingevity, and Arkansas Asphalt Pavement Association (AAPA) for providing test materials and logistic support for this study. The authors are also thankful to Dr. Hashim Ali and Dr. Kotaiba for their help with FTIR tests of this study.

TECHNICAL DOCUMENTATION PAGE

1. Project No.	2. Government Accession No.	3. Recipient's Catalog No.
20BASU23		

4. Title and Subtitle	5. Report Date
Effectiveness of Softening Agents for Enhancing Properties of Asphalt Mixes with High RAP Contents.	Aug. 2021
	6. Performing Organization Code
7. Author(s)	**8. Performing Organization Report No.**
PI: Zahid Hossain https://orcid.org/0000-0003-3395-564X Co-PI: Ashraf Elsayed https://orcid.org/0000-0003-1506-2784 GRA: Sumon Roy https://orcid.org/0000-0001-6183-6619	
9. Performing Organization Name and Address	**10. Work Unit No. (TRAIS)**
Transportation Consortium of South-Central States (Tran-SET) University Transportation Center for Region 6 3319 Patrick F. Taylor Hall, Louisiana State University, Baton Rouge, LA 70803	**11. Contract or Grant No.** 69A3551747106
12. Sponsoring Agency Name and Address	**13. Type of Report and Period Covered**
United States of America Department of Transportation Research and Innovative Technology Administration	Final Research Report Aug. 2020 – Aug. 2021
	14. Sponsoring Agency Code

15. Supplementary Notes

Report uploaded and accessible at Tran-SET's website (http://transet.lsu.edu/).

16. Abstract

A high percentage of reclaimed asphalt pavement (RAP) in new asphalt concrete can lead to developing premature failure of asphalt pavements due to fatigue or low-temperature cracking. The use of softening agents in asphalt binders can resolve these problems. The aim of this study is to evaluate the effectiveness of softening agents for enhancing the properties of asphalt mixes with high RAP contents. Two waste products, namely, waste cooking oil (WCO), and engine bottom oil (EBO) along with a commercially produced rejuvenator were investigated in this study. The following three types of Performance Grade (PG) binders, each collected from two different sources, were considered in this study: PG 64-22, PG 70-22, and PG 76-22. These PG binders blended with different amounts (0, 15, 25, 40, and 60%) of RAP binders were rejuvenated with different dosages (0, 10, 15, and 20%) of the selected softening agents. Empirical tests (e.g., penetration and pH), Superpave tests, Atomic Force Microscope (AFM), Scanning Electron Microscope (SEM), Fourier Transform Infrared Spectroscopy (FTIR), and limited laboratory and field performance of asphalt mixture samples were also evaluated. It was found that the rejuvenators reduced the viscosity of the binder samples. The results showed that the rejuvenated binders reduce the production temperatures as well as the brittleness of the hard binders. The AFM results showed that modulus and deformation values of rejuvenated binders were significantly less than those of their unrejuvenated counterparts. Similarly, distinct peaks were observed in the FTIR peaks due to the rejuvenation. The findings of this study will help pavement professionals in selecting suitable rejuvenators in the construction of pavements with high RAP contents.

17. Key Words	18. Distribution Statement
Reclaimed Asphalt Pavement, Rejuvenator, Waste Cooking Oil, Engine Bottom Oil, Atomic Force Microscope, Pavement Durability, Asphalt Binder.	No restrictions. This document is available through the National Technical Information Service, Springfield, VA 22161.

19. Security Class if. (of this report)	20. Security Class if. (of this page)	21. No. of Pages	22. Price
Unclassified	Unclassified	72	

Form DOT F 1700.7 (8-72) **Reproduction of completed page authorized.**

SI* (MODERN METRIC) CONVERSION FACTORS

APPROXIMATE CONVERSIONS TO SI UNITS

Symbol	When You Know	Multiply By	To Find	Symbol
		LENGTH		
in	inches	25.4	millimeters	mm
ft	feet	0.305	meters	m
yd	yards	0.914	meters	m
mi	miles	1.61	kilometers	km
		AREA		
in^2	square inches	645.2	square millimeters	mm^2
ft^2	square feet	0.093	square meters	m^2
yd^2	square yard	0.836	square meters	m^2
ac	acres	0.405	hectares	ha
mi^2	square miles	2.59	square kilometers	km^2
		VOLUME		
fl oz	fluid ounces	29.57	milliliters	mL
gal	gallons	3.785	liters	L
ft^3	cubic feet	0.028	cubic meters	m^3
yd^3	cubic yards	0.765	cubic meters	m^3
		NOTE: volumes greater than 1000 L shall be shown in m^3		
		MASS		
oz	ounces	28.35	grams	g
lb	pounds	0.454	kilograms	kg
T	short tons (2000 lb)	0.907	megagrams (or "metric ton")	Mg (or "t")
		TEMPERATURE (exact degrees)		
^oF	Fahrenheit	5 (F-32)/9 or (F-32)/1.8	Celsius	^oC
		ILLUMINATION		
fc	foot-candles	10.76	lux	lx
fl	foot-Lamberts	3.426	$candela/m^2$	cd/m^2
		FORCE and PRESSURE or STRESS		
lbf	poundforce	4.45	newtons	N
lbf/in^2	poundforce per square inch	6.89	kilopascals	kPa

APPROXIMATE CONVERSIONS FROM SI UNITS

Symbol	When You Know	Multiply By	To Find	Symbol
		LENGTH		
mm	millimeters	0.039	inches	in
m	meters	3.28	feet	ft
m	meters	1.09	yards	yd
km	kilometers	0.621	miles	mi
		AREA		
mm^2	square millimeters	0.0016	square inches	in^2
m^2	square meters	10.764	square feet	ft^2
m^2	square meters	1.195	square yards	yd^2
ha	hectares	2.47	acres	ac
km^2	square kilometers	0.386	square miles	mi^2
		VOLUME		
mL	milliliters	0.034	fluid ounces	fl oz
L	liters	0.264	gallons	gal
m^3	cubic meters	35.314	cubic feet	ft^3
m^3	cubic meters	1.307	cubic yards	yd^3
		MASS		
g	grams	0.035	ounces	oz
kg	kilograms	2.202	pounds	lb
Mg (or "t")	megagrams (or "metric ton")	1.103	short tons (2000 lb)	T
		TEMPERATURE (exact degrees)		
^oC	Celsius	1.8C+32	Fahrenheit	^oF
		ILLUMINATION		
lx	lux	0.0929	foot-candles	fc
cd/m^2	$candela/m^2$	0.2919	foot-Lamberts	fl
		FORCE and PRESSURE or STRESS		
N	newtons	0.225	poundforce	lbf
kPa	kilopascals	0.145	poundforce per square inch	lbf/in^2

TABLE OF CONTENTS

LIST OF FIGURES

LIST OF TABLES

ACRONYMS, ABBREVIATIONS, AND SYMBOLS

AASHTO	American Association of State Highway and Transportation Officials
AC	Asphalt Concrete
AFM	Atomic Force Microscopy
ARDOT	Arkansas Department of Transportation
ASTM	American Society for Testing and Materials
ASU	Arkansas State University
BBR	Bending Beam Rheometer
DSR	Dynamic Shear Rheometer
DMT	Derjaguin, Muller, and Toropov
DOT	Department of Transportation
EBO	Engine Bottom Oil
EDX	Energy Dispersive X-Ray
EVF	An engineered (commercially produced) rejuvenator
FHWA	Federal Highway Administration
FTIR	Fourier Transform Infrared Spectroscopy
HAP	Hard Asphalt Particles
HCA	Heat Cast Approach
HMA	Hot Mix Asphalt
HR1	Hydrocarbon Resin
HT PG	High Temperature Performance Grade
KBr	Potassium Bromide
L-SBS	Linear SBS Polymer
LT PG	Low Temperature Performance Grade
MR	Resilient Modulus
MSCR	Multiple Stress Creep Recovery
NCHRP	National Cooperative Highway Research Program
nPB	n-Propyl Bromide
OBA	Optimized Bio-Asphalt
PAV	Pressure Aging Vessel
PFQNM™	Peak-Force Quantitative Nanomechanical Mapping
PG	Performance Grade
PPA	Polyphosphoric Acid
RAB	Reclaimed Asphalt Binder
RAP	Reclaimed Asphalt Pavement
Rej	Rejuvenator
R-LDPE	Recycled Low Density Polyethylene
RTFO	Rolling Thin Film Oven
RV	Rotational Viscosity
S1	Source 1
S2	Source 2
SARA	Saturates, Aromatics, Resins and Asphaltenes
SBS	Styrene-Butadiene-Styrene
SEM	Scanning Electron Microscope

SHRP	Strategic Highway Research Program
S-value	Creep Stiffness
TBT	Texas Boiling Test
TranSET	Transportation Consortium of South-Central States
TRB	Transportation Research Board
TSR	Tensile Strength Ratio
TTI	Texas Transportation Institute
U.S.	United States
USDOT	United States Department of Transportation
WCO	Waste Cooking Oil
WCORs	Waste Cooking Oil Residues
%	Percent
%R	Percent Creep Recovery
°C	Degree Celsius (Unit of Temperature)
°F	Degree Fahrenheit (Unit of Temperature)
G*	Complex Shear Modulus
g/gm	Gram (Unit of weight)
hrs	Hours
Hz	Unit of Frequency used in DSR Test
in.	Inch
Jnr	Non-Recoverable Creep Compliance
kPa	Kilo Pascal
L	Liter
lb	Pound
min	Minute(s)
mJ/m^2	Unit of Cohesion Energy
mm	Millimeter
MPa	Mega Pascal; Unit of DMT Modulus
m-value	Slope of the Stiffness Curve
nm	Nanometer (Unit of Surface Roughness and Deformation)
nN	Adhesion Force
Pa.s	Pascal.sec ($N.s/m^2$) Unit of Dynamic Viscosity
psi	lb/in^2
rpm	Rotation per Minute
Rq	Roughness
s	Second
δ	Phase Angle
μm	Micrometer

EXECUTIVE SUMMARY

The use of reclaimed asphalt pavement (RAP) has increased in the construction of hot mix asphalt (HMA) pavements in the United States and around the world in recent years. Approximately, more than 90% of roads and highways in the U.S. are constructed with the HMA (2). Thus, a huge amount of RAP is generated annually from the repairing of existing asphalt pavements and reconstruction of new pavements. However, the use of high RAP content in pavement construction is a major concern to the state departments of transportation (DOTs) due to the performance of RAP-modified asphalt pavement during the service life. The main objective of this study is to evaluate the effectiveness of different softening agents for improving the properties of asphalt mixes with high RAP contents. Asphalt binder samples used for this study were collected from two different sources (S1 and S2). The tested binders included an unmodified (PG 64-22) binder and two polymer-modified (PG 70-22 and PG 76-22) binders. Two RAP samples were collected and evaluated in the laboratory in this study. Four RAP blends (0%, 15%, 25%, 40%, and 60% by weight) were prepared and tested in this study. To find the rejuvenators effects, two waste-based softening agents such as waste cooking oil (WCO) and engine bottom oil (EBO) along with a commercially produced rejuvenator (henceforth called EVF) were investigated in this study.

To fulfill the objectives of this project, a series of laboratory tests were conducted and test data were analyzed to draw meaningful conclusions and provide recommendations for further study. The performance test also called "Superpave tests" such as Rotational Viscometer (RV), Dynamic Shear Rheometer (DSR), Rolling Thin-Film Oven (RTFO), Pressure-Aging Vessel (PAV), Bending Beam Rheometer (BBR), and Multiple Stress Creep Recovery (MSCR) tests were performed to evaluate the rheological properties of the tested binder samples. Additionally, empirical tests such as penetration were also included to find the qualitative effects of rejuvenators on the consistency of the binder. To evaluate the moisture resistance of the asphalt mixtures, Texas Boiling tests (TBT) were conducted on loose mixture samples. Besides the conventional test methods, some advanced technological tests such as atomic force microscopy (AFM) were considered to investigate the properties of rejuvenated asphalt binders at the molecular level. The AFM tool was also used to characterize the microscopic morphology (roughness) and micro-mechanical properties (e.g., adhesion, DMT modulus, and deformation) of the asphalt binders at the molecular level. Furthermore, a Scanning Electron Microscope (SEM) was included in this study to examine the effects of rejuvenators in the binders' surface morphology and microstructures. For the chemical analysis of the rejuvenated binders, this study also included the pH test to examine binders' polarity and the Fourier Transform Infrared Spectroscopy (FTIR) test to detect the presence of any functional group due to the addition of rejuvenators.

The RV results showed that the addition of rejuvenators reduced the dynamic viscosity of the RAP-blended significantly and resulted in lower production temperatures. The DSR test results revealed that the rejuvenated binders possess lower rutting factors at a higher testing temperature. The empirical test results showed that rejuvenated binders become softer due to rejuvenation and these findings agree with the binders' performance test results. The AFM results also showed that the morphologies of the rejuvenated binders were changed and nanomechanical properties were found to be decreased noticeably. The FTIR test results showed the appearance of distinct peaks in the rejuvenated binder blends. The TBT results also showed that the WCO-modified RAP blend showed better performance than EBO. About 10% of WCO was found to be optimum for surfaces mixes with 25% RAP. The findings of this study will help pavement professionals in selecting suitable rejuvenators in the construction of pavements with high RAP contents.

1. INTRODUCTION

1.1. Problem Statement

The use of reclaimed asphalt pavement (RAP) in hot mix asphalt (HMA) has increased in recent years due to the rising costs and demand for crude oils and aggregates. However, a high RAP content in new mixes may have some adverse effects on their performance such as low resistance due to fatigue and low-temperature cracking. This is mainly due to the occurrence of oxidative aging of RAP binders. This problem can be avoided by using a softer binder (e.g., PG 58-22) or softening agents such as rejuvenators. However, the use of a softer binder puts the contractors in a non-compliance situation as it is not often an approved PG binder of the agency. For example, the Arkansas Department of Transportation (ARDOT) allows only three binders for roadway construction in Arkansas, and they are PG 64-22, PG 70-22, and PG 76-22. Furthermore, softer binders such as a PG 58-22 binder are more expensive than the base binder (PG 64-22). The alternative solution could be the use of a softening agent to enhance the performance of the mixes with high RAP as it will allow contractors to use the ARDOT-approved binders without increasing the cost of materials significantly.

This study aims to determine the effectiveness of different rejuvenators on blended binders' rheological and mechanistic properties through traditional test methods (e.g., Superpave) and non-traditional techniques such as the AFM. Two RAP samples collected from local highways in Arkansas (AR) were also used for asphalt binder extraction and recovery in the laboratory. The recovered binders were then blended with the base binders. An engineered (i.e., commercially produced) rejuvenator along with two waste-based softening agents, namely, waste cooking oil (WCO) and engine bottom oil (EBO) were also investigated in this study.

1.2. Background

In recent years, the reclaimed asphalt pavement (RAP) has become an important source in the construction of HMA pavements in the United States (U.S.) and around the world. The binder extracted and recovered from the RAP materials is known as reclaimed asphalt binder (RAB) *(1).* According to a Federal Highway Administration (FHWA) study, more than 90% of roads, and highways in the U.S. are constructed with the HMA (2). Therefore, a huge amount of RAP is generated annually from the maintenance and rehabilitation work of existing asphalt pavements and the reconstruction of new pavements. The FHWA has highlighted the use of recycled materials in the highway construction industry due to their engineering, economic, and environmental benefits *(3).* Thus, the use of RAP in the construction of the asphalt pavement can become an important source of energy and cost savings *(4).* It has been reported that the use of RAP in highway construction is becoming more popular to pavement professionals, particularly, to reduce the amount of virgin binder as RAP contains old asphalt binder. Therefore, usage of RAP offers the additional benefit of reducing the amount of virgin binder in new mixes *(5).* However, the use of high RAP content in pavement construction is a major concern to the transportation agencies as it is necessary to predict the performance of RAP-modified asphalt pavement during the design period.

According to the AASHTO M 323 specifications, the contractors are not allowed to change the binder grade in the mix in the case of a RAP amount of less than 15% *(2).* It recommends selecting a virgin binder one grade softer than the normal grade, for instance, a PG 58-28 binder will be selected instead of PG 64-22 when RAP is in between 15 to 25%, and the blending charts are to

be used when RAP is more than 25%. Based on the ARDOT Standard Specifications for Highway Construction (6), the contractors are restricted to use RAP in the job mixture where the mixture must contain a minimum of 70% virgin material. The ARDOT has provisions to use RAP with some restrictions, which include that a softening agent along with the accompanying specifications should be submitted and approved before using it with the binders. A temperature-viscosity curve for the blending of RAP and virgin asphalt is required to be supplied by the contractors as well. However, the contractors are exempted to provide the temperature-viscosity curve if the design incorporates less than 15% RAP and uses the PG 64-22 binder. Therefore, the contractors often limit the usage of RAP to no more than 15% as there are no specific guidelines of the RAP usage over 15%. Furthermore, the ARDOT allows only three types of virgin binders, namely, PG 64-22, PG 70-22, and PG 76-22 for construction roads and highways. While many state Departments of Transportation (DOTs) increased the amount of RAP to be used in HMA, the use of high RAP (25% or more RAP in an asphalt mixture by weight of the total mix) in new mixes is still not common in Arkansas. Like many other states, ARDOT has not experimented with the HMA with high RAP and mostly limited up to 15% of RAP usage by contractors. However, some neighboring states (i.e., Texas, Kansas, Mississippi, Tennessee, and Missouri) have experimented or routinely use high RAP while contractors in Arkansas do not usually use any RAP on surface course and no more than 15% RAP in binder course. The limitations on ARDOT's current specification, lack of expertise in processing such as the variability of RAP, lack of the availability of quality RAP, and lack of prior experience, the usage of more than 15% of RAP in the mixture is not practiced very often. The Federal Highway Administration stated the most common barriers among state transportation agencies include the quality concerns, consistency of RAP, binder grade and blending, mix design procedures, volumetric requirements, durability, and cracking performance *(2).* Conversely, the most common barriers among contractors are the state DOTs' specifications, quality control of RAP, dust and moisture content, and increased quality control of the new mixes. For example, the latest ARDOT Standard Specifications *(6)* states that a mixture must contain a minimum of 70% virgin material when RAP is used.

Asphalt concrete is a composite material composed of asphalt binder and mineral aggregates. The durability and performance of the asphalt concrete may be affected due to the aging process of the asphalt binders. Multiple researchers reported that the rheological parameters (e.g., penetration, softening point, viscosity, and complex shear modulus), as well as chemical fractions (e.g., saturates, aromatics, resins, and asphaltenes (SARA)), are changed due to volatilization and oxidation of the reclaimed asphalt binder (RAB) *(7-9).* Past research also showed that the RAB binder already oxidized and could result in an increase in stiffness and brittleness due to high-temperature mixing during production and long-term exposure to air and sunlight during service life *(10,11).* However, the rheological properties of the aged binder can be restored and maintained by rejuvenating the aged binder in the RAP materials *(12).* According to Zaumanis et al. *(13),* rejuvenators can restore the original characteristics of the aged binder, which can be obtained from different materials, such as a soft binder, vegetable oils, waste engine oils, derived oils, as well as composite rejuvenator *(13).*

2. OBJECTIVES

The main objective of this study is to evaluate the effectiveness of different softening agents (commercially produced as well as waste-based) in RAP blended binders' rheological and mechanistic properties. Specific objectives of this study are given as follows: (i) Determine consistency and penetration and changes in PG grades of the RAP-blended binders, (ii) Determine the optimum amounts of different softening agents, (iii) Evaluate the effectiveness of softening agents on binders' rheological properties, (iv) Observe the changes in morphological phases and interactions of virgin and aged binders at the molecular level, and (v) Evaluate plant mixes with high RAPs and monitor the field performance.

3. LITERATURE REVIEW

A comprehensive literature review has been conducted throughout the study to understand practices for using the RAP and softening agents along with the asphalt binders and fine-tune the associated tasks and methodologies. The following paragraphs represent major findings based on the literature review, which have been conducted based on previous and current research on the effectiveness of softening agents in mixes with high RAP, and their effects on changes of rheological, morphological, mechanical, and chemical properties in the unrejuvenated and rejuvenated RAP blends.

3.1. Use of Rejuvenators for Improving Asphalt Binders' Properties

The influence of softening agents on rheological, chemical, morphological, and mechanical properties has been studied by many researchers. For instance, Hugener et al. *(14)* reported that the properties of the aged binder from RAP can be reactivated properly by using vegetable oil-based rejuvenators *(14).* They used a commercial rejuvenator (BRW), two vegetable oils (i.e., rapeseed oil and linseed oil), and waste oil (frying oil), and the concentration of each rejuvenator was 0.32 % by the weight in the mixture. Zaumanis et al. *(15)* studied 100% RAP samples using six different rejuvenators (waste vegetable oil, waste vegetable grease, organic oil, distilled tall oil, aromatic extract, and waste engine oil) at 12% dose by mass of the binder. Their test results revealed that the waste vegetable oil produced better rejuvenating effects, which improved the fatigue resistance of the aged binder *(15).*

Moreover, Shen et al. *(16)* investigated the effects of the soft binder containing a low asphaltene content (2% by the weight of the bine) on the properties of the aged binder and recycling asphalt mixtures. They evaluated a total of three recycled mixture samples using rejuvenated aged binders at 0%, 2.0%, and 7.4% of rejuvenating percentages, respectively, and one virgin mixture sample. They reported that the rutting resistance of the aged binder was decreased with the increase of soft binder dosage and the dynamic stability of mixtures showed the same trend *(16).*

Dony et al. *(17)* examined the performance of the 60% RAP aged binders rejuvenated by vegetable oil, aromatic oil, and soft binder. Their experimental results indicated that the binder rejuvenated using the vegetable oil showed a better fatigue resistance *(17).* Romera et al. *(18)* also studied the suitability of three types of rejuvenators (commercial oil, motor recycling oil, and a 150/200 penetration grade bitumen) in rejuvenating RAP binders. The results demonstrated that the permanent deformation of recycling asphalt mixtures rejuvenated by the motor oil could be delayed.

Furthermore, some researchers reported that the mixing and compaction temperature can be reduced by using motor oil *(18).* Chen et al. *(19)* also conducted a comparative study of three different rejuvenators (composite rejuvenator, cooking oil, and cotton seed oil) with three different percentages (0%, 5%, and 10%). They found that the rutting resistance factor and the complex modulus of rejuvenated binders decreased due to the addition of the rejuvenator, cotton seed oil, or waste cooking oil whereas their phase angles increased. They also reported that a small amount of waste cooking oil or cotton seed oil in the aged asphalt could more easily achieve the demand of a PG 64-XX binder in meeting the rutting resistance factor, phase angle, complex modulus, and failure temperature compared with those of the binder with the rejuvenator. The results also

showed that waste cooking oil or cotton seed oil can slightly reduce the viscosity value of the aged asphalt and thus, decrease the mixing and compaction temperatures of the mixture *(19).*

Sun et al. *(20)* evaluated the waste cooking oil residues (WCORs)-based optimized bio-asphalt (OBA) and found that the bio-asphalt containing high content of WCOR (33.3% by weight) had an excellent mechanical and chemical performance. Based on the rheological test results, the authors reported that the OBA had similar high-temperature performance to SBS modified asphalt (SBS-MA), and it exhibited much better low-temperature performance than either SBS-MA or PEN 70 base asphalt (PEN 70). These researchers performed the FTIR test and mentioned that OBA had some special chemical composition: the acids and esters originated from the addition of WCOR. The mixture performance tests results confirmed that the OBA mixture possessed similar rutting resistance and moisture susceptibility to the SBS-MA mixture, and it exhibited more satisfying low-temperature capability than either of SBS-MA or PEN 70 mixture. The OBA mixture also showed noticeable fatigue performance at different strain levels. Moreover, the optimum blending proportion of the bio-asphalt was determined as 33.3% WCOR, 31.8% hard asphalt particles (HAP), 30.3% hydrocarbon resin (HR1), 4.6% recycled low-density polyethylene (R-LDPE), and external 4% linear SBS polymer (L-SBS) based on the formula of the uniform design method.

Majidifard et al. *(21)* investigated the short-term and long-term binder performance of high-RAP mixtures containing WCO. In this study, these researchers used 60% and 100% of RAP with different percentages of WCO. The results showed that increment of the amount of WCO in the high-RAP mixtures increases their workability and low-temperature performance, whereas it decreases the moisture damage resistance and rutting resistance. The results showed that the binder with 16% oil had the best performance for low-temperature (LT) PG. On the other hand, the binder with crumb rubber exhibited the best high-temperature (HT) PG. By interpolating between the percentage of oil and continuous PG of the two tested binders, it was found that the addition of 13% oil resulted in a continuous grade of PG 63.2-25.1 and met the properties of the fresh binder. Moreover, the linear regression of the LT PG and percentage of added oil showed that the percentage of oil required to soften the artificial RAP binder was found to be 2.9% for LT and 9.2% for HT.

Cavalli et al. *(22)* studied the aging effect on rheology and cracking behavior of reclaimed binders with bio-based rejuvenators. This research focused on evaluating the low temperature cracking as well as rheological behavior of RAP binder modified with bio-based rejuvenators at aged and unaged conditions. It also analyzed the oxidation caused by aging and the effects of rejuvenators on RAP binders' functional groups. In this study, the total binder content was 5.6% (by the weight of the RAP mixture), and three types of bio-based products namely, seed oil (A), cashew nut shell oil (B), and tall oil (C) were investigated. The rejuvenator's dosage of this study was 5% (by the mass of the recovered RAP binder). The results showed that with the addition of 5% of each bio-based product, the RAP binder had similar rheological performances to the virgin binder at low temperatures. It was found that RAP+5% B and RAP+ 5% C had a higher softening potential of the RAP binder in the entire frequencies/temperature range than RAP+5% A. It was evident that rejuvenators would restore the aged RAP binder mechanically by showing significant differences in the modulus and phase angle results. Moreover, it was found that the mechanical changes due to rejuvenators were not caused by changes at the chemical bonds/functional groups level.

Loise et al. *(23)* conducted a comprehensive review on bitumen rejuvenation including its mechanisms, effects on chemical structure and microstructural features, investigation techniques to distinguish between various additives along a critical analysis of the state-of-the-art practices of rejuvenations. The authors mentioned that a rejuvenating agent can act in two different sub-mechanisms: (i) by lowering the viscosity of the aged binder, for example, flux oil, lube stock, and slurry oil, known as softening agents, and (ii) by restoring the physical and chemical properties employing real rejuvenators. These researchers highlighted the studies conducted by Król et al. *(24)* and Somé et al. *(25)* that used vegetable oils produced from various raw materials such as rapeseed oils, soybean oil, sunflower oil, and linseed oil, and they investigated binders modified with the vegetable oils of different dosage levels up to a 10%. These researchers also performed chemical actions to prepare other additives in which they used methyl esters of fatty acid obtained by transesterification of vegetable oils.

Zargar et al. *(26)* used a WCO as a rejuvenator and found that the performance of the aged binder can be restored at a 3% WCO content, and its performance can be improved further by the addition of a 5% WCO. These results were also interpreted on a chemical basis using the FTIR technique. Elkashef et al. *(27)* used thermal stability analysis to evaluate the effect of a 12% soybean oil on RAP. Cavalli et al. *(22)* used three commercial bio-based rejuvenators: (i) a natural seed oil, (ii) a cashew nut shell oil, and (iii) a rejuvenator based on tall oil. They used a 5% dosage level of these rejuvenators and performed the FTIR analysis. These researchers observed mechanical changes in rejuvenated binders by the rearrangements of polar/nonpolar components. However, the chemical changes at the functional groups level were not found to be responsible for the mechanical changes.

Zhu et al. *(28)* studied the effects of a bio-rejuvenator where they 5% or 10% bio-rejuvenator with styrene-butadiene-styrene (SBS)-modified PAV-aged samples. Mokhtari et al. *(29)* investigated the potential of the FTIR to investigate the effect of two different rejuvenators: (i) a petroleum oil, and (ii) a product derived from refined tall oil. They used petroleum oil at dosage levels of 15% and 30% (by the weight of the binder) and the tall oil at amounts of 10% and 20% (by weight) as the lower and upper limits of these rejuvenators. Yu et al. *(30)* used the AFM technique to analyze the materials' surface morphology where two types of rejuvenators namely, ((i) frying oil and (ii) an aromatic extract containing approximately 75% of aromatic oil and resin compounds with a small amount of saturated oil to observe their effectiveness. Kuang et al. *(31)* compared the effect of adding the conventional rejuvenating (CR) and the solubilized rejuvenating (SR) on the aged bitumen with a dose rate of 10%. Nahar et al. *(32)* explored the potentiality of AFM techniques to investigate the effect of two types of rejuvenators using the dose rate of 10%, 20%, and 25%, and performed AFM analyses.

Most recently, Zhang et al. *(33)* investigated the influence of four types of rejuvenators (soft binder, vegetable oil, waste engine oil, and composite rejuvenator) on the rheological behavior of the aged binder and dynamic response of recycled asphalt mixtures with 60% RAP. They determined the optimum dosages of these rejuvenating agents, which restored the penetration grade of the recovered aged binder. They found that optimum dosages of soft binder, vegetable oil, waste engine oil, and composite rejuvenator were 39%, 9%, 10%, and 8%, respectively. They also reported that the dynamic modulus of the RAP mixture increased while the fatigue life was reduced due to a high RAP content. The researchers demonstrated that the use of rejuvenating

agents would restore the visco-elastic behavior of recycled asphalt mixtures, but it was difficult to achieve the dynamic modulus and fatigue life similar to the previous level.

Mamun and Al-Abdul Wahhab *(34)* also conducted the comparative laboratory evaluation of WCO-rejuvenated asphalt mixtures with a high RAP content. In this study, three different percentages of (13%, 20%, and 27%) of WCO (by the mass of the RAP binder content) were evaluated for three different percentages (30%, 40%, and 50%) of RAP. The indirect tensile strength (ITS) test results showed that the ITS value decreases with the increase of the rejuvenator's percentage. It was found that only 13% of WCO could be used to rejuvenate the asphalt mixtures with up to 50% RAP. Moreover, the resilient modulus (MR) values were found to be decreased with the increase of the rejuvenator's content and RAP percentage. Based on the test results, it was observed that the MR values of 13% WCO-rejuvenated mixtures containing up to 50% RAP were comparable with mixtures without any RAP content. The MR values of rejuvenated mixtures were also comparable with that of the commercial rejuvenated mixtures. It was noticed that the WCO content higher than 13% and the RAP content greater than 40% in mixtures increased the susceptibility to moisture damage significantly.

While designing the test matrices of the current study, the findings of the aforementioned studies were taken into consideration. Also, information and science found in the previous and some of the concurrent studies of other research groups were used to discuss test results and draw meaningful conclusions.

4. METHODOLOGY

This chapter represents the required materials, equipment, research tools, and a brief description of the test procedures employed in this study. To fulfill the objectives of this study along with their suitability in different state DOTs, and highway agencies, the required materials such as base asphalt binders, RAPs, rejuvenators, and appropriate test methods were selected in this study. As the main goal of this study is to study the effectiveness of different softening agents in RAP blended asphalt binders' properties, both traditional test methods (e.g., Superpave) and advanced-level techniques (e.g., AFM, SEM, and FTIR.) of asphalt binders in addition to the asphalt mixtures performance tests such as Texas Boiling test (TBT) and the retained stability test were performed in this study.

4.1. Preparation of Test Plan

To achieve the goals of the study, a systematic study plan and a detailed test matrix were developed where suitable test methods were selected based on the review of relevant research. A project flow diagram, shown in Figure 1, was developed to illustrate major steps and associated tasks toward the successful completion of the project.

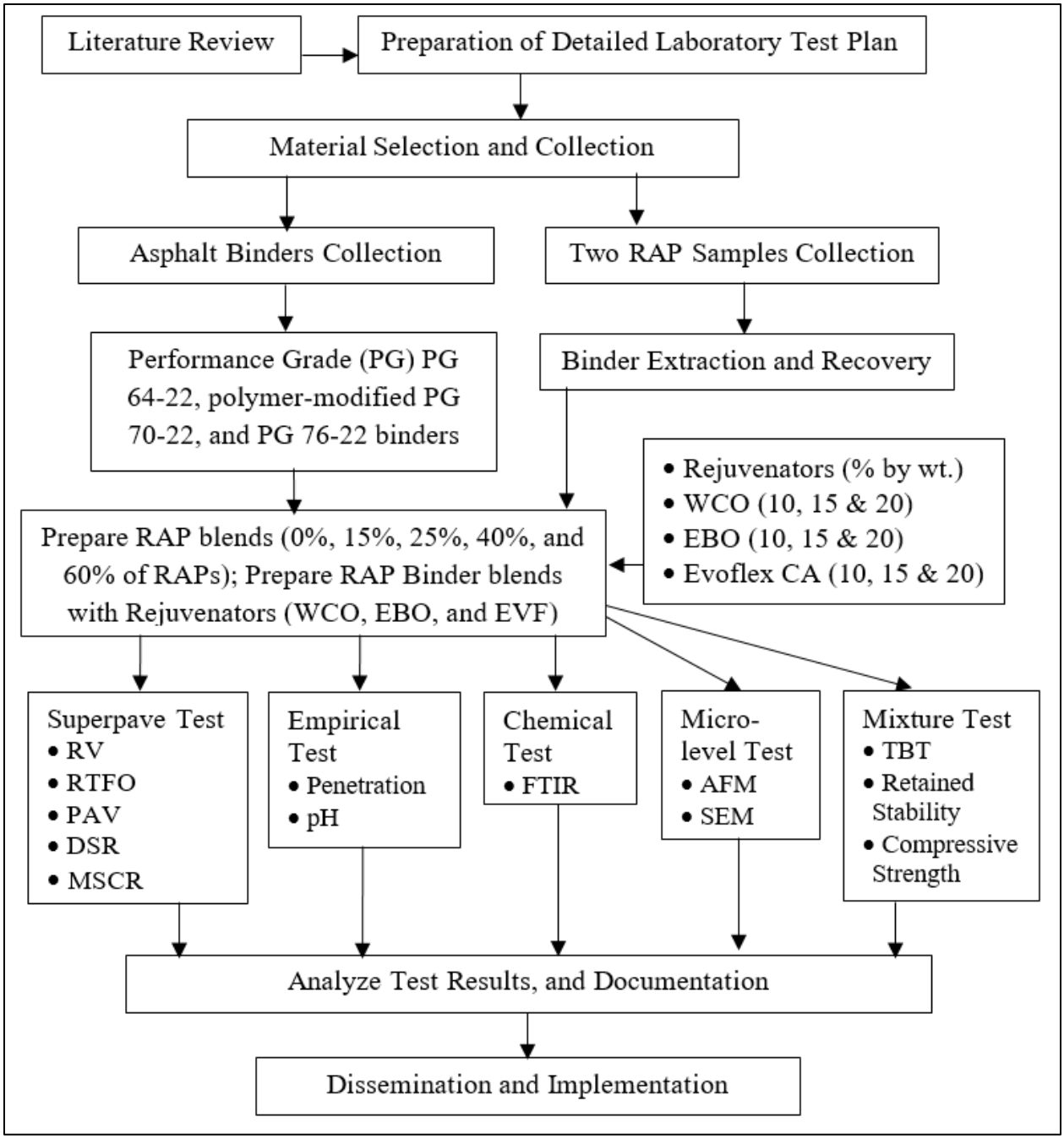

Figure 1. Detailed Project Flow Diagram Showing the Tasks.

4.2. Materials

4.2.1. Asphalt Binder, RAPs, and Rejuvenators

Based on the Qualified Product List (QPL) of the ARDOT, the following three types of PG asphalt binders were collected from two different sources: one PG 64-22 binder, two polymer-modified PG 70-22, and PG 76-22 binders. The first set of asphalt binders was prepared from a Canadian

crude source. The second set of binders was made from an Arabian crude source, which is a combination of "sweet and sour crudes." Table 1 shows some of the details of the asphalt binders used for this study.

Two RAP samples were collected with the help of a local contractor in Jonesboro, AR, and they were investigated in this study. One RAP sample was originated from a roadway section on Interstate 555 (I-555) between Marked Tree and I-55 while the other RAP sample was obtained from U.S Highway 67 (Hwy 67) between the Lawrence County line and Hwy 62 in Pocahontas, AR. The collected RAP samples were used for binder recovery in the laboratory. The recovered binders of different percent were blended with the PG binders, and they were further blended with softening agents. Table 2 shows the details of the RAP samples used in this study along with their amounts in the blended asphalt binder samples

An engineered (i.e., commercially produced) rejuvenator, henceforth named EVF, was collected from its manufacturer's plant. Additionally, two waste-based softening agents, namely, WCO and EBO were collected from a local restaurant and an automobile dealer, respectively. The WCO and EBO samples (each about 5 gallons) were no more than a one-day cumulative waste of soybean and motor (mostly SAE 10W-30) oils, respectively. The soybean oil is generally composed of five fatty acids: palmitic acid (~10%), stearic acid (~4%), oleic acid (~18%), linoleic acid (~55%), and linolenic acid (~13%). The EBO is a blend of base oils composed of petroleum-based hydrocarbons, polyalphaolefins, or their mixtures with a flashpoint of about 215 ^{o}C. The dosage level of WCO and EBO was selected as 10% (by weight of total binder blend) for the laboratory testing and evaluations. This dosage level was chosen based on evidence from in-house laboratory data as well as recommendations from relevant studies available in the public domain. Table 3 shows the details of the rejuvenators used for this study. A higher dosage level (15% or 20% by the weight of the binder) of the rejuvenators was not found to be effective based on preliminary test results as blended binders were highly soft. Thus, a 10% dosage level of the rejuvenator was explored further.

Additionally, sandstone aggregates, collected from a local quarry, that passed a 3/8-inch sieve and retained on an ASTM No. 4 Sieve were used to evaluate the performance of asphalt mixtures in this study.

Table 1. Details of Asphalt Binders along with their Properties.

Asphalt Binders				
Crude Source	**Asphalt Binders**	**Modifiers**	**Flash Point (°C)**	**Viscosity at 135°C (mPa.s)**
Canadian (Source 1; S1)	PG 64-22	None	318.00	390
	PG 70-22	Polymer	312.78	1180
	PG 76-22	Polymer	322.78	1580
Arabian (Source 2; S2)	PG 64-22	None	356.00	474
	PG 70-22	Polymer	342.00	954
	PG 76-22	Polymer	320.00	1779

Table 2. Details of RAP Samples used in the Study.

Reclaimed Asphalt Pavements (RAPs)		
RAP Type	**Amount of RAP Used (% by wt.)**	**Origin/Collection Source**
RAP1	0%, 15%, 25%, 40%, and 60%	I-555; between Marked Tree and I-55, AR
RAP2	0%, 15%, 25%, 40%, and 60%	Hwy 67;between the Lawrence County line and the Hwy 62 in Pocahontas, AR

Table 3. Details of Rejuvenators used in the Study.

Softening Agents		
Agent Type	**Dosage (%) (wt. of the total binder)**	**Origin/Collection Source**
WCO	10%, 15%, and 20%	Local Restaurant, Jonesboro, AR
EBO	10%, 15%, and 20%	Automobile Dealer, Jonesboro, AR
EVF	10%, 15%, and 20%	Commercial Lab

4.3. Laboratory Tests

Asphalt binder samples (unmodified and polymer modified), two RAP samples, and three different rejuvenators were tested in the laboratory. Superpave tests were conducted for characterizing the rheological properties of asphalt binders. These tests include the Rotational Viscosity (RV) as per AASHTO T 316, Dynamic Shear Rheometer (DSR) as per AASHTO T 315, Rotational Thin Film Oven (RTFO) as per AASHTO T 240, Pressure Aging Vessel (PAV) as per AASHTO R 28, Bending Beam Rheometer (BBR) as per ASHTO T 313 and Multiple Stress Creep Recovery (MSCR) as per AASHTO T 350-14. Additionally, the penetration test (AASHTO T 49) was performed to find the consistency of the asphalt binders. The pH tests were conducted to find the acidic or basic nature of the rejuvenated and unrejuvenated binders by following the Western Research Institute (WRI)-based methodology in the laboratory.

Furthermore, an Atomic Force Microscope (AFM) was used to observe the changes in morphological phases and interactions of the asphalt binders at the molecular level. The Scanning Electron Microscope (SEM) technique was also used to examine the microstructures and surface morphology of the tested asphalt binders. Moreover, the FTIR test was performed on an asphalt binder to detect any in the functional group that might have occurred due to any modification. In the end, a mixture test, namely, the Texas Boiling test (TBT) as per ASTM D3625 followed by the guideline established by Texas Transportation Institute (TTI), was conducted to evaluate the performance of the rejuvenated binder mixtures. All of these tests were conducted on the unmodified and modified binders with different percentages of RAP contents under different aging environments (unaged, RTFO-aged, and PAV-aged) in the laboratory.

Table 4 shows the summary of the test methods used in the laboratory. The brief descriptions of all the laboratory tests along with procedures included in this study to achieve the desired goals are given below.

Table 4. Summary of the Laboratory Test Methods Used in the Study.

Test Name	Standard	Purpose(s)
Superpave Tests		
Rotational Viscosity (RV)	AASHTO T 316	• Measures the viscosity (workability, pumpability, and mixability) of the asphalt binders • Determine mixing and compaction temperatures.
Dynamic Shear Rheometer (DSR)	AASHTO T 315	• Measures the complex shear modulus (G*) and phase angle (δ) • Determine rutting and fatigue parameters
Rotational Thin Film Oven (RTFO)	AASHTO T 240	• Simulates asphalt binder aging (hardening) during the hot-mix asphalt (HMA) production and construction
Pressure Aging Vessel (PAV)	AASHTO R 28	• Simulates the asphalt binder's aging (hardening) during the HMA service life
Multiple Stress Creep Recovery (MSCR)	AASHTO T 350-14	• Measures the percent recovery and non-recoverable creep compliance
Micro-Level Tests		
Atomic Force Microscope (AFM)	PFQNM™ mode	• Finds the surface morphology and mechanical properties
Scanning Electron Microscope (SEM)	SNE-4500MPlus	• Examines the microstructures and surface morphology
Empirical Tests		
Penetration Test	AASHTO T 49	• Determines the depth of penetration
pH Test	WRI	• Finds the acidic or basic nature
Chemical Analysis		
Fourier Transform Infrared Spectroscopy (FTIR**)**	AASHTO T 302	• Detect any change in functional group
Mixture Test		
Texas Boiling Test (TBT)	TTI	• Measures the moisture damage resistance of the asphalt mixtures
Compressive Strength Test	AASHTO T 22	• Measures compressive strength of concrete samples
Retained Stability	ARDOT 455A-11	• Evaluate the moisture effects on the strength of compacted asphalt mixtures.

4.3.1. RAP Binder Extraction and Recovery

The collected RAP samples were used for the extraction and recovery of RAP binders in the laboratory by using a centrifuge as per AASHTO T 164 (Figure 2) and a Rotavapor as per ASTM D5404, respectively (Figure 3). For the extraction of binder from the RAP, n-Propyl Bromide (nPB) was used as a solvent because of its minimal effects on the properties of the recovered binder *(35)*.

Binder Extraction Procedures:

In this method, the following major steps were followed:

- At first, the core sample was loosened using a gravity convection oven at 110 ^{o}C ± 5 ^{o}C.
- When the asphalt core sample became soft enough, it was then removed from the oven and placed on a metal pan.
- The aggregates coated with asphalt binder were then separated from the compacted state to the loose state by hands.
- The loose asphalt mix was then placed in the extraction bowl as per the AASHTO T 164 requirements.
- In this study, approximately 1000 g of loose asphalt was filled in the bowl for the one cycle of the extraction process.
- A sufficient amount of nPB was poured into the bowl to fill it up and then allowed nearly 1 hour to dissolve the asphalt binder into the nPB solution.
- The bowl was then placed into the centrifuge extraction chamber.
- 1000 mL glass beaker was placed at the ejection/discharge channel to receive the solution of the extracted binder.
- The extractor was then started rotating after securing the chamber cover. The rotation speed was slowly increased up to 3000 rpm and continued until the extract stopped flowing out from the ejection pipe.
- The extracted binder solution was then allowed to rest for nearly 15 minutes to settle down the fine particles at the bottom of the beaker.
- Finally, the extracted binder solution from the top portion was then transferred to a flask for the recovery process.

Figure 2. The Centrifuge Extractor for Asphalt Binder Extraction Process.

Binder Recovery Procedures: In this study, a rotavapor was used to recover the asphalt binder in the laboratory. The asphalt binder recovery from the extracted nPB solution was performed followed by the ASTM D5404 standard. This method included the evaporation of the nPB from the extracted solution using the rotavapor, cooling it down to liquid form using a condenser, and leaving the asphalt binder in the flask. The laboratory setup for the recovery of the binder is shown in Figure 3.

Figure 3. Binder Recovery using the Rotary Evaporation Method.

As shown in Figure 3, the major steps of the recovery process used in this study are given below.

- Firstly, the flask was carefully fitted with the glass pipe and the oil bath was heated at a temperature of 140 ^{o}C ± 3 ^{o}C.
- The flask was then slightly submerged in the hot oil bath and set to rotate at nearly 40 rpm.
- The coolant was then run through the condenser.
- A vacuum pressure of 5.3 kPa ± 0.7 kPa (53 mbar ± 7 mbar) below the atmospheric pressure was applied, and nitrogen gas at a rate of nearly 500 mL/min was supplied to the flask.
- When the bulk amount of nPB was removed from the solution, the vacuum pressure was gradually increased up to 80.0 kPa ± 0.7 kPa (800 mbar ± 7 mbar) below the atmospheric pressure, and the nitrogen supply was adjusted to about 600 mL/min with a rotation speed of 45 rpm.
- The vacuum pressure was adjusted if any bubble formation was noticed in the flask.
- The setup was run for 10 minutes after the forming of the last bubble.
- After 10 minutes, the rotation of the flask was slowly stopped, the flask was removed and the RAP binder was transferred to the container.
- During the transferring process, the flask-container setup was kept in an oven preheated at a temperature of 163 ^{o}C that accelerated the transferring time of asphalt binder to the container.

4.3.2. Blending of Asphalt Binders

A blending protocol, originally developed by Hossain et al. *(36),* for mixing RAP binder along with additives and virgin binder in the laboratory was followed in this study. In a recent relevant study of the current research team, the same blending protocol was also used to examine some of the morphological and nanomechanical properties of selected rejuvenated asphalt binders containing high RAP binders *(37).* Figure 4 shows a snapshot of the manual blending protocol of the RAP binders.

The major steps involved in the blending of asphalt binders used in this study are given below.

- Firstly, a sufficient amount of neat binder was heated in the aluminum can at 160 ^{o}C for nearly 20 minutes to make it workable.
- The container of the RAP binder was heated separately at the same time. The required amount of RAP binder was poured into the base binder container.
- The container of RAP and neat binder were kept in the oven at 160 ^{o}C for nine minutes.
- A glass rod was used for stirring the mixture for one minute vigorously and uninterruptedly.
- The mixture was then kept in the oven for heating for another 9 minutes and followed by 1 minute of stirring.
- This cycle (heating for 9 minutes and stirring for 1 minute) was repeated a total of six times that allowed sixty minutes (one hour) of blending time for every mixing type.
- During the blending process, the interior wall of the sample container was scrapped periodically to prevent the accumulation of RAP binders to the sides of the container.
- To prepare the rejuvenated RAP blends, the required amount of softening agent (e.g., WCO, EBO, and EVF) was added into the container of the base binder along with the RAP binder before starting the “heating and stirring” cycle.
- In end, the blended asphalt binder was then allowed to cool down to room temperature and stored for further testing.

Figure 4. Manual Blending of RAP Binder.

4.3.3. Penetration Test

The penetration test was the most widely used asphalt testing method before the Viscosity grading system. The penetration test measures the penetration of a standard needle into the asphalt binder sample under 100 gm of load at a temperature of 25°C for 5 seconds. The penetration test was conducted per AASHTO T 49. Although AASHTO T 49 is an empirical test method, this test is routinely performed as part of the quality control practices of the ARDOT. In this study, the penetration device was used to conduct the penetration test on unaged binders only. Figure 5 shows the penetration test arrangement in the laboratory used in this study.

The major steps followed in this test are given below.

- A total of 100 g weight (including the needle holder and loading frame) was allowed to penetrate for five seconds on a smooth surface of the asphalt binder at room temperature.
- The depth of penetration was recorded at least three times and the average value was reported for analysis.
- The penetration device measures the penetration depth in units of 1/10 of a millimeter (mm). For example, the depth of penetration of 7 mm under specific conditions indicates the penetration grade of 70.

Figure 5. Penetration Device.

4.3.4. pH Test

The pH tests were conducted to find the acidic or basic nature of the selected binder samples in the laboratory. In this study, the methodology proposed by the researchers at the Western Research Institute (WRI) was used with a minor modification for measuring the pH of a binder *(38).* Figure 6 shows the pH measurement of the rejuvenated asphalt binders.

The major steps followed in the laboratory are given below.

- Firstly, approximately a 5 gm asphalt binder sample was taken in a 250 mL beaker.
- 30 mL of toluene (HPLC grade) was added to the sample and heated gradually to dissolve the binder into the toluene.
- The dissolved sample was then allowed to cool down to room temperature.
- The solution was then transferred into a 250 mL separatory funnel.
- 15 mL of deionized water was added to the solution and shaken for 2 minutes to extract the water-soluble materials from toluene into the aqueous layer.
- The aqueous layer was then centrifuged to separate the clear water for measuring the pH.
- A pH meter was used to measure the pH of the asphalt binder. Before taking any readings, the pH meter was calibrated with a buffer solution of pH 7.00.

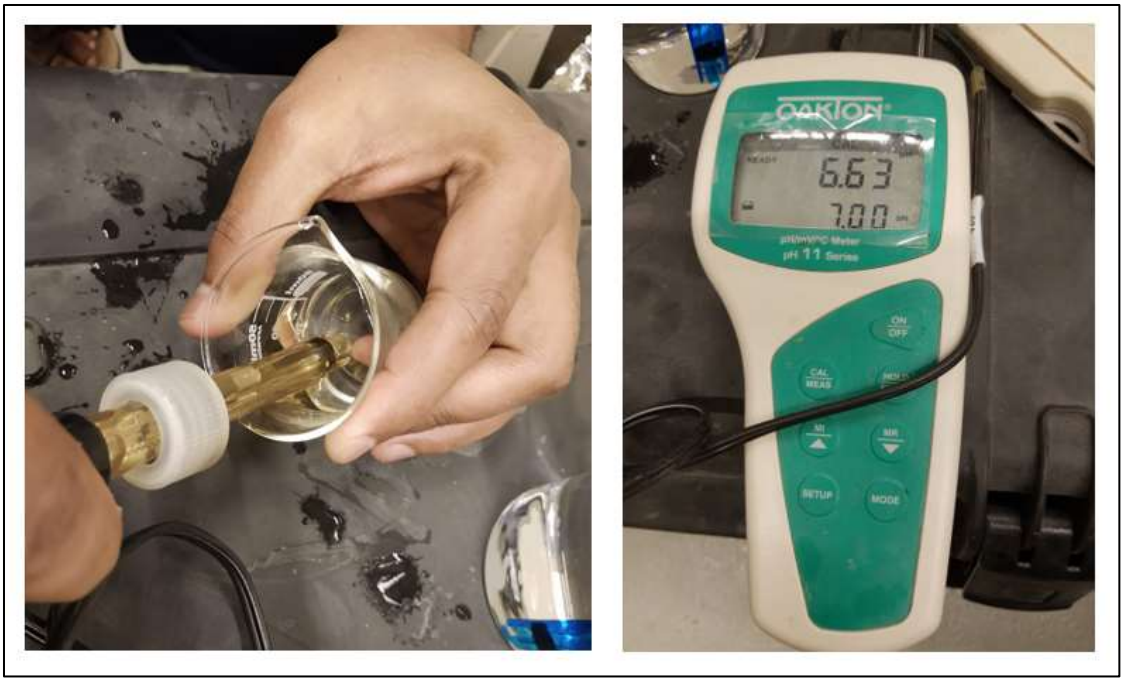

Figure 6. pH Measurement of Rejuvenated Asphalt Binders.

4.3.5. Rotational Viscosity (RV) Test

The viscosity of the asphalt binder measures the workability, pumpability, and mixability of the asphalt binders at high manufacturing and construction temperatures. The RV test was performed on selected asphalt binder samples as per AASHTO T 316 in the laboratory. In this study, a DV-II+ Pro rotational viscometer (RV) from Brookfield Engineering Inc. was used to perform the tests, shown in Figure 7. The RV test is performed to measure the viscosity of asphalt binders at higher temperatures, usually above 135℃. In particular, the RV test was done at a temperature of 135 ℃ up to 180 ℃ at an interval of 15 ℃. The Superpave specification for unaged asphalt binder is that the viscosity of the binder should be ≤ 3 Pa.s at 135 ℃.

In the RV test, the major procedures per AASHTO T 316 followed in this study are given below.

- Firstly, the spindle, sample chamber, and viscometer environmental chamber were Preheat at 135 ℃.
- The asphalt binder sample was heated until sufficiently fluid to pour. During this period, the sample was stirred carefully so that there was no entrapped air bubble.
- Approximately 10 gm of binder sample was poured into the sample chamber.
- The sample chamber was then inserted into the RV temperature controller unit and lower spindle into the sample slowly and carefully.
- The desired testing temperature of the sample was reached within approximately 30 minutes.
- Once the test temperature reached the desired level, an additional time of 10 minutes was allowed to ensure the stability of the test temperature.
- The motor was turned on and the spindle rotation was set for 20 rpm. The amount of torque required to maintain a constant rotational speed (20 rpm) of the cylindrical spindle indicates the viscosity of the binder at a constant temperature.

- At every test temperature, a total of three viscosity readings from the RV display were taken at an interval of 1 minute.
- Finally, the viscosity of the asphalt binder sample was reported as the average of three readings.
- Afterward, the chamber temperatures were set at different levels, from 135 °C to 180 °C at 15°C increments, and the viscosity values at each testing temperature were reported.

Figure 7. RV Test Device.

4.3.6. Dynamic Shear Rheometer (DSR) Test

The Dynamic Shear Rheometer (DSR) test is performed to characterize the viscous and elastic behavior of asphalt binder samples at high and intermediate service temperatures *(39).* The DSR measures the complex shear modulus (G*) and phase angle (δ) of asphalt binders at desired temperatures and frequency of loading. The G* is the measure of the total resistance of the binder to deformation when repeatedly sheared. As shown in Figure 8, the G* consists of two components: (i) storage modulus or the elastic part, and (ii) loss modulus or the viscous part *(40).*

In this study, an Anton Paar MCR 302 DSR machine was used, shown in Figure 9. In the DSR test, the asphalt binder sample is sandwiched between the fixed plate and an oscillating plate, shown in Figure 10. As shown in Figure 10, when torque is applied to the oscillating plate, it starts from point A and moves to point B; later, the plate moves back from point B and goes to point C passing the point A.; again, it returns to point A from point C; thus, it completes one cycle of oscillation. All Superpave DSR tests are conducted at a frequency of 10 radians per second which is equivalent to about 1.59 Hz.

The DSR tests are performed at a frequency of 10 radians per second (1.59 Hz) per AASHTO T 315. The DSR tests were conducted on unaged, RTFO-aged, and PAV-aged asphalt binder samples. Based on the Superpave asphalt binder specification, the rutting parameter was calculated from the ratio of G* to sinδ (i.e., G*/sinδ) for unaged and RTFO-aged binders whereas, the fatigue factor was calculated by multiplying G* and sinδ (i.e., G*.sinδ) for PAV-aged binders. In the DSR test, the gaps between the two plates were 1.00 mm and 2.00 mm respectively, for 25-mm and 8-mm parallel plates. The Superpave specifications of the DSR test are presented in Table 5.

Table 5. Superpave Specifications for the DSR Test Parameters.

Material	Value	Test Temperature (^{o}C)	Specification
Unaged Binder	G*/sinδ	High Service	≥ 1.0 kPa (0.145 psi)
RTFO-aged Binder	G*/sinδ	High Service	≥ 2.2 kPa (0.319 psi)
PAV-aged Binder	G*.sinδ	Intermediate Service	≤ 5000 kPa (725 psi)

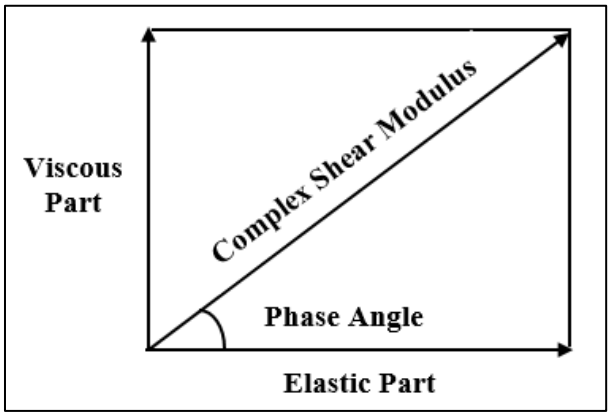

Figure 8. Principle Components of Complex Shear Modulus (G*).

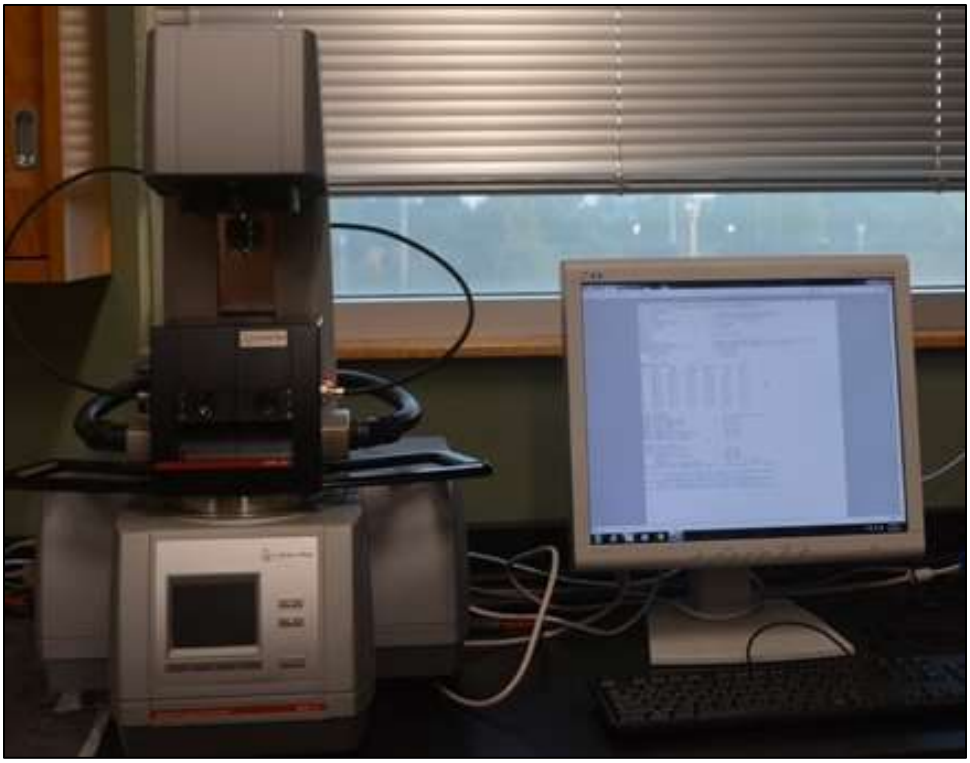

Figure 9. Dynamic Shear Rheometer (DSR).

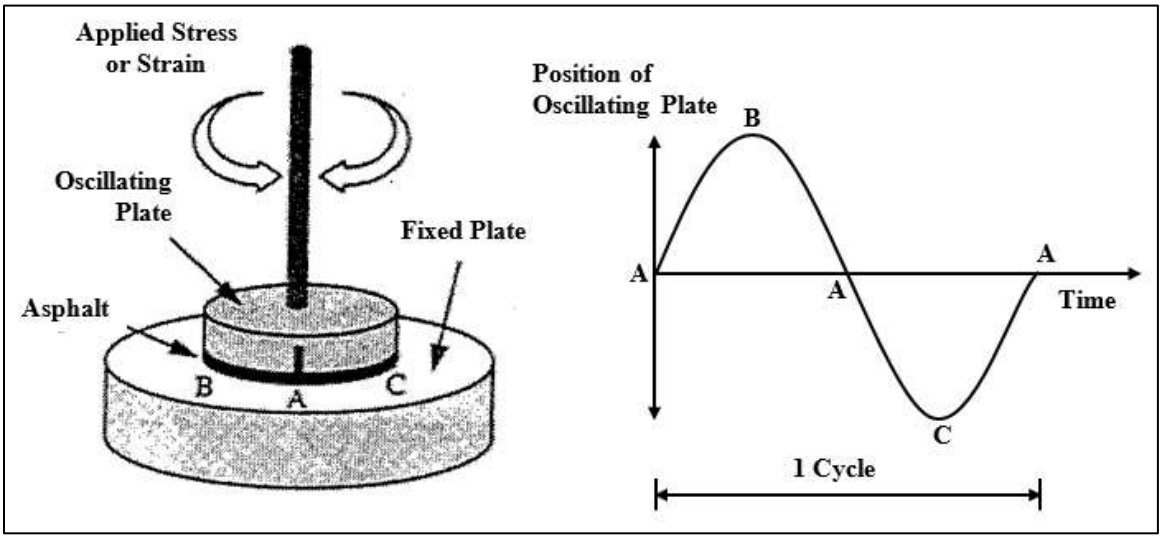

Figure 10. Principle of DSR *(40)*.

4.3.7. Bending Beam Rheometer (BBR) Test

The low-temperature stiffness and stress relaxation properties of asphalt binders were measured by the BBR test. These parameters indicate asphalt binders' resistance to low temperature cracking as well as provide the low service temperature of the PG grading. From the BBR test, creep stiffness and the slope of the master stiffness curve referred to as "m-value" at 60 seconds (s) were measured. The test was performed as per AASHTO T 313. A typical BBR device is shown in Figure 11 and the Superpave specifications for the BBR test are presented in Table 6.

Figure 11. Bending Beam Rheometer (BBR).

Table 6. Superpave Specification for BBR Test.

Parameters	Test Temperature (°C)	Specification
"m-value" at 60 second	Low Service Temperature +10°C	≥ 0.300
Stiffness at 60 seconds	Low Service Temperature +10°C	≤ 300 MPa

The degassed PAV-aged binders were used to prepare a 0.246 x 0.492 x 5.000 inch (6.25 x 12.5 x 127 mm) solid asphalt beam for conducting this test. This beam was loaded at its midpoint in a simply supported set-up where the two supports are 4.02 inches (102 mm) apart and the load was 0.22 lb. (100 g). Afterward, the beam deflection was measured at 8, 15, 30, 60, 120, and 240 seconds. A stiffness master curve was plotted for these points. From the curve, slopes were drawn at 8, 15, 30, 60, 120, and 240 seconds to calculate the "m" values. The test was performed on rejuvenated samples from Source 1 (S1) at -9 °C and -12 °C. To simulate the low service temperature, the time-temperature superposition principle was used.

4.3.8. Multiple Stress Creep Recovery (MSCR) Test

The Multiple Stress Creep Recovery (MSCR) test measures the percent recovery and non-recoverable creep compliance of asphalt binder samples. The MSCR test was conducted per AASHTO T 350 using the DSR at a temperature of 64 °C. In the MSCR test, the percent recovery value is used as the measurement of elastic response and stress dependence of polymer modified and unmodified asphalt binders.

The following are the major steps involved in conducting the MSCR test in this study.

- In the MSCR test, the RTFO-aged asphalt binder was subjected to 10 loading cycles at a temperature of 64 ^{o}C at two stress levels such as 0.1 kPa and 3.2 kPa.
- Each loading cycle was set for a total of 10 seconds duration, consisting of a one-second of loading and nine seconds of recovery.
- For each stress level, the binder sample was subjected to 10 cycles of loading/unloading. Thus, this test was run for a total of 20 cycles for the stress level of 0.1 kPa and 3.2 kPa.
- The change in shear strain for the creep/recovery cycle of the applied stress was measured.
- Afterward, the test results were processed to calculate the two major parameters: i) Percent Creep Recovery (%R) and ii) Non-Recoverable Creep Compliance (Jnr) using the following Equations. Figure 12 shows a typical plot of creep and recovery obtained in the MSCR test.

$$\text{Percent Recovery} = \text{Percent of Recoverable Shear Strain} \quad (1)$$

$$J_{nr} = \frac{\text{Non-Recoverable Starin}}{\text{Applied Stress}} \ (\text{kPa}^{-1}) \quad (2)$$

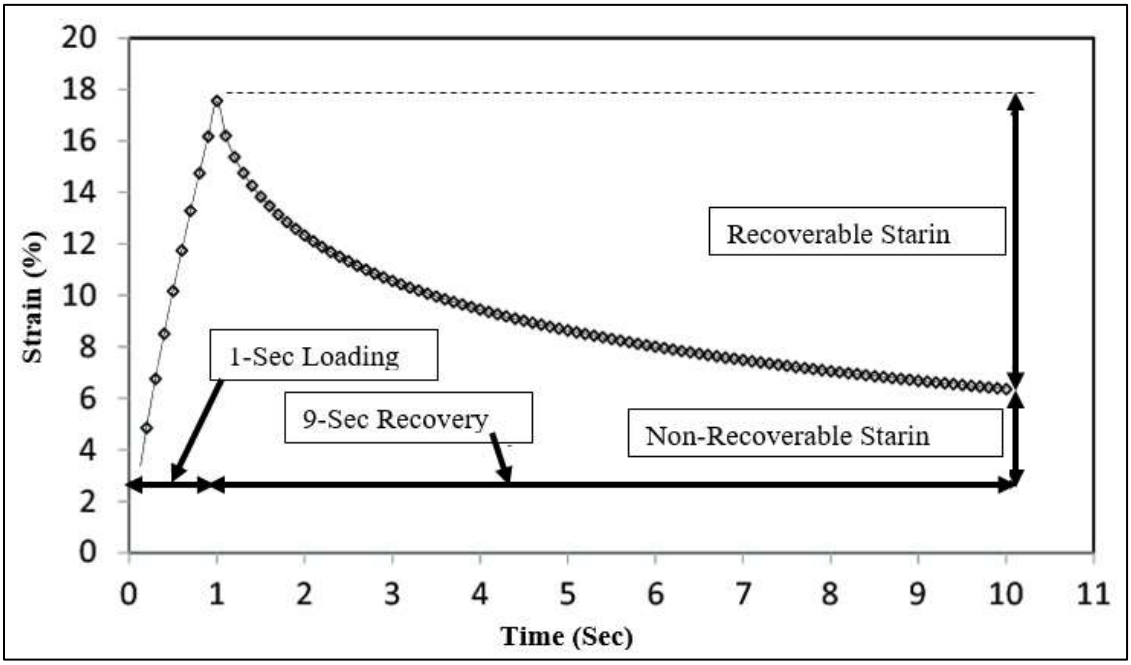

Figure 12. A Typical Plot of Creep and Recovery Obtained in MSCR Test.

4.3.9. Rotational Think Film (RTFO) Aging

In the laboratory, the asphalt binder is generally subjected to elevated temperatures to simulate manufacturing and placement aging. The Rolling Thin-Film Oven (RTFO) aging process is intended to simulate the short-term aged asphalt binder for physical property testing. The RTFO aging was performed per AASHTO T 240. The RTFO aging was used to Simulate asphalt binder aging (hardening) during the hot-mix asphalt (HMA) production and construction. An RTFO oven used for this study is shown in Figure 13.

The basic procedures followed in RTFO aging are stated below.

- Firstly, the asphalt binder sample was heated until it was sufficiently fluid to pour into the RTFO bottles. During this period, the sample was stirred carefully so that there was no entrapped air bubble.
- Approximately 35 ± 0.5 g of asphalt binder was poured into each sample bottle. The bottles were properly labeled.
- The heating chamber of the RTFO was preheated at 163 °C ±1 °C.
- After preheating, the glass bottles were placed into the RTFO sample rack.
- The sample rack was then set to rotate at a speed of 15 rpm for 85 minutes.
- An airflow of 4 liters/min was started to directly blow the asphalt binders into the bottles.
- After completing the rotation time, turned off the heating and airflow.
- The residue from each bottle was then transferred to a single container. The transferring was done by simply pouring as much material as possible at first and then scraping the sides of the bottles with a scraping tool to remove any remaining residue.
- Finally, the RTFO aged binders were stored for further testing and usage.

Figure 13. Rolling Thin Film Oven (RTFO).

4.3.10. Pressure Aging Vessel (PAV)

The PAV simulates the asphalt binder's aging (hardening) during the HMA service life. The PAV aging was done per AASHTO R 28 in this study. The PAV was preheated to the test temperature without applying any pressure. RTFO aged asphalt binder was then placed in PAV and exposed to a temperature of 100°C and pressure of 2.07 MPa for twenty hours. Figure 14 shows the PAV equipment that was used for this purpose.

The major steps followed in this study are given below.

- At first, the RTFO aged asphalt binder was heated until it was sufficiently fluid to pour.
- The sample was stirred and poured 50 g into a preheated thin film oven pan.

- The samples were stacked on a vertical rack (pan holder) and placed inside preheated PAV.
- The temperature was set for 100 °C during this aging process. The PAV was pressurized to 2.07 MPa for 20 hours ± 10 minutes.
- At the end of the aging period, the pressure was released slowly and the pans were removed from the PAV.
- Finally, the aged samples were taken out from the PAV and transferred to a can.
- The transferred samples were then placed in a vacuum oven preheated at 170 °C and degassed for 30 minutes to remove entrapped air.

Figure 14. Pressure Aging Vessel (PAV).

4.3.11. Atomic Force Microscope (AFM) Test

The Atomic Force Microscopy (AFM) technique has been used by multiple researchers to study the properties of asphalt binders at micro-scale in recent years. The AFM tools can capture the microstructures presented on the asphalt binder surface and provide the mechanical properties by correlating its morphological properties as well.

In this study, the Dimension Icon AFM from Bruker has been used to observe the surface roughness/morphology and the mechanical properties such as the DMT modulus, adhesion force, deformation, and dissipated energy of the asphalt binders in the laboratory, shown in Figure 15. The PeakForce Quantitative Nanomechanical Mapping (PFQNM™) mode of the AFM system has been chosen as it provides maps for the surface roughness and mechanistic properties simultaneously at the molecular level. Similar to the tapping mode, the peak force tapping provides the surface morphology and the force-displacement curve of any point under the scan area which are analyzed through the quantitative nanomechanical mapping to find the properties of the scanned surface.

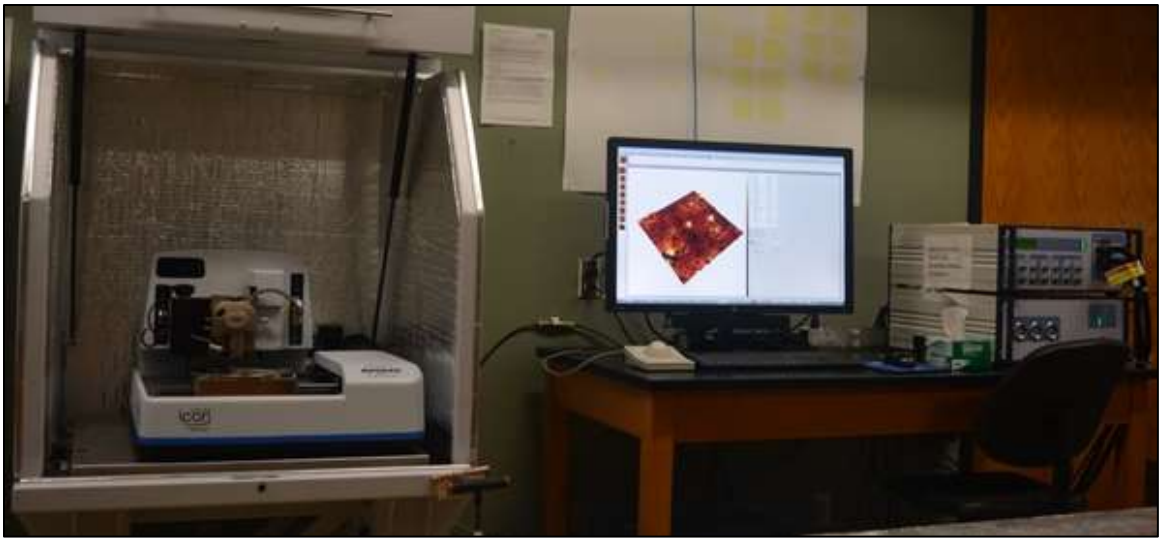

Figure 15. AFM System Installed in the Laboratory.

To prepare the specimens for the AFM tests from the selected binder samples, the heat cast method was followed which has been used by several researchers in the characterization of asphalt binders *(37, 41-53).*

The major steps involved in preparing the AFM test specimens are given below.

- At first, the asphalt binder sample was heated in a preheated oven at 160 °C until it became sufficiently fluid to pour.
- A very small amount of asphalt binder, generally 2 drops, was placed on a thin glass plate of 2" by 3" in size.
- Afterward, the samples with the glass plates were placed in the oven for nearly 15 minutes to create a uniform and smooth surface of the binder. However, in the case of stiff binders, like SBS, the heating time was extended until the desired result was obtained.
- The prepared specimens were then cooled at room temperature for 30 minutes and stored in a humidity-controlled desiccator for 24 hours before testing.
- The AFM tests were conducted using the prepared specimens of the asphalt binders.
- After conducting the AFM tests, the scanned maps were analyzed offline using the NanoScope (version 9.0) software to quantify the roughness and mechanical properties of asphalt binders.

4.3.12. Scanning Electron Microscope (SEM) Test

The Scanning Electron Microscope (SEM) has become a popular technique for the observation of microstructures in asphalt binders in recent years *(54).* These microstructures can be further investigated into rheological properties, modification mechanism, the interaction between modifier and binder's structural, viscoelastic, and physicochemical properties. SEM technique can be effectively used to observe dispersion and distribution of the modifier particles and/or softening agents in the asphalt binder samples *(55).* Moreover, Shirzad et al. *(56)* utilized the SEM technique to evaluate the effects of asphalt rejuvenators (e.g., sunflower oil and PennzSuppress) on asphalt binder and their effectiveness in reversing the aging of asphalt binder. They analyzed the SEM images to observe the morphology and size of the rejuvenator-modified binder as a function of agitation rate, temperature, healing time, and shell thickness.

In this study, the SEM technique was used to examine the microstructures and surface morphology of the tested asphalt binders. Moreover, SEM has the potential to detect the cohesion within the binder and adhesion to the other material. The SEM images will be analyzed to verify if the softening agents are blended smoothly in the RAP mixtures with the asphalt without visible discontinuity at the asphalt-modifier interface. The asphalt binder specimens were coated with gold for 4 minutes before testing. SNE-4500M Plus SEM was operated at an accelerated voltage of 20 kV with a magnification of 100X. SEM has a built-in Energy Dispersive X-Ray (EDX) detector which was used for the compositional analysis of the binder samples. Figure 16 shows the SEM system installed in the laboratory.

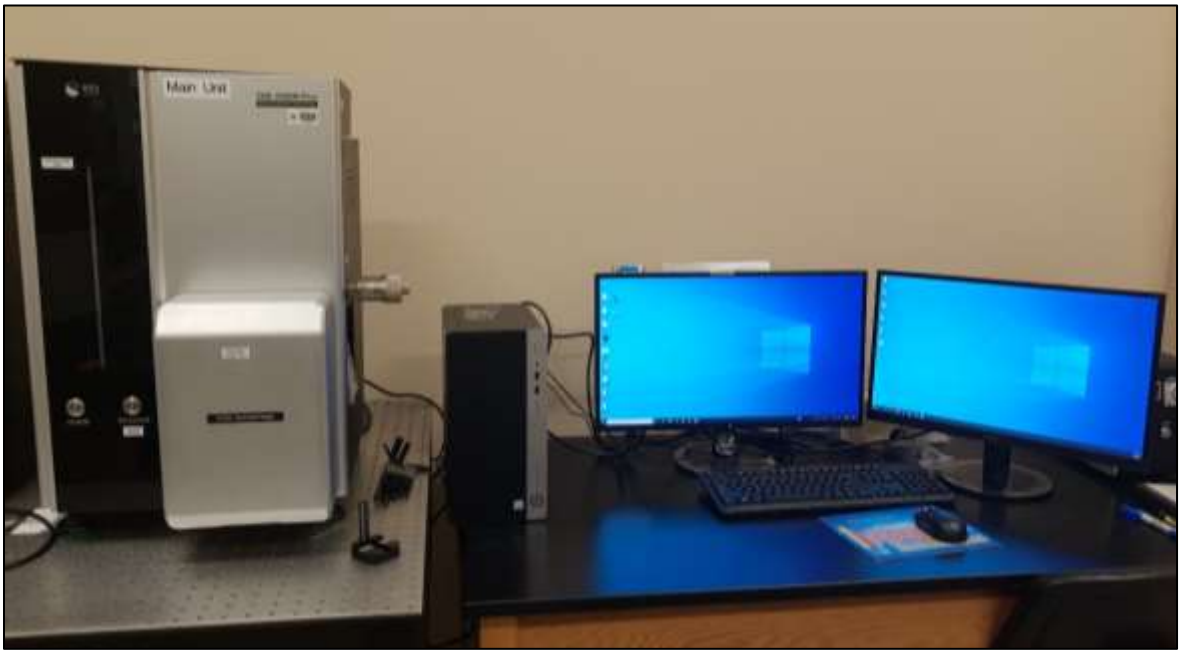

Figure 16. SEM System Installed in the Laboratory.

4.3.13. Fourier Transform Infrared Spectroscopy (FTIR) Test

The FTIR test was conducted on the selected asphalt binder samples to detect the presence, if any, functional group after the modification. The FTIR test is commonly used in the asphalt industry on chemically modified asphalt binder samples *(57).* The test was also performed on RTFO and PAV aged samples to detect any change in the functional group due to the occurrence of oxidative aging.

In this test, a vibrational Infra-Red (IR) light is passed through the sample in question. When the natural vibrational frequencies of a specific molecule match with the frequency of the IR radiation, the molecule absorbs the energy and increases the amplitude of vibrational motion is detected as a peak in the interferogram. In FTIR analysis, the natural vibrations of the covalent bonds among the molecules are exploited in any detection. As every type of bond has a different natural frequency of vibration, and two of the same type of bond in two different compounds are in two slightly different environments, therefore, no two molecules of the different structures have the same IR absorption pattern *(58).* A mapping tool that lists the functional groups and the wavenumbers of their occurrence was followed in this study. Figure 17 illustrates the schematic diagram of the infrared spectrum, which will be used as a mapping tool in the FTIR test *(58).*

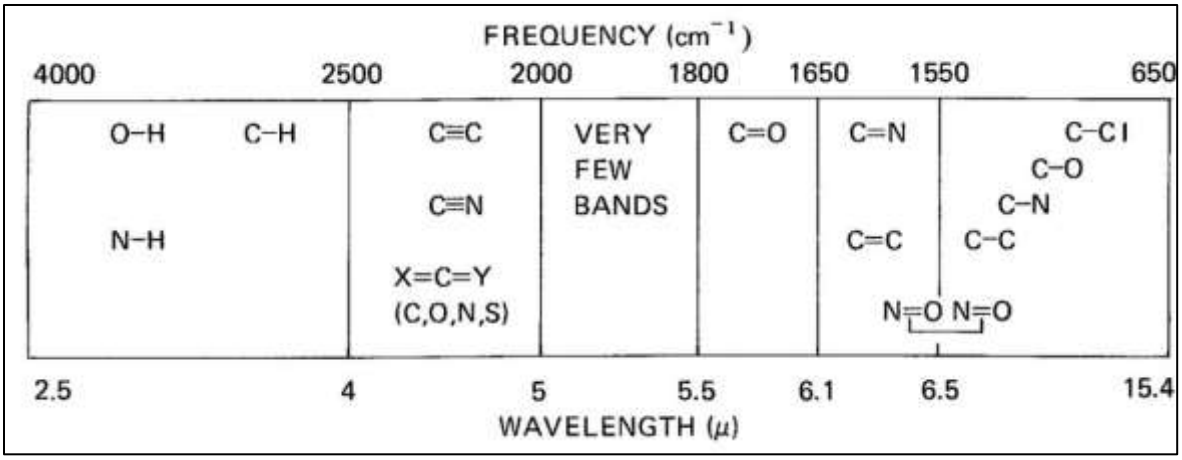

Figure 17. Approximate Regions where Various Common Types of Bonds Absorb (only Stretching Vibrations; Bond Variations (Bending and Twisting) are Omitted) *(58).*

In this study, disposable Real Crystal IR cards, containing the potassium bromide (KBr) substrate, were used for the sample preparation. A blank card was scanned before starting the test. A Nicolet 8700 spectrometer was used in this study. To prepare the sample, Firstly, the asphalt binder was heated at 163 °C until it became sufficiently fluid and workable. A small amount of hot asphalt binder was dropped right outside the aperture and dragged over the KBr substrate to make the coating of the sample on the KBr plate. The aperture of the hole in the plate was 15 mm. A spectrum range of 350 to 7400 cm-1 was used in this study. The samples were run over 50 scans at 4 cm-1 resolutions for 30 seconds. The test was conducted at a relative humidity under 5%. Finally, the test data were analyzed using Omnic 6.2 software. Figure 18 shows a blank IR card and four specimens of PG 70-22 S2 rejuvenated binders.

From the FTIR test, the changes in the quantities of functional groups of asphalt binders before and after rejuvenation were estimated by using the carbonyl (C=O), sulfoxide (S=O) peaks, and the Trans-Butadiene index (ISBS). The values of carbonyl index (IC=O), the sulfoxide index (IS=O), and the Trans-Butadiene index were quantitatively calculated using Equations (3), (4), and (5) *(59,60).*

- Carbonyl Index (C=O),

$$I_{C=O} = \frac{Area\ of\ the\ Carbonyl\ band\ around\ 1700\ cm^{-1}}{Area\ of\ the\ spectral\ band\ between\ 2000\ cm^{-1}\ and\ 600 cm^{-1}} \quad (3)$$

- Sulphoxide-Index(S=O),

$$I_{C=O} = \frac{Area\ of\ the\ Carbonyl\ band\ around\ 1030\ cm^{-1}}{Area\ of\ the\ spectral\ band\ between\ 2000\ cm^{-1}\ and\ 600 cm^{-1}} \quad (4)$$

- Trans-Butadiene Index (S=O),

$$I_{SBS} = \frac{Area\ of\ the\ Carbonyl\ band\ around\ 968\ cm^{-1}}{Area\ of\ the\ spectral\ band\ between\ 4000\ cm^{-1}\ and\ 650 cm^{-1}} \quad (5)$$

Figure 18. A Blank IR Card and Four Specimens of PG 70-22 S2 Rejuvenated Binders.

4.3.14. Mixture Tests and Field Performance Evaluation

However, limited testing and evaluation of asphalt mixes would be conducted to generate some preliminary data for future projects containing high RAP. To this end, two plant mixes containing RAP will be collected for laboratory evaluation of volumetric properties (ARDOT 464) such as voids in total mix, voids in mineral aggregates, and voids filled with asphalt.

Texas Boiling Test (TBT): The Texas Boiling Test is a simple and quick method for evaluating the moisture damage resistance of the asphalt mixtures. This test requires less labor to identify the moisture susceptibility of the asphalt mixtures which is also used by the transportation agencies. The stripping of the asphalt mixtures is determined based on visual observation after 10-minutes of boiling the asphalt mixtures in hot water. The asphalt mixture for this test is prepared using either individual aggregates or total aggregate mixtures. For individual aggregate mixture, the aggregates could be used on the following criteria: i) passing 3/8 inch retained on No. 4, ii) passing No. 4 retained on No. 10, iii) passing No. 10 retaining on No. 40, and iv) passing No. 40 retaining on No. 80. For evaluating the total aggregate mixture, the sample should have the same gradation as proposed for the construction works. Typically, the aggregates greater than 7/8 inches are discarded to conduct this test.

The major steps involved in conducting this test are given below.

- Texas boiling test includes heating the mixture inside a glass beaker with boiling water.
- Firstly, a 1000 ml beaker was filled with 500 ml of distilled water and heated to a boiling temperature (100 ^{o}C).
- The asphalt mixture was added to the boiling water and increased the heat for maintaining the boiling temperature. The heat was applied to the glass beaker at a rate so that the water will start re-boiling within two to three minutes.
- The asphalt mixture with water was set for boiling for approximately ten minutes and stirred with a glass rod at three-minute intervals.
- During the boiling, the stripped asphalt came to the water surface was removed using the paper towel to stop recoating of the aggregates.
- After the boiling test, the water was drained out from the beaker; the mixture was emptied on a paper towel; allowed to cool and dry to room temperature for nearly 30 minutes.
- Finally, the percentage of asphalt retention on the surface of the aggregates was reported by following the guideline established by the Texas Transportation Institute (TTI) as shown in Figure 19.

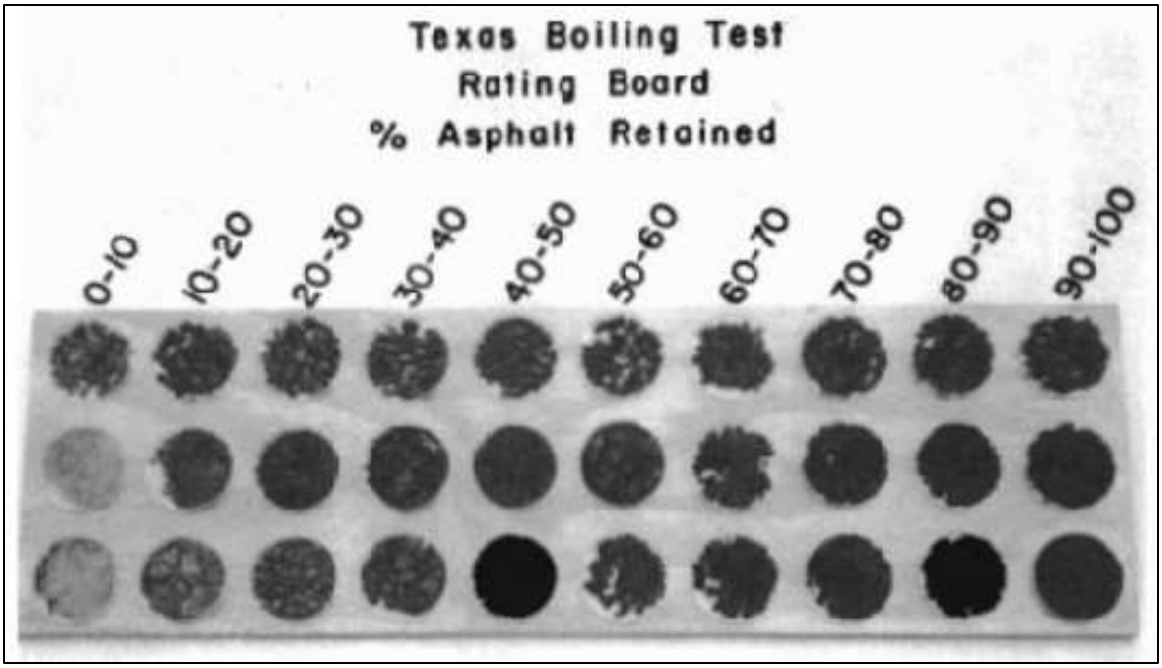

Figure 19. Rating Board for Texas Boiling Test *(61).*

Compressive Strength Test: To conduct the compressive strength tests, the required specimens are usually prepared using a Superpave gyratory compactor (SGC) by compacting the HMA specimens. A Pine Gyratory Compactor installed in the LSW Lab#132 at Arkansas State University was used for compacting the sample specimen, shown in Figure 20.

The major steps involved in conducting this test are given below.

- The specimens were collected from a nearby company, namely, Delta Asphalt, Inc. located at Paragould, Arkansas.
- According to AASHTO TP4-93, approximately 4700 g sample was placed in a flat pan and kept at 135 ^{o}C for 4 hours for compacting the sample for one specimen of 6" by 6" of size.
- The mold used for the compaction was also heated for 30 minutes in the oven before compacting the specimen.
- After proper heating of the mold, a paper disk was placed on the bottom of the mold and a properly hot mix loose asphalt sample was placed inside the mold with another paper disk on the top of the sample.
- Afterward, the mold was placed and set up in the gyratory compactor.
- To achieve the goals of the project, the maximum number of gyration (Nmax) was set as 115 for 0.3 to 3.0 M ESALS of traffic. The compaction was done with proper speed, angle, and the number of gyrations, as required.
- The compacted sample was taken out of the compactor after compaction and used for conducting the compressive strength test.
- The specimen was capped using the reusable capping sets as used in testing Portland Cement Concrete cylinders (AASHTO T 22). This system consists of two steel retainers, each containing a 50-durometer Neoprene pad. The compression tests will be performed at a loading rate of 7.5 mm/min.

Figure 20. Pine Gyratory Compactor (left) and HMA Specimen after Heating.

Retained Stability (ARDOT Test Method 455A-11) Test: This test method is used to evaluate the effects of water on the strength of compacted bituminous mixtures. In this test, a numerical index of reduced strength is obtained by comparing the Marshall Stability at 60° C (140° F) of cured specimens with that of duplicate specimens that have been immersed in water at 60° C (140° F) under a condition of vacuum saturation.

The major steps involved in conducting this test are given below.

- Firstly, the test specimens are separated into two groups identified as Group A and Group B.
- Then, the stability values of Group A, known as SA, specimens were tested according to AASHTO T 245.
- For Group B specimens, specimens are completely submerged in the water bath for 24 hours at 60 + 1°C after one hour of vacuum period.
- Afterward, the stability of Group B specimens, known as SB, was determined as per AASHTO T 245.
- The numerical index of water sensitivity is expressed as the percentage of stability retained after water immersion, which was calculated using the following equation.

$$Retained\ Stability, R\ (\%)\ = \frac{S_B}{S_A}\ x\ 100 \qquad (6)$$

where,

SA = average Marshall stability of Group A in lbs. (kN)

SB = average Marshall stability of Group B (water-immersed specimens) in lbs. (kN).

5. ANALYSIS AND FINDINGS

5.1. Performance (Superpave) and MSCR Test Results

5.1.1. Rotational Viscosity of Asphalt Binders

The RV tests were conducted on unrejuvenated and rejuvenated RAP blends in this study. Detailed RV test data of RAP1 and RAP2 blends along with various dosage levels of the selected softening agents are presented in Appendix A of this report. From the RV test results, it is seen that the viscosity data of RAP1 is very comparable with that of RAP2 even though their sources and histories are different from each other. Also, it is observed that a higher dosage (e.g., 15 or 20%) of the softening agents is not beneficial. Further, previous literature review data suggest that 10% (by the weight of the binder blend) is optimum. Thus, RV test data of RAP1 blends (0, 15, 25, 40, and 60% by the weight of the total binder) of all three binders (PG 64-22, PG 70-22, and PG 76-22) from both sources (S1 and S2) with 0% (Control) and 10% softening agents have been evaluated and explained thoroughly here.

Figures 21 to 23 represent the viscosity values of RAP1-blended S1 binders rejuvenated with 10% softening agents. In the RV tests, a total of three replicate specimens were tested for each test temperature of 135 °C, 150 °C, 165 °C, and 180 °C. For each specimen, three viscosity readings were recorded at 1-minute intervals at each test temperature, and the average values were taken into consideration for data interpretation. As seen from these figures, the rejuvenators decreased the viscosity of all binder blends irrespective of the binder grade and test temperature. It is also evident that the reduction of the viscosity values of 25% RAP1 blends followed a similar trend in the cases of WCO and EVF rejuvenators compared to EBO, which showed the most reduction of viscosity values. The reduction of viscosities is expected to facilitate lower production temperatures (mixing and compaction) for rejuvenated asphalt binder mixes compared to their unrejuvenated counterparts, as shown in Figure 24.

In this study, for naming the test samples, the following nomenclature was used: the binder source was followed by binder grade, which is followed by RAP No. and amount (%), which is followed by rejuvenator type and amount (%), and then lastly the aging condition (U for unaged, R for short-term aged, and P for long-term aged). For example, S1PG64-22+RAP1(25)+EVF(10)U denotes the test sample is a Source 1 PG 64-22 binder with 25% RAP1 that is rejuvenated with 10% EVF and the binder is unaged.

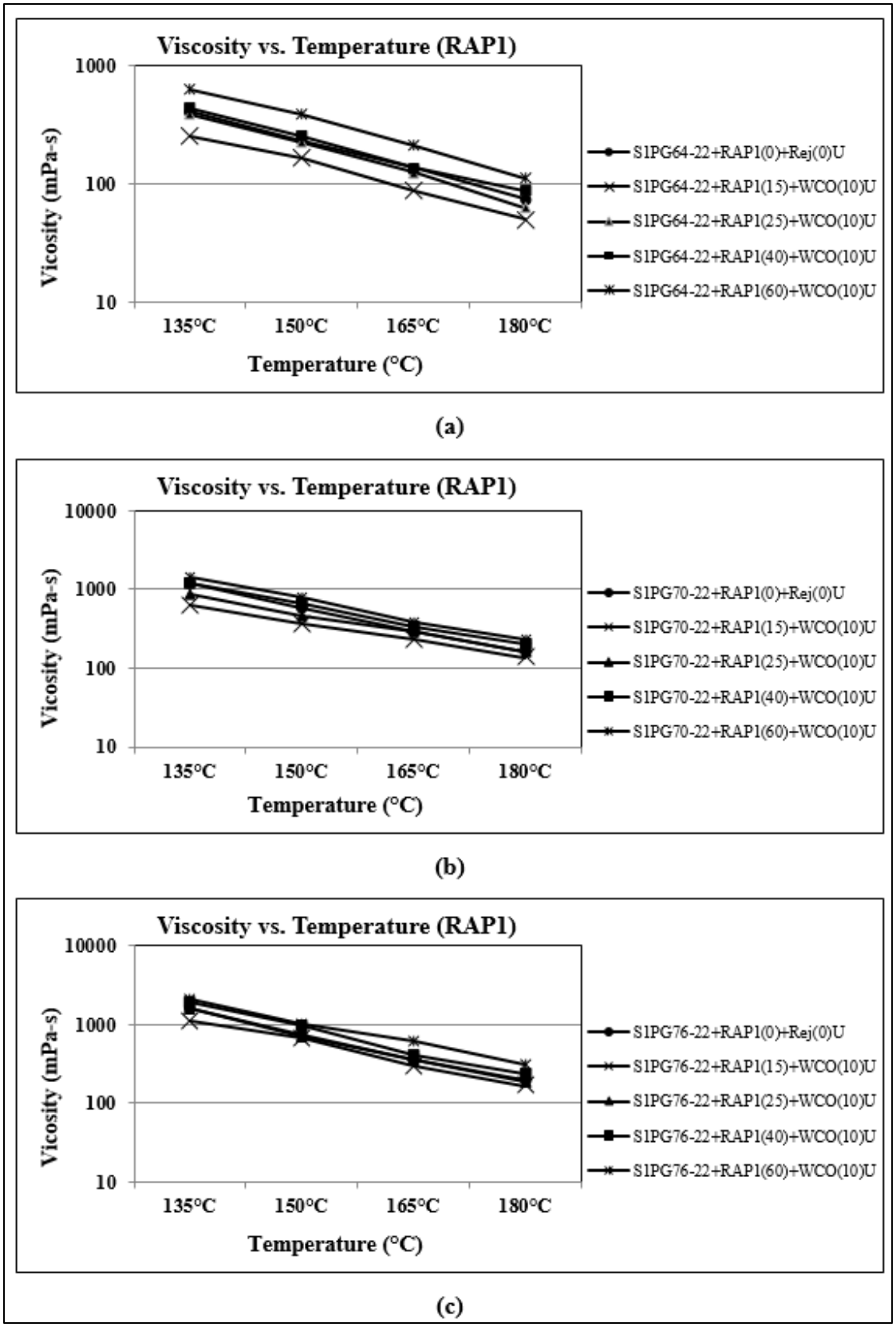

Figure 21. Rotational viscosity (mPa.s) Test Results of 10% WCO-Rejuvenated RAP1 Binders from S1.

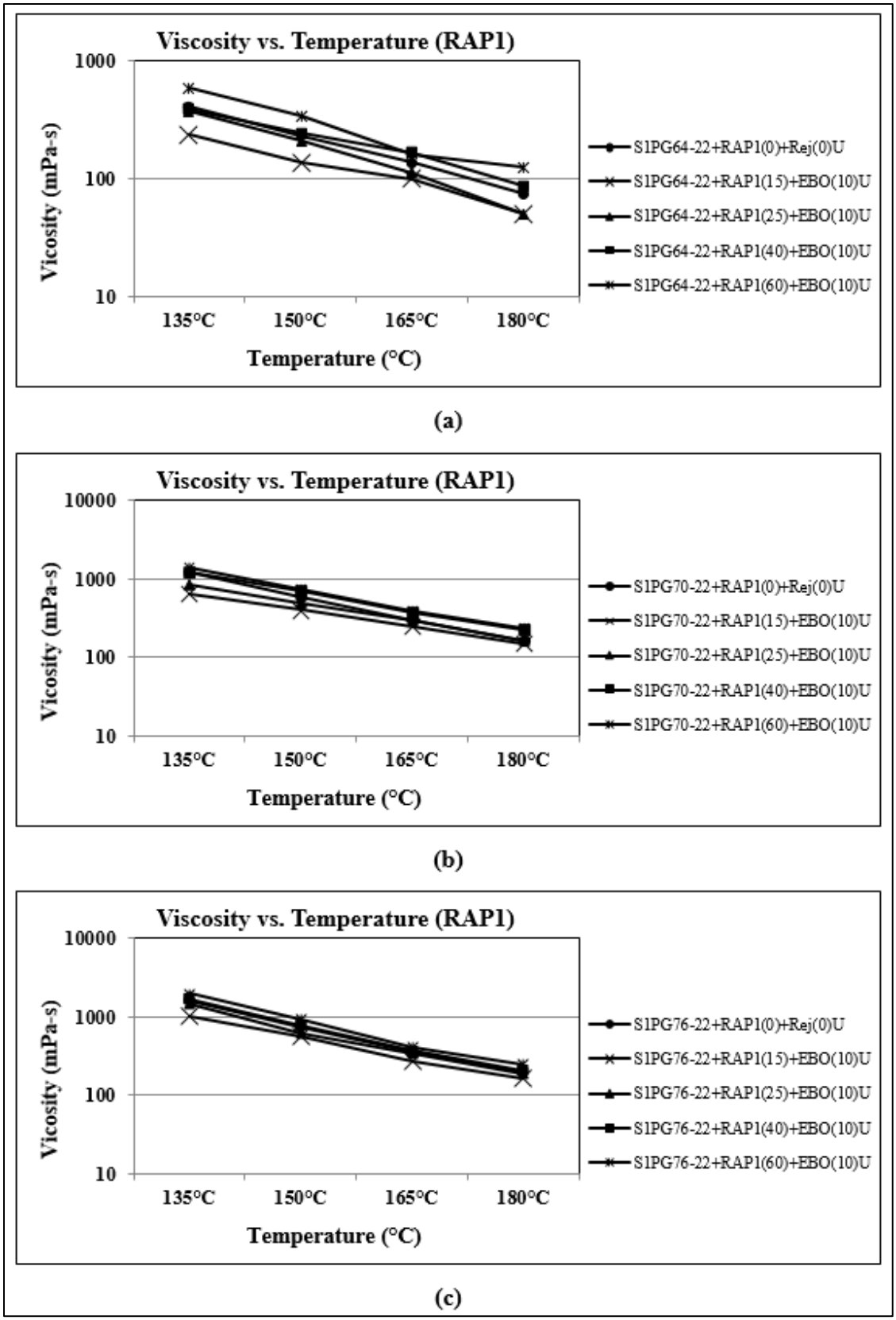

Figure 22. Rotational viscosity (mPa.s) Test Results of 10% EBO-Rejuvenated RAP1 Binders from S1.

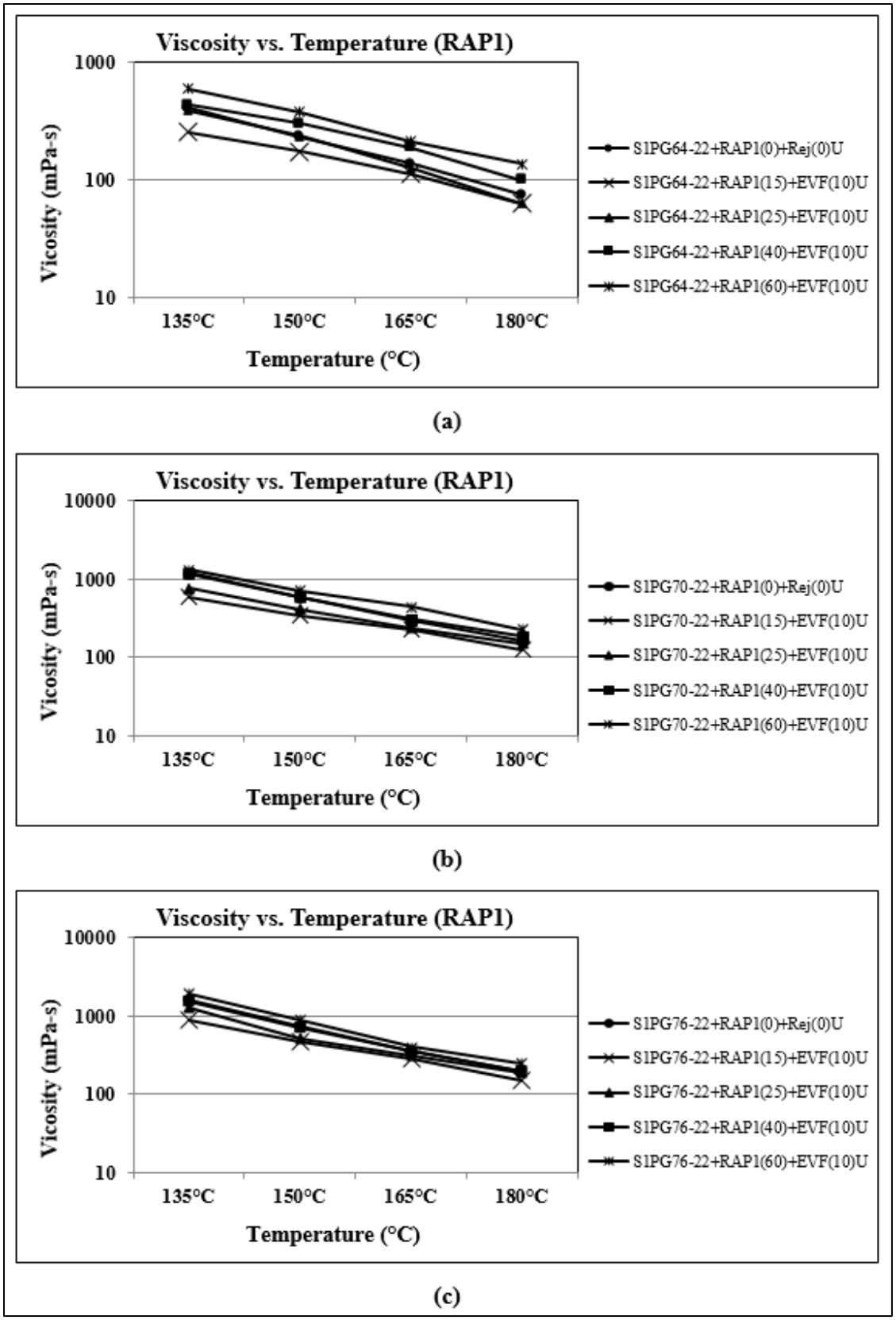

Figure 23. Rotational viscosity (mPa.s) Test Results of 10% EBO-Rejuvenated RAP1 Binders from S1.

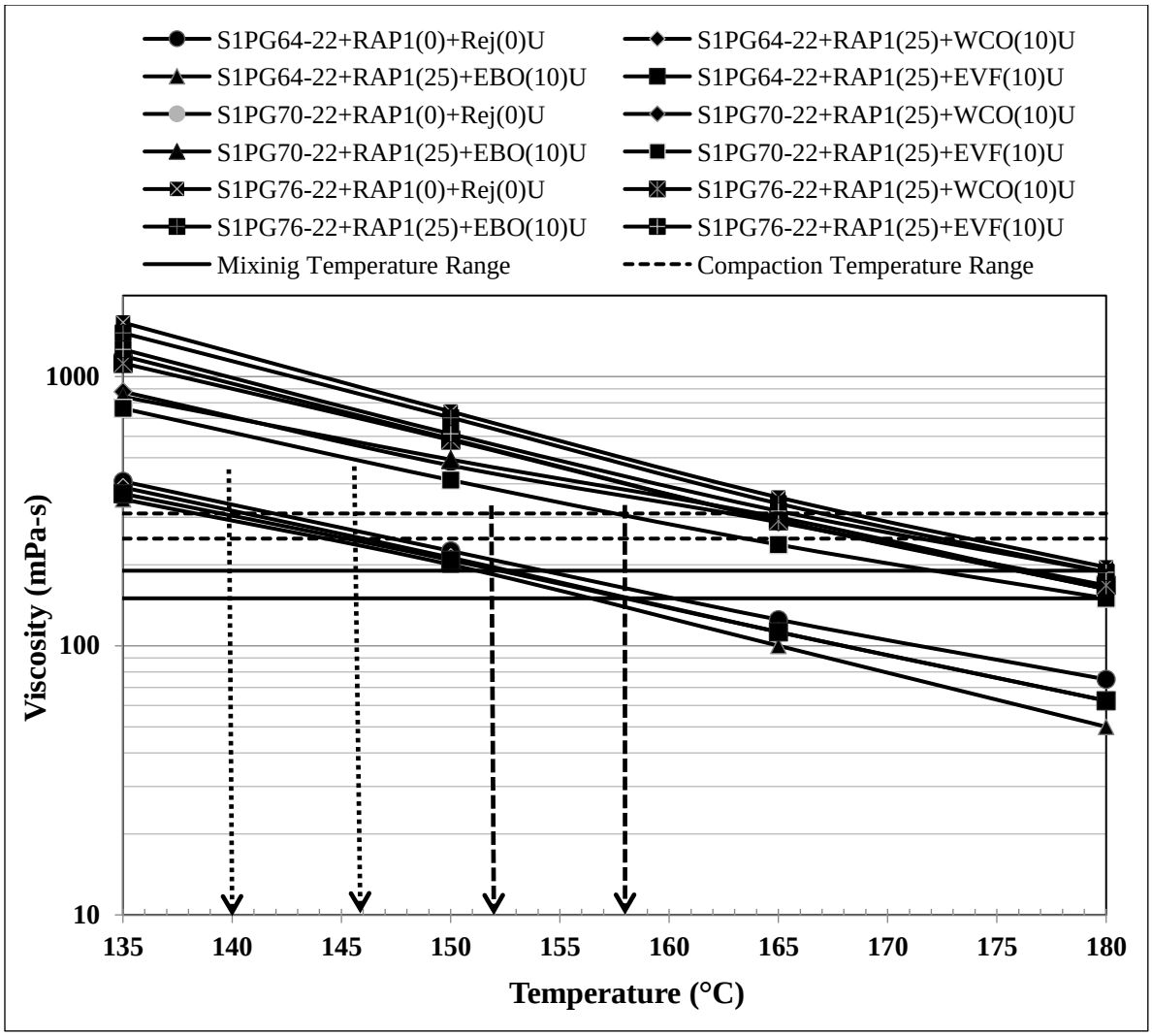

Figure 24. Comparison of Viscosities and Determination of Mixing and Compaction Temperatures of Rejuvenated Binders from S1.

Figure 24 shows the ranges of the mixing and compaction temperatures for all rejuvenated blends from S1. The mixing and compaction temperatures of HMA are expressed in ranges of temperature based on the viscosities of asphalt binders as per ASTM D 2493. The viscosity values of 170±20 mPa-s and 280±30 mPa-s are recommended for determining the mixing and compaction temperatures, respectively. The addition of the rejuvenators reduced the viscosities at each test temperature of all binders containing 25% of RAP compared to their corresponding unrejuvenated binders. For instance, a mixing temperature range of 152 °C - 158 °C was found for rejuvenated 25% RAP blend with 10% EVF for PG 64-22, designated as S1PG64-22+RAP1(25)+EVF(10)U in Figure 24. The compaction temperature range of this binder blend was found to be in the range of 140 °C - 146 °C. Therefore, it can be said that this rejuvenated blend can be mixed at 155 °C ± 3°C and compacted at 143 °C ± 3 °C that contains 25% of RAP binder. On the other hand, the mixing and compaction temperatures of the corresponding unrejuvenated binder i.e., S1PG64-22+RAP1(25)+Rej(0)U are 157 ^{o}C ± 3 ^{o}C and 145 ^{o}C ± 3 ^{o}C, respectively. Thus, the reductions of mixing and compaction temperatures of the EVF-rejuvenated PG 64-22 binder with 20% RAP binder are about 2 ± 2 ^{o}C and 2 ^{o}C, respectively. Tables 7 to 9 represent the mixing and compaction

temperatures of all rejuvenated binders from S1. The RV test data further suggest that binder blends with 25% RAP binder meet the Superpave criterion with 10% of any of the softening agents, especially for surface mixes when hard binders (PG 70-22 or PG 76-22) are used. Again, a 25% RAP in surface mixes denotes the mix with a high RAP content. As explained later in this report, the field demonstrations of two surface mixes also contain 25% RAP. Hence, most of the other laboratory testing of the project has focused on 25% RAP and 10% softening agent in the cases of all three PG binders considered in this study.

Table 7. Mixing and Compaction Temperatures of Rejuvenated Binders from S1: PG 64-22.

Binder Description	Mixing Temperature (°C)		Compaction Temperature (°C)	
	Low	High	Low	High
S1PG64-22+RAP1(0)+Rej(0)U	154	160	142	148
S1PG64-22+RAP1(25)+WCO(10)U	152	158	140	145
S1PG64-22+RAP1(25)+EBO(10)U	151	156	139	144
S1PG64-22+RAP1(25)+EVF(10)U	152	158	140	146

Table 8. Mixing and Compaction Temperatures of Rejuvenated Binders from S1: PG 70-22.

Binder Description	Mixing Temperature (°C)		Compaction Temperature (°C)	
	Low	High	Low	High
S1PG70-22+RAP1(0)+Rej(0)U	176	182	164	179
S1PG70-22+RAP1(25)+WCO(10)U	174	180	161	167
S1PG70-22+RAP1(25)+EBO(10)U	173	180	159	165
S1PG70-22+RAP1(25)+EVF(10)U	172	179	158	164

Table 9. Mixing and Compaction Temperatures of Rejuvenated Binders from S1: PG 76-22.

Binder Description	Mixing Temperature (°C)		Compaction Temperature (°C)	
	Low	High	Low	High
S1PG76-22+RAP1(0)+Rej(0)U	181	187	168	174
S1PG76-22+RAP1(25)+WCO(10)U	176	182	164	169
S1PG76-22+RAP1(25)+EBO(10)U	177	183	156	171
S1PG76-22+RAP1(25)+EVF(10)U	174	184	161	167

5.1.2. Dynamic Shear Rheometer (DSR) Test Results

Figures 25 and 26 show the effects of rejuvenators on all RAP binder blends in the PG temperatures. The Superpave acceptance criterion is shown with the horizontal lines in these figures. As seen in these figures, the rejuvenated RAP blends became softer than their corresponding unmodified binders; so, they failed earlier at high test temperatures. For instance, the high PG temperature was found to be reduced from 82 °C to 76 °C for the PG 76-22 binder blends. The DSR test results show that the high PG temperature corresponding to the Superpave rutting factor of rejuvenated RAP blends of PG 64-22, PG 70-22, and PG 76-22 binders range from 61°C to 64°C, from 76 °C to 73 °C, and from 79°C to 76°C, respectively. It is seen that the EBO-modified RAP blends exhibited lower failure temperatures compared to WCO and EVF among all binders. Generally, the range of high PG temperature of rejuvenated blends containing 25% RAP binders is slightly lower than that of the unrejuvenated counterparts. Thus, it can be said the rejuvenators acted as the binder softeners for all RAP blends. It is also expected that the low PG temperatures of these RAP blends would also be slightly lower, which will be discussed in the following section. Based on the DSR test results, either EVF or WCO is found to be superior to EBO as a softening agent for the RAP blended binders.

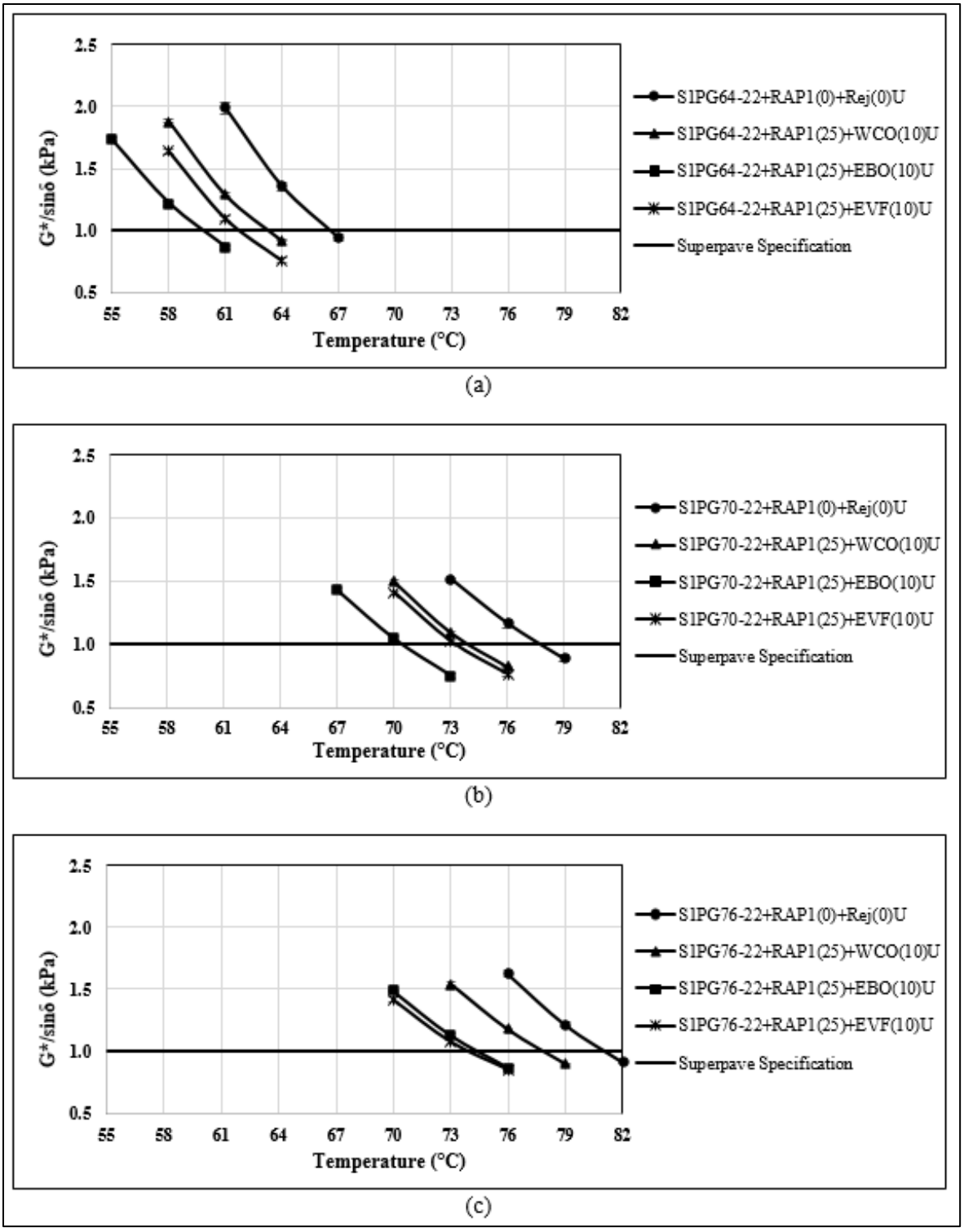

Figure 25. DSR Test Results of Unaged Rejuvenated RAP1 Binders from S1.

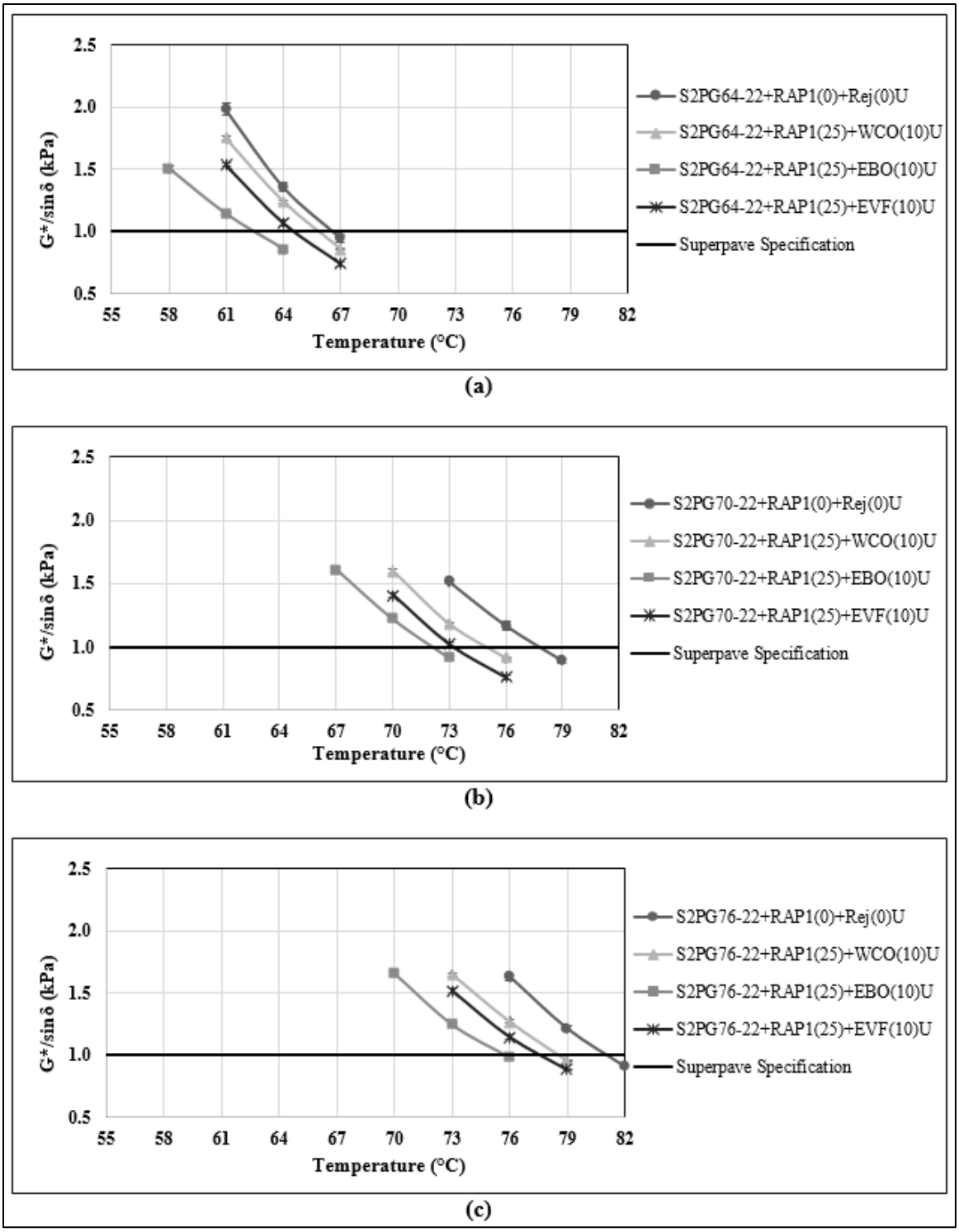

Figure 26. DSR Test Results of Unaged Rejuvenated RAP1 Binders from S2.

5.1.3. Bending Beam Rheometer (BBR) Test Results

The BBR tests were conducted on selected rejuvenated asphalt binder samples to evaluate their low-temperature performance. In this study, the BBR test was done for the PG 70-22 and PG 70-22 binder samples from S1 modified with 25% of RAP1 binder contents and all three rejuvenators (i.e., WCO, EBO, and EVF). The other binder, PG 64-22, was not considered for BBR tests as it is a soft binder and its low critical temperature (i.e., -22) is the same as the other two binders. For all tested binder samples, the measured creep stiffness and m-value at the 60s at -9 °C and -12 °C are shown in Figures 27 to 30.

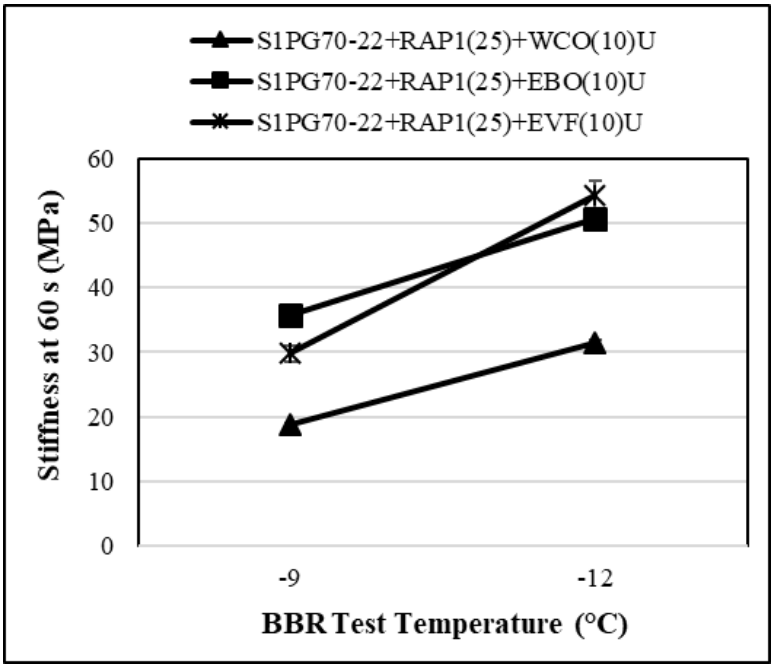

Figure 27. Creep Stiffness of Rejuvenated RAP1 Binders from S1: PG 70-22.

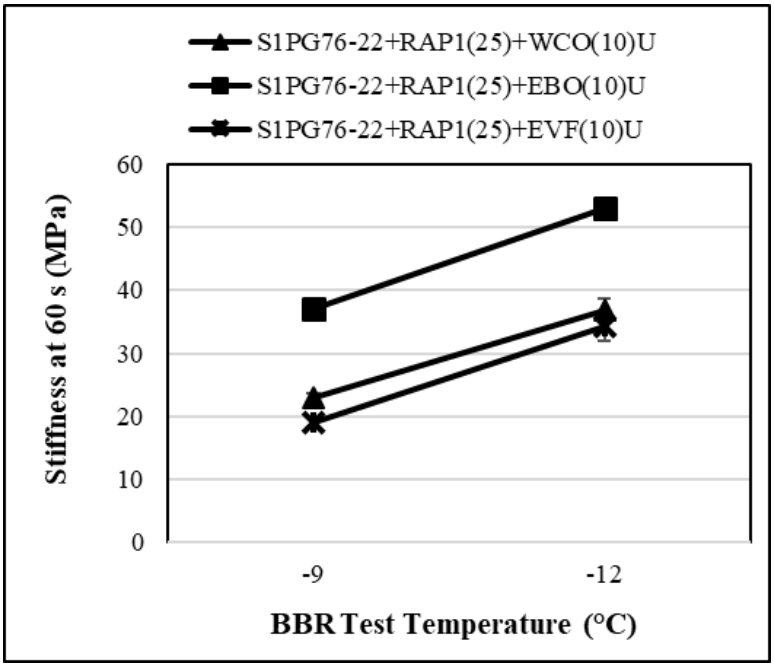

Figure 28. Creep Stiffness of Rejuvenated RAP1 Binders from S1: PG 76-22.

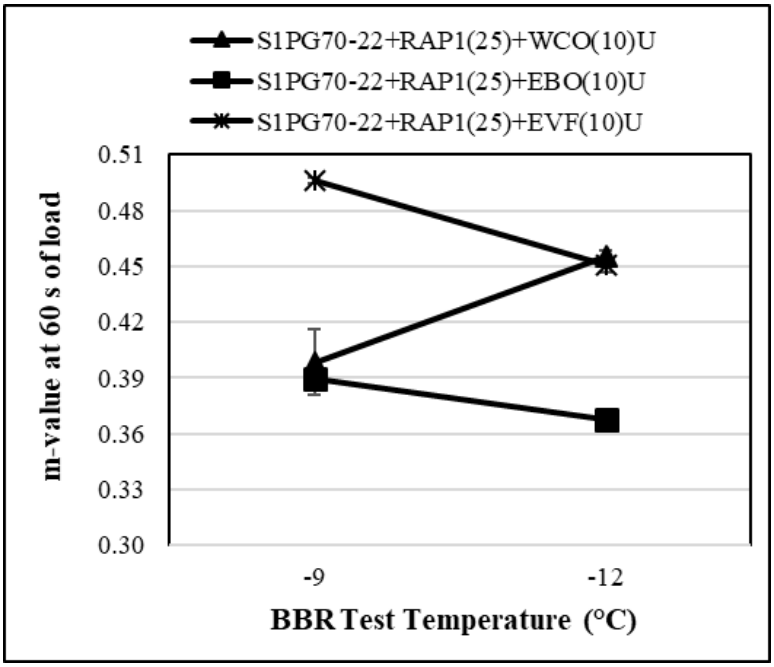

Figure 29. "m-values" of the Rejuvenated RAP1 Binders from S1: PG 70-22.

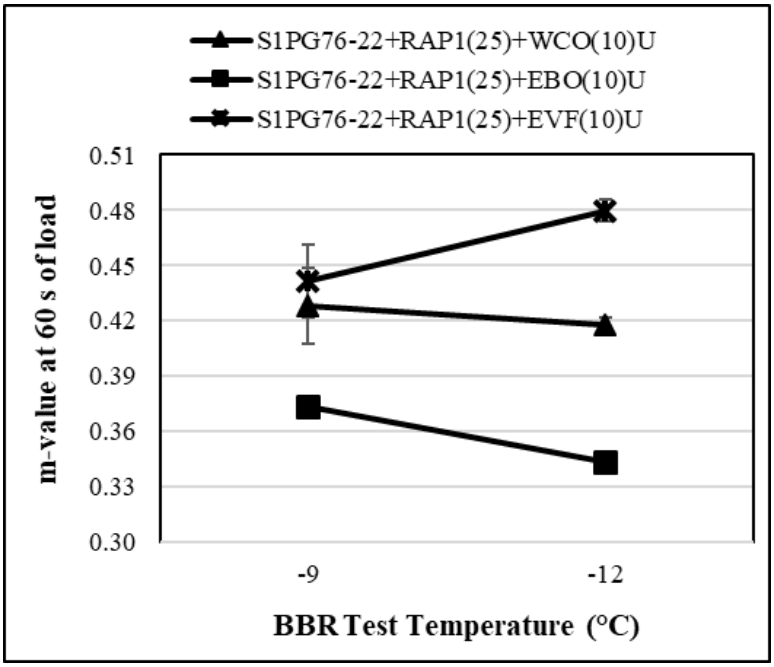

Figure 30. "m-values" of Rejuvenated RAP1 Binders from S1: PG 76-22.

From Figures 27 and 28, it is seen that the stiffness values at 60 s were increased at the testing temperature from -9 °C and -12 °C for all rejuvenated blends. At -9 °C, the RAP blends rejuvenated with EBO showed higher stiffness values compared to EVF and WCO-modified blends. As expected, the stiffness values of all rejuvenated asphalt binders increased with a decrease of the testing temperature, but they were well below the Superpave acceptance criteria of 300 MPa at a BBR testing temperature of -12 °C (i.e., low PG temperature of -22 °C).

As seen in Figures 29 and 30, the "m-values" of most of the samples were found to be reduced with a reduction of test temperature (i.e., from -9 °C and -12 °C), which was expected. However, in the cases of "S1PG70-22+RAP1(0)+Rej(0)U" and "S1PG76-22+RAP1(25)+EVF(10)U," a reverse trend was noticed. The root cause of this unexpected trend is unknown to the research team. One of the probable reasons could be due to the testing of the beam specimens after a longer period since their preparation. After noticing this unusual trend, an extra pair of beam specimens at both testing temperatures (-9 °C and -12 °C) were tested again, but the m-values agreed with the results of the previous pair. It was observed that the EBO-modified binders exhibited the lowest "m-values" at 60 s of load among all rejuvenated binders. Thus, the major finding from the BBR test results is that the softening agents increased the "m-value" (rate of stress relaxation) of RAP-blended binders indicating their beneficial effects. From the "m-value" perspective, EVF and WCO were found to outperform EBO. However, at a testing temperature of -12°C, all tested rejuvenated RAP-blended binders comfortably met the Superpave criterion for the rate of stress relaxation (m-value ≥ 0.300).

5.1.4. Multiple Stress Creep Recovery (MSCR) Test Results

The MSCR tests were conducted on rejuvenated asphalt binder samples from S1. The percent recovery and non-recoverable creep compliance (Jnr) values of these binders are shown in Figures

31 and 32. From Figure 31, it is seen that the percent recovery (%R) values were higher for base binders in the case of PG 76-22 and PG 70-22 binders compared to other binders. Figure 32 shows that the Jnr values were found to be lower for hard binders, particularly for PG 76- 22 binders, compared to the others. In the cases of rejuvenated PG 64-22 binders, the Jnr values were found to be higher than the other two PG binders tested in this study. Moreover, the %R and Jnr showed a similar trend in all binder blends, as evident in Figures 31 and 32.

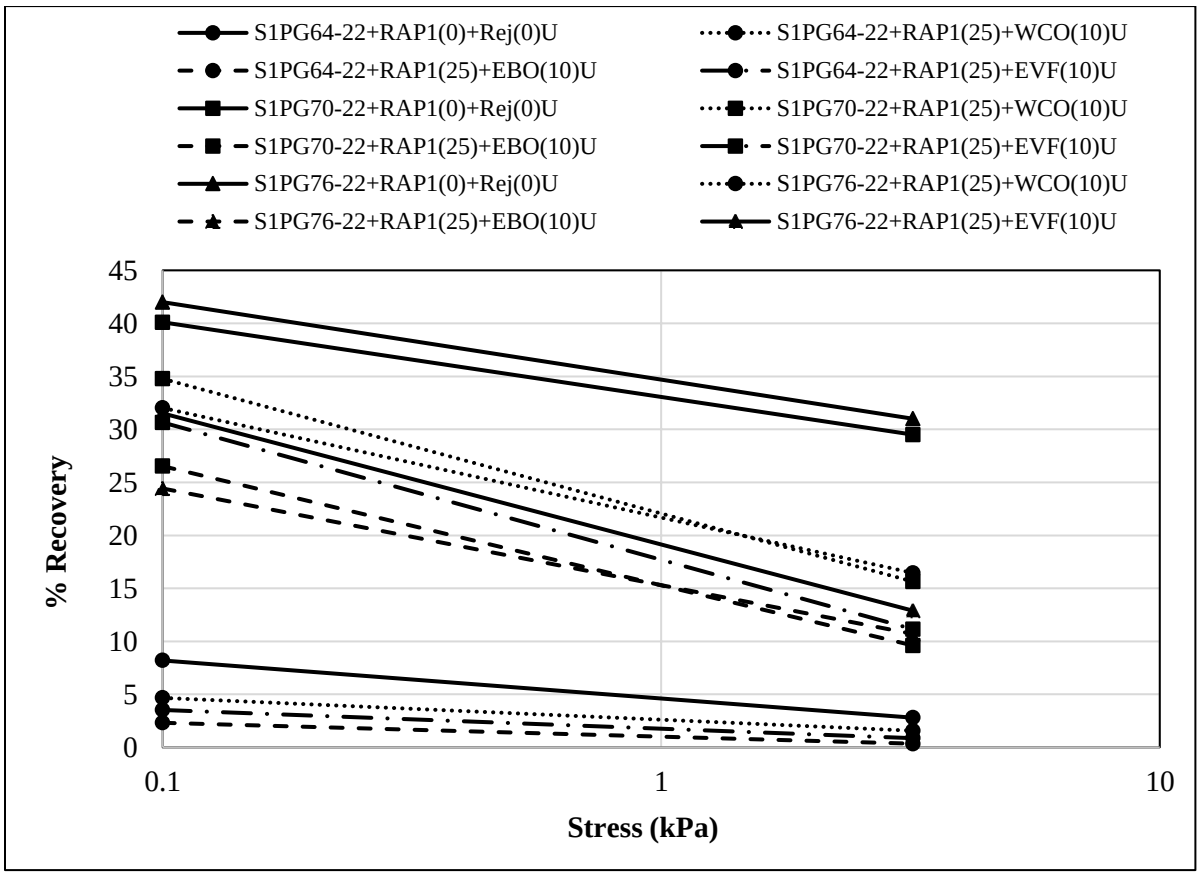

Figure 31. Percent Recovery vs. Stress for Rejuvenated RAP1 Binders from S1.

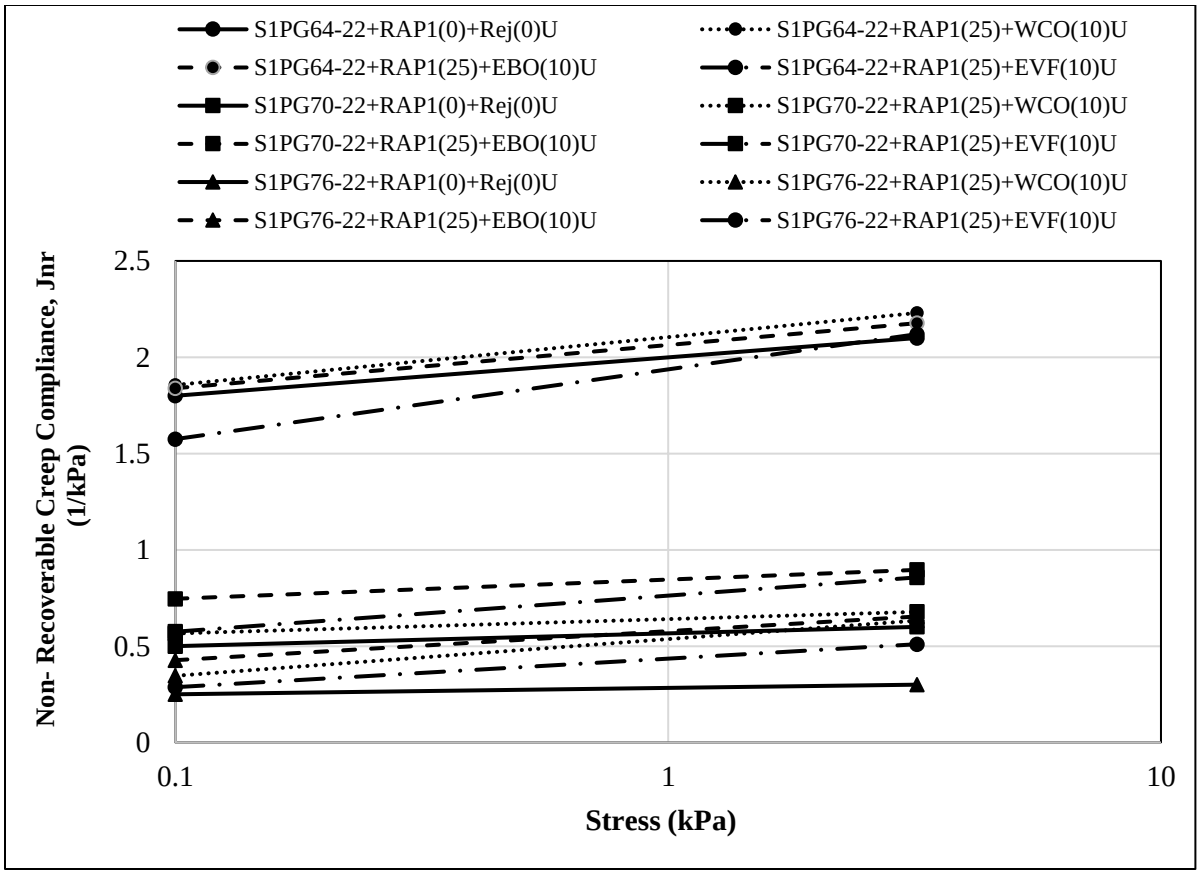

Figure 322. Non-Recoverable Creep Compliance vs. Stress for Rejuvenated RAP1 Binders from S1.

5.2. Empirical Test

5.2.1. Penetration Test Results

The comparative results of the penetration tests of unrejuvenated and rejuvenated RAP1 binders from S1 and S2 are presented in Figures 33 and 34, respectively. A total of six base binders, 25% of RAP1 rejuvenated blends with 10% of different softening agents (WCO, EBO, and EVF) were considered for conducting the penetration test. As seen from the figures, the addition of rejuvenators increased the penetration values of all blends compared to their corresponding base binders regardless of binder grade and crude source. Among all rejuvenators, EBO showed the maximum penetration value in the cases of PG 64-22 and PG 70-22 binders from S1 and S2, whereas EVF had slightly higher penetration values in both sources.

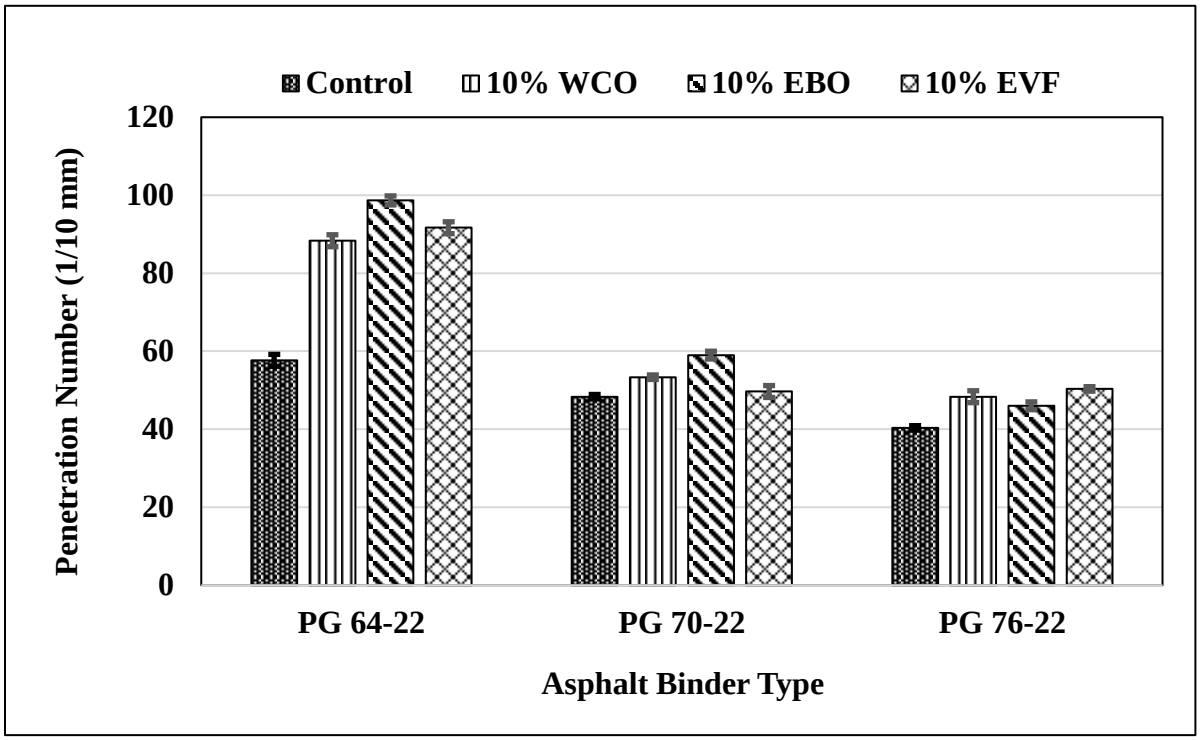

Figure 33. Penetration Test Results of Asphalt Binders from S1.

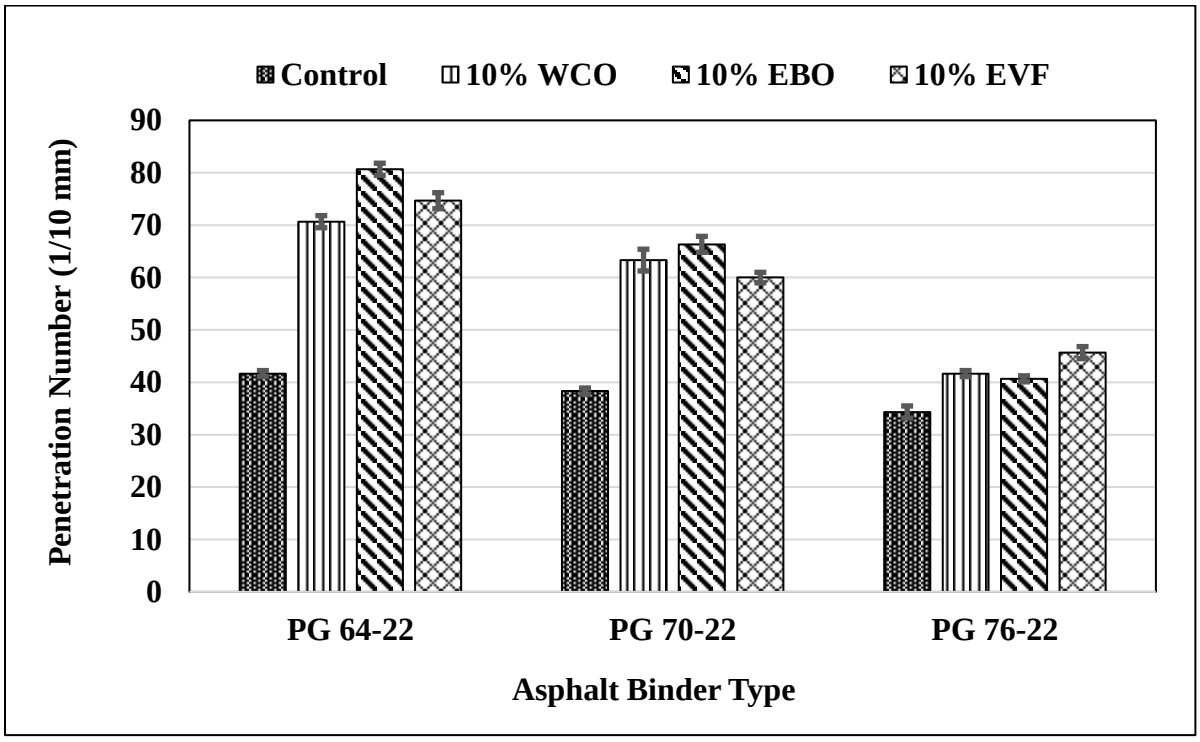

Figure 34. Penetration Test Results of Asphalt Binders from S2.

5.3. Chemical Analysis of Rejuvenated Binders

5.3.1. pH Test Results

Figures 35 and 36 show the pH test results of unrejuvenated and rejuvenated RAP1 binder blends from S1 and S2 are presented respectively. As seen in Figures 35 and 36, pH measurements revealed that the base binder (PG 64-22) from S1 was basic with a pH value of 8.3, whereas that from S2 is acidic. For It was found that the acidity values were increased (as pH decreased) with the addition of WCO and EBO for PG 64-22 and PG 70-22 binders from S1 while the corresponding binders from S1 did not follow this trend. In the case of EVF, these binders showed a significant increment of the pH values, which resulted in a pH value of higher than 7.0 in all cases of S1 and S2 binders except for PG 76-22 S1 binder. Among all rejuvenators, EVF exhibited a higher pH value for binders from both sources.

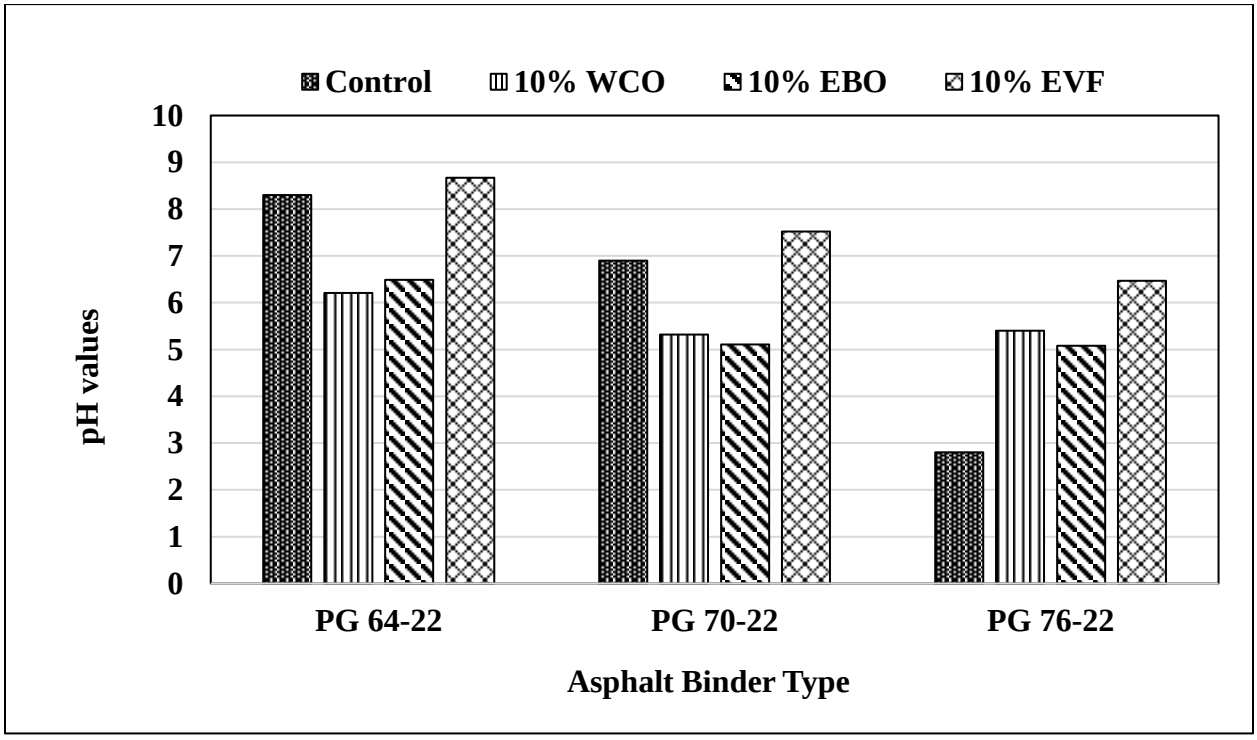

Figure 35. pH test results of Asphalt Binders from S1.

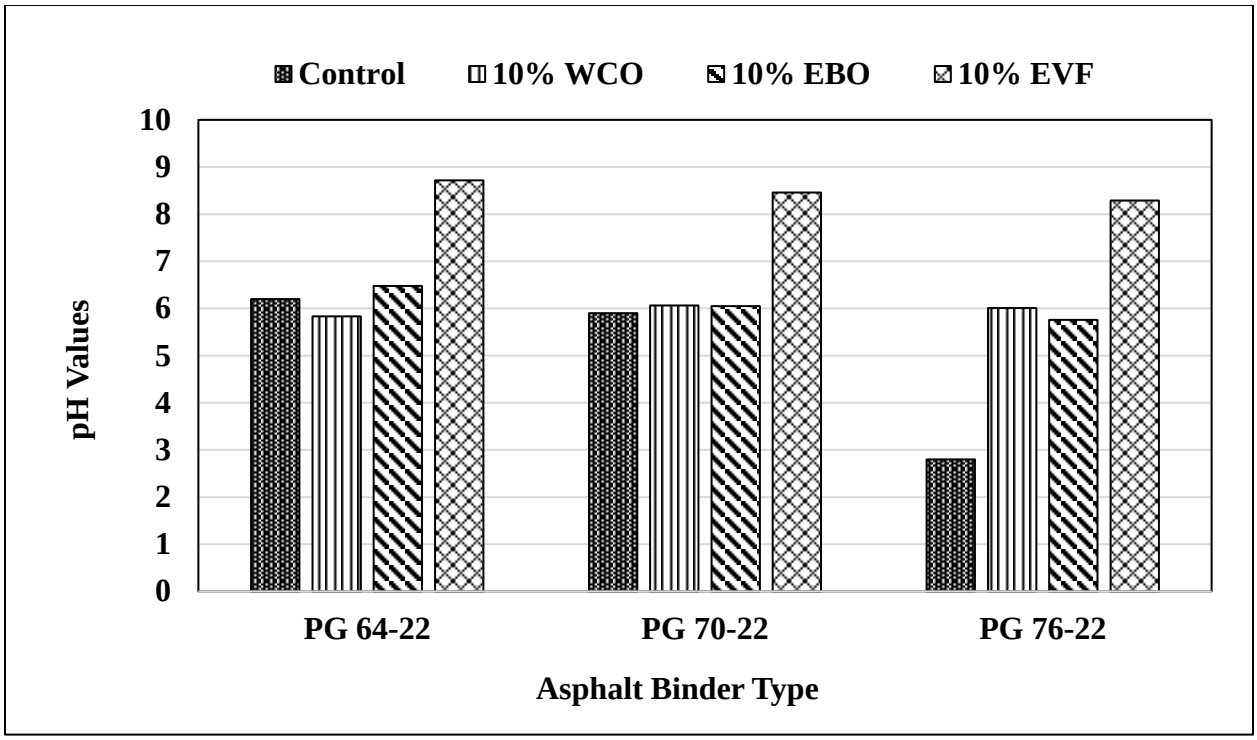

Figure 36. pH test results of Asphalt Binders from S2.

5.3.2. Fourier Transform Infrared Spectroscopy (FTIR) Test Results

The FTIR tests were conducted on unaged rejuvenated binder samples from S1 and S2, shown in Figures 37 and 38, respectively. As seen in these figures, the peak at certain wavenumbers displayed a higher signal, which indicated that the rejuvenations had introduced some increase in certain quantities in the rejuvenated binder samples.

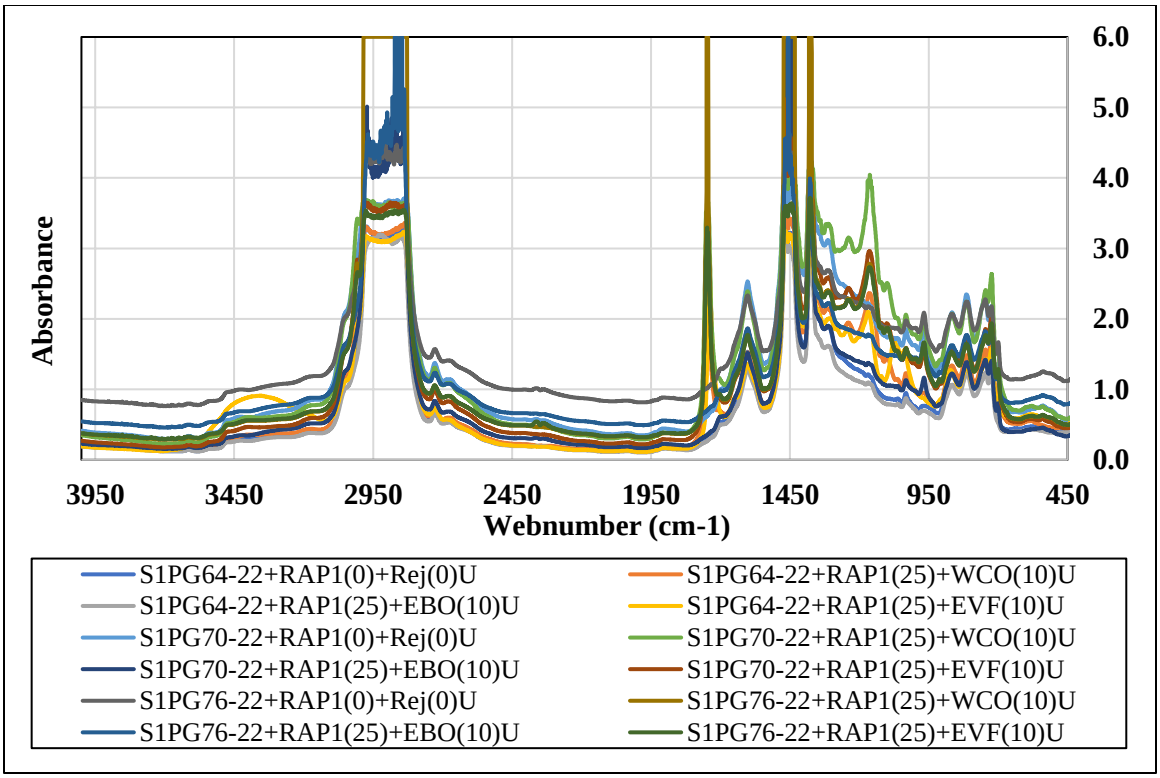

Figure 37. The FTIR Spectra of Rejuvenated RAP1 Binders from S1.

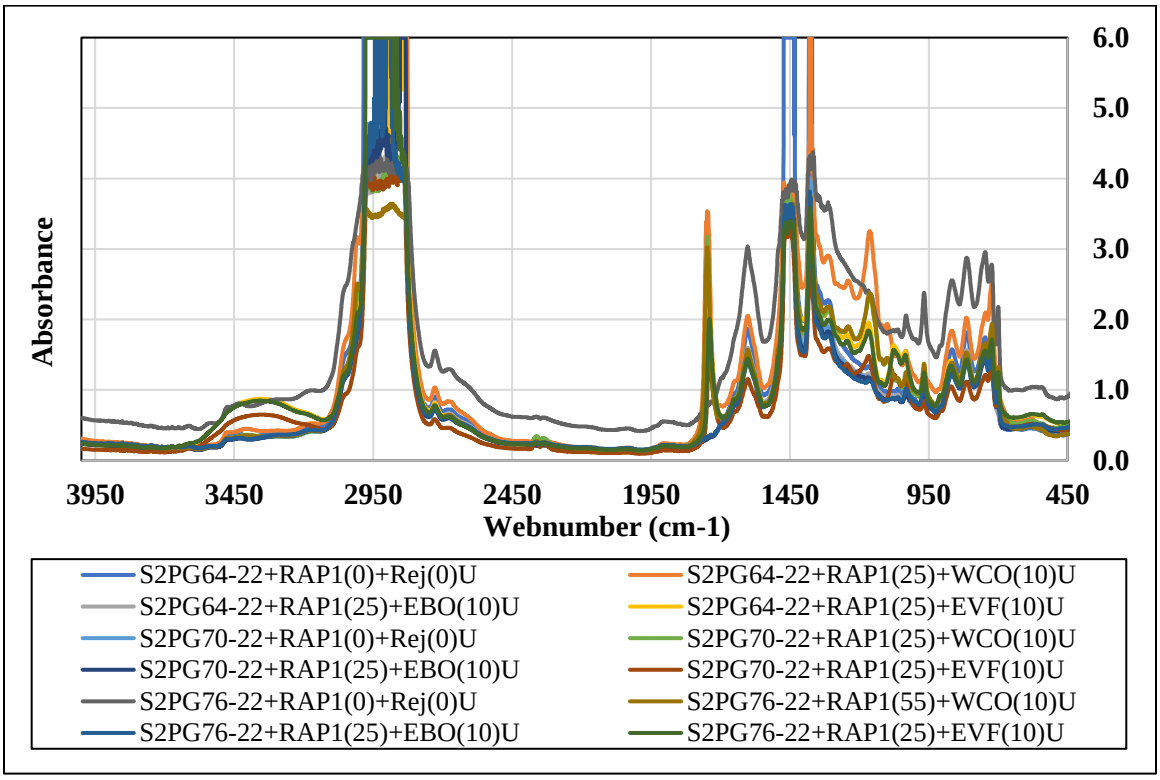

Figure 38. The FTIR Spectra of Rejuvenated RAP1 Binders from S2.

Tables 10 and 11 represent the area under the curve corresponding to the specified three peaks and three indices were calculated using Eqs. (3), (4), and (5) for rejuvenated binders from S1, and S2, respectively. From these tables, it is seen that carbonyl index was found to be increased for the EVF-modified rejuvenated PG 64-22 (S1 and S2) and PG 76-22 (S2) binders; EBO-modified PG 70-22 (S1) and PG 76-22 (S2) binders; and WCO-modified PG 76-22 (S1) binder. It is also found that the sulfoxide index was increased significantly with the addition of EBO in the case of PG 64-22 (S1 and S2) and PG 76-22 (S2) binders. Moreover, the Trans-Butadiene index was found to be increased for EBO-modified PG 76-22 (S1) and PG 64-22 (S2) binders than the control binder.

Table 10. Different Indices Obtained from the FTIR Spectra for Rejuvenated Binders from S1.

Binder Description	**Total Area (2000 cm^{-1} to 650 cm^{-1})**	**Area for Wavenumber (1700 cm^{-1})**	**I (C=O) for Wavenumber (1700 cm^{-1})**	**Area for Wavenumber (1030 cm^{-1})**	**I (S=O) for Wavenumber (1030 cm^{-1})**	**Area for Wavenumber (968 cm^{-1})**	**I (SBS) for Wavenumber (968 cm^{-1})**
S1PG64-22+RAP1(0)+Rej(0)U	987	0.00	*0.0000*	2.22	*0.0022*	2.76	*0.0028*
S1PG64-22+RAP1(25)+WCO(10)U	1251	0.05	*0.0000*	3.70	*0.0030*	2.18	*0.0017*
S1PG64-22+RAP1(25)+EBO(10)U	858	1.58	*0.0018*	3.83	***0.0045***	2.20	*0.0026*
S1PG64-22+RAP1(25)+EVF(10)U	1106	48.08	***0.0435***	3.16	*0.0029*	0.18	*0.0002*
S1PG70-22+RAP1(0)+Rej(0)U	1629	0.00	*0.0000*	3.53	*0.0022*	9.10	*0.0056*
S1PG70-22+RAP1(25)+WCO(10)U	1956	0.22	*0.0001*	3.87	*0.0020*	9.10	*0.0047*
S1PG70-22+RAP1(25)+EBO(10)U	1139	1.56	***0.0014***	2.44	*0.0021*	5.69	*0.0050*
S1PG70-22+RAP1(25)+EVF(10)U	1589	0.18	*0.0001*	3.83	***0.0024***	6.79	*0.0043*
S1PG76-22+RAP1(0)+Rej(0)U	1169	0.00	*0.0000*	2.34	*0.0020*	6.53	*0.0056*
S1PG76-22+RAP1(25)+WCO(10)U	1416	44.99	***0.0318***	1.40	*0.0010*	5.81	*0.0041*
S1PG76-22+RAP1(25)+EBO(10)U	1092	0.54	*0.0005*	2.02	*0.0018*	6.24	***0.0057***
S1PG76-22+RAP1(25)+EVF(10)U	1411	0.28	*0.0002*	2.48	*0.0018*	2.11	*0.0015*

Table 11. Different Indices Obtained from the FTIR Spectra for Rejuvenated Binders from S2.

Binder Description	Total Area (2000 cm^{-1} to 650 cm^{-1})	Area for Wavenumber (1700 cm^{-1})	I (C=O) for Wavenumber (1700 cm^{-1})	Area for Wavenumber (1030 cm^{-1})	I (S=O) for Wavenumber (1030 cm^{-1})	Area for Wavenumber (968 cm^{-1})	I (SBS) for Wavenumber (968 cm^{-1})
S2PG64-22+RAP1(0)+Rej(0)U	1337	0.00	*0.0000*	4.69	*0.0035*	3.24	*0.0024*
S2PG64-22+RAP1(25)+WCO(10)U	1718	0.04	*0.0000*	5.01	*0.0029*	3.84	*0.0022*
S2PG64-22+RAP1(25)+EBO(10)U	1045	0.19	*0.0002*	4.00	***0.0038***	2.81	***0.0027***
S2PG64-22+RAP1(25)+EVF(10)U	1152	4.99	***0.0043***	1.51	*0.0013*	0.33	*0.0003*
S2PG70-22+RAP1(0)+Rej(0)U	996	0.00	*0.0000*	2.91	*0.0029*	5.93	*0.0060*
S2PG70-22+RAP1(25)+WCO(10)U	1247	0.10	*0.0001*	3.23	*0.0026*	5.82	*0.0047*
S2PG70-22+RAP1(25)+EBO(10)U	971	0.51	*0.0005*	3.56	*0.0037*	5.33	*0.0055*
S2PG70-22+RAP1(25)+EVF(10)U	887	0.03	*0.0000*	2.64	*0.0030*	2.12	*0.0024*
S2PG76-22+RAP1(0)+Rej(0)U	1738	0.00	*0.0000*	6.61	*0.0038*	14.24	*0.0082*
S2PG76-22+RAP1(25)+WCO(10)U	1319	0.12	*0.0001*	4.34	*0.0033*	8.25	*0.0063*
S2PG76-22+RAP1(25)+EBO(10)U	941	6.93	***0.0074***	4.22	***0.0045***	6.93	*0.0074*
S2PG76-22+RAP1(25)+EVF(10)U	1085	38.81	***0.0358***	4.02	*0.0037*	4.56	*0.0042*

5.4. Micro-level Test

5.4.1. Atomic Force Microscope (AFM) Test Results

In this study, the AFM tests were conducted to investigate the microscopic surface roughness and the micromechanical properties of the unrejuvenated and rejuvenated binders. Figure 39 represents the surface roughness of rejuvenated PG 76-22 binders from S1. The effect of rejuvenators is seen in the binder's surface morphology by observing the microstructural features (e.g., "bee

structures”). The DMT Modulus and the deformation of rejuvenated PG 76-22 and PG 70-22 binders are shown in Figures 40 and 41, respectively.

The details of microstructural properties such as roughness, the number of phases observed, dominant phase, the appearance of the dispersed phase, wrinkling (dispersed phase), development of new phase, microstructure recovery, the shape of bees, etc. of rejuvenated PG 64-22, PG 70-22, and PG 76-22 binders are presented in Tables 12, 13, and 14, respectively.

From these tables, it is found that three distinct phases namely, (i) dispersed phase or Catana/bee structure), (ii) interstitial phase or peri phase, and (iii) matrix or para phase were presented in control binders. However, the addition of rejuvenators may eliminate these phases and create a new phase on the binder surface. For example, phases (i) and (ii) were found to be disappeared in the case of EVF-modified binders and a new phase consisting of black dots/spot, circular-shaped phase (iv) was generated. Moreover, the wrinkling pattern on the binder surface was missing due to the rejuvenation using the EVF. In most rejuvenated binders, the dispersed phase was found to be dominant with an appearance of well-dispersed along with some clustering. The shapes of the bees were found to be either elliptical or, irregular and conical hill-shaped for control, WCO- and EBO-modified rejuvenated binders while circular-shaped black spots were observed in the case of EVF-modified binders. It is also seen that the surface roughness values were found to be lower in the rejuvenated binders compared to corresponding control binders except for EVF-modified binders. It is also found that the WCO- and EBO-rejuvenated binders were found to be useful in the recovery of microstructures compared to EVF-rejuvenated binders, as depicted in Figure 39.

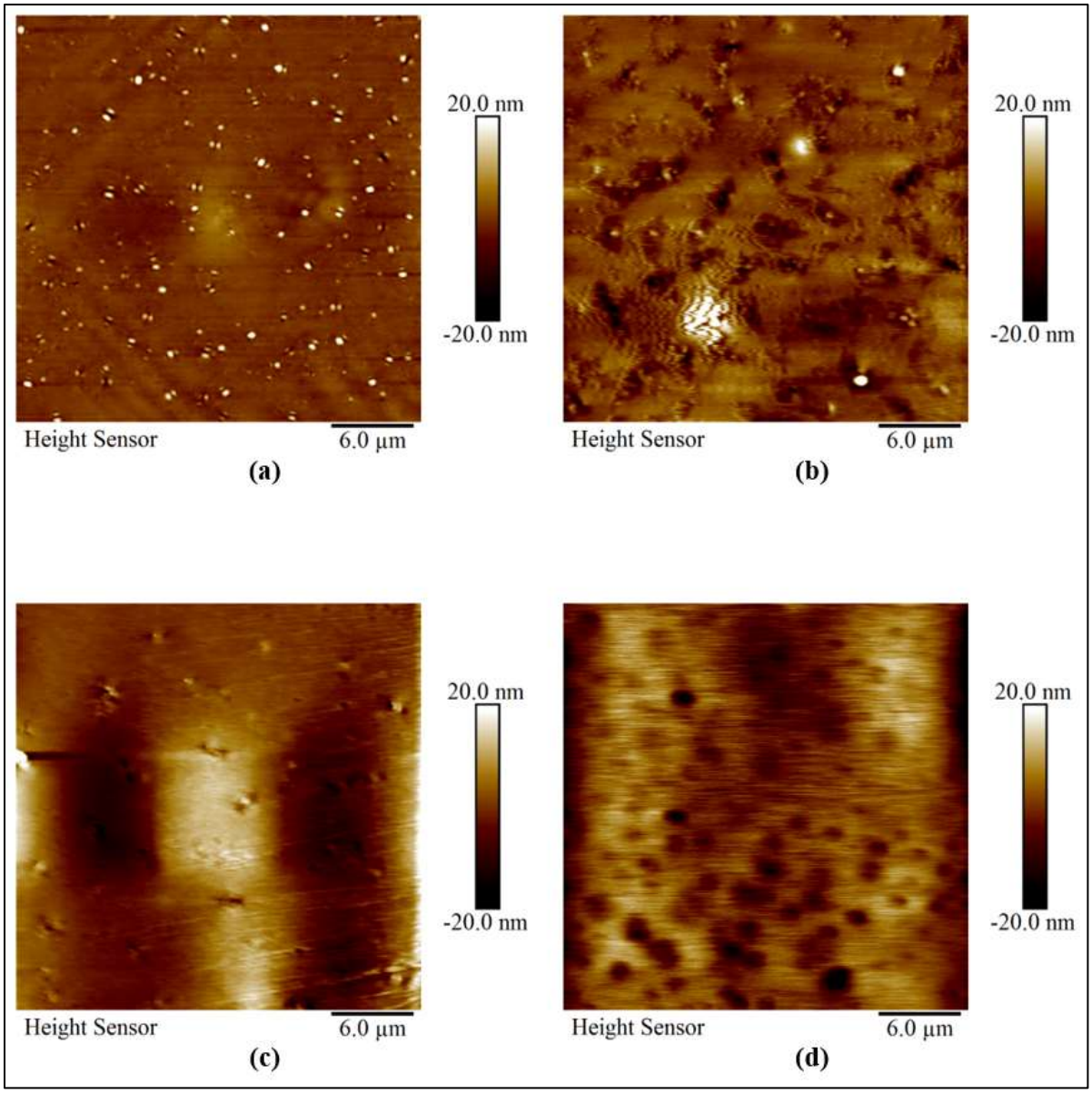

Figure 39. Surface Roughness of Rejuvenated PG 76-22 S1 Binders: (a) S1PG76-22+RAP1(0)+Rej(0)U (unmodified); (b) S1PG76-22+RAP1(25)+WCO(10)U; (c) S1PG76-22+RAP1(25)+EBO(10)U; (d) S1PG76-22+RAP1(25)+EVF(10)U.

Table 12. Qualitative Microstructural Properties of Rejuvenated Binders from S1: PG 64-22.

Microstructural Features	**S1PG64-22+RAP1(0)+Rej(0)U**	**S1PG64-22+RAP1(25)+WCO(10)U**	**S1PG64-22+RAP1(25)+EBO(10)U**	**S1PG64-22+RAP1(25)+EVF(10)U**
Roughness (Rq) (nm)	3.08	9.52	4.19	9.36
Number of Phases* observed	3 (i+ii+iii)	2 (i+iii)	2 (iii+iv)	3 (i+ii+iii)
Dominant Phase	Dispersed phase	Dispersed phase	Matrix phase	Dispersed phase
Appearance of Dispersed Phase	Well dispersed, some clustering	Well dispersed, some clustering	Isolated	Well dispersed, some clustering
Wrinkling (Dispersed Phase)	Present	Present	Present	Present
Development of New Phase	No	No	(iv)	No
Microstructure Recovery	Control	Yes	No	Yes
Shape of Bees	Elliptical	Irregular hill-shaped	Elliptical	Irregular hill-shaped

Table 13. Qualitative Microstructural Properties of Rejuvenated Binders from S1: PG 70-22.

Microstructural Features	S1PG70-22+RAP1(0)+Rej(0)U	S1PG70-22+RAP1(25)+WCO(10)U	S1PG70-22+RAP1(25)+EBO(10)U	S1PG70-22+RAP1(25)+EVF(10)U
Roughness (Rq) (nm)	2.29	1.99	1.59	4.3
Number of Phases* observed	3(i+ii+iii)	2(i+iii)	3(i+ii+iii)	2(iii+iv)
Dominant Phase	Dispersed phase	Matrix phase	Dispersed phase	Matrix phase
Appearance of Dispersed Phase	Well dispersed, some clustering	Well dispersed, some clustering	Well dispersed, some clustering	Not present
Wrinkling (Dispersed Phase)	Present	Present	Present	Not present
Development of New Phase	No	No	No	(iv)
Microstructure Recovery	Control	Yes	Yes	No
Shape of Bees	Elliptical	Irregular hill-shaped	Elliptical	Circular

Table 14. Qualitative Microstructural Properties of Rejuvenated Binders from S1: PG 76-22.

Microstructural Features	S1PG76-22+RAP1(0)+Rej(0)U	S1PG76-22+RAP1(25)+WCO(10)U	S1PG76-22+RAP1(25)+EBO(10)U	S1PG76-22+RAP1(25)+EVF(10)U
Roughness (Rq) (nm)	2.27	3.92	2.48	5.73
Number of Phases* observed	3(i+ii+iii)	3(i+ii+iii)	3(i+ii+iii)	2(iii+iv)
Dominant Phase	Dispersed phase	Dispersed phase	Dispersed phase	Matrix phase
Appearance of Dispersed Phase	Well dispersed, some clustering	Well dispersed	Well dispersed	Not present
Wrinkling (Dispersed Phase)	Present	Present	Present	No
Development of New Phase	No	No	No	(iv)
Microstructure Recovery	Control	Yes	Yes	No
Shape of Bees	Elliptical	Conical hill-shaped	Elliptical	Circular

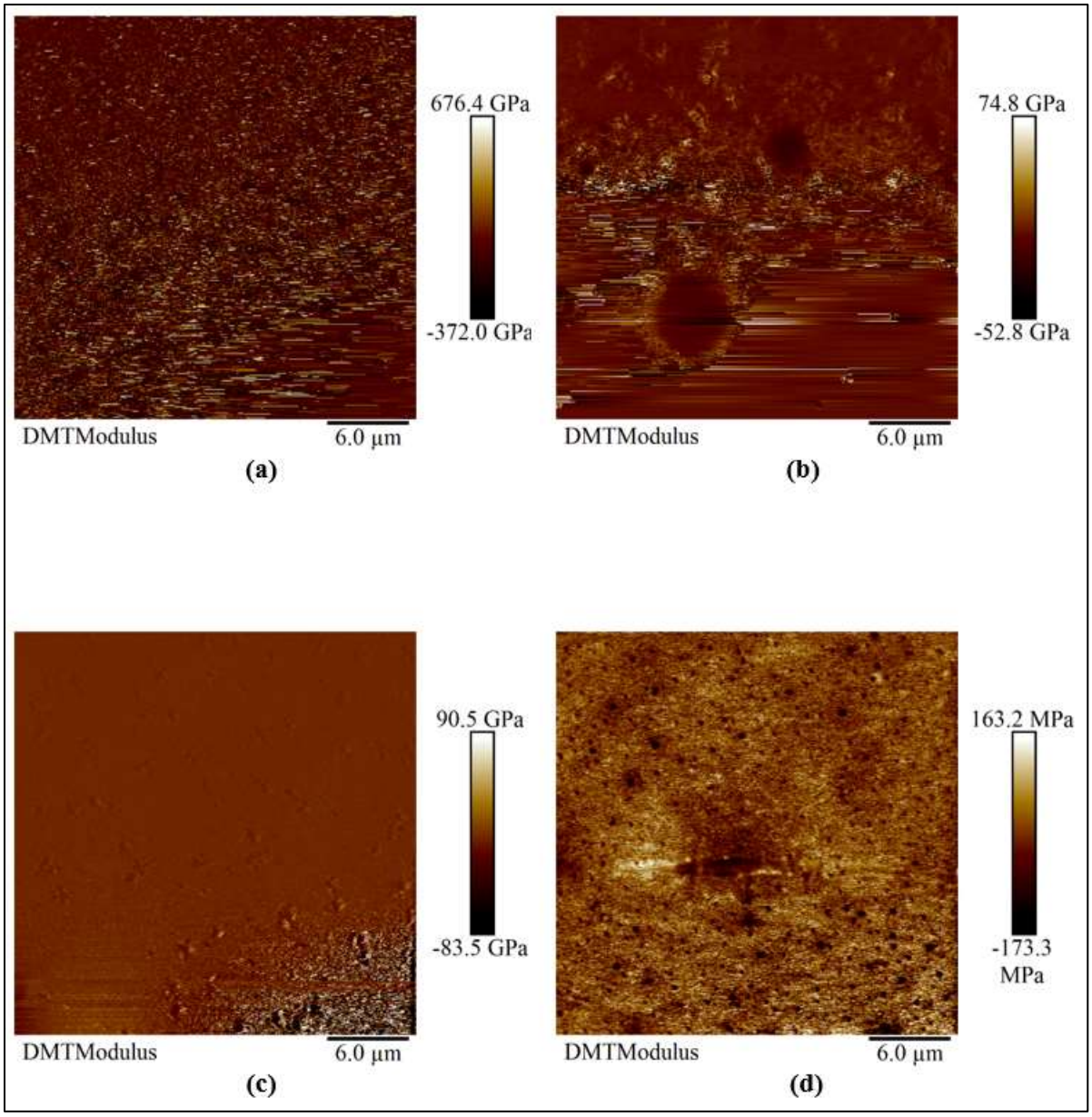

Figure 40. DMT Modulus of Rejuvenated PG 70-22 S1 Binders: (a) S1PG70-22+RAP1(0)+Rej(0)U (unmodified); (b) S1PG70-22+RAP1(25)+WCO(10)U; (c) S1PG70-22+RAP1(25)+EBO(10)U; (d) S1PG70-22+RAP1(25)+EVF(10)U.

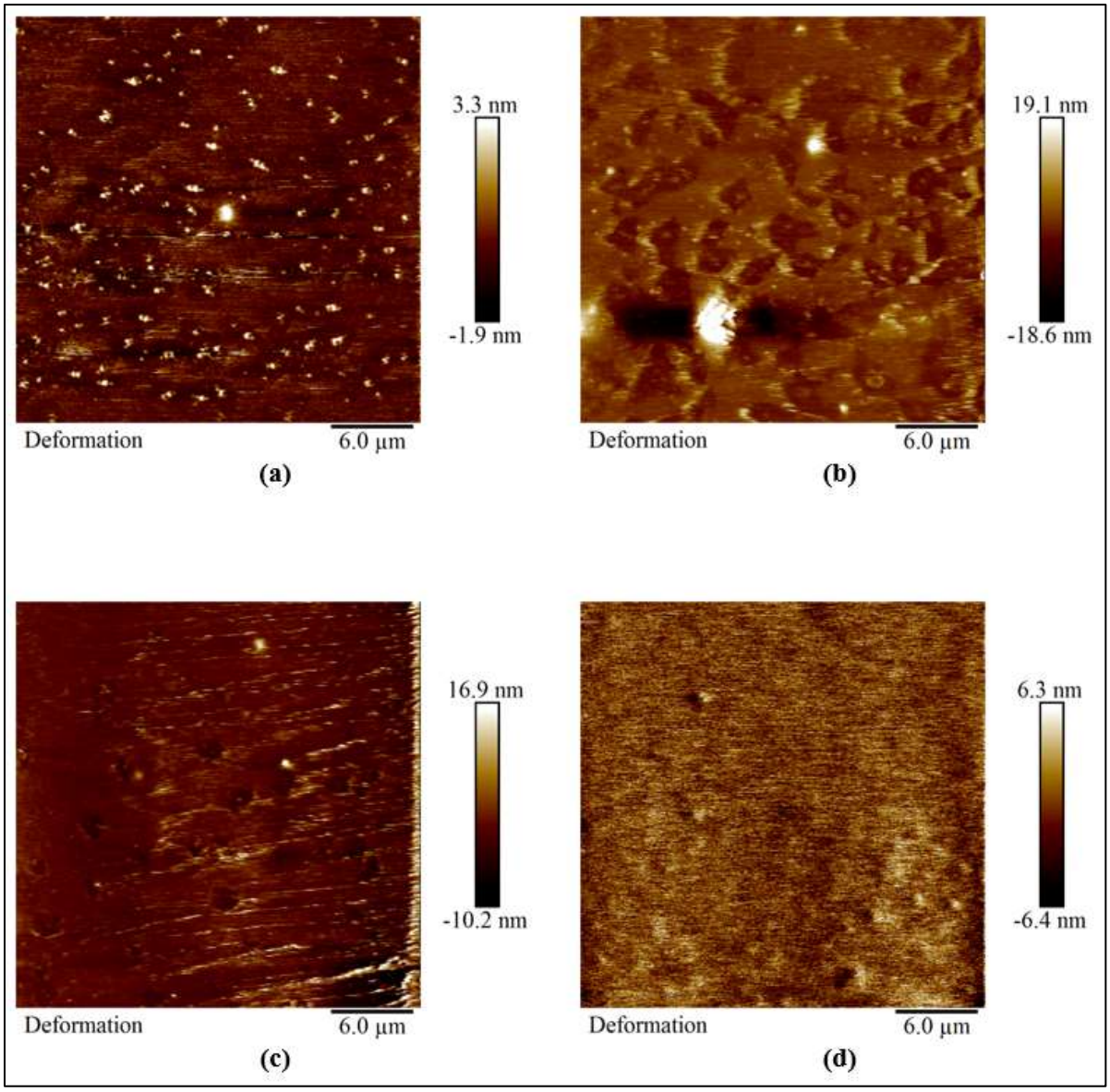

Figure 41. Deformation of Rejuvenated PG 76-22 S1 Binders: (a) S1PG76-22+RAP1(0)+Rej(0)U (unmodified); (b) S1PG76-22+RAP1(25)+WCO(10)U; (c) S1PG76-22+RAP1(25)+EBO(10)U; (d) S1PG76-22+RAP1(25)+EVF(10)U.

Table 15 shows average values of the mechanical properties (e.g., DMT modulus in MPa and deformation in nm) of rejuvenated binder samples from S1. The AFM test results revealed that the average modulus value for the control PG 76-22 binder was 521 MPa, and it varied from 510 MPa to 610 MPa in the dispersed and interstitial phases, whereas it was found to ranging from 450 MPa to 536 MPa in the recessed areas (matrix phase). Due to the increment of RAP contents, the binder blend typically provides higher modulus values than the control binder and it makes the binder stiffer. However, as seen in Table 5, 25% of RAP blends did not show any increment of modulus values because of the rejuvenation of the RAP blends using WCO, EBO, and EVF, which resulted in lower modulus values. Although the decreasing trend had different for each rejuvenator, the least modulus value was found for EVF while WCO had the maximum modulus and EBO had an intermediate modulus between these two rejuvenators irrespective of the binder grades.

From Table 15, it is seen that the average values of deformation for the control PG 76-22 binder were found to be 5.0 nm over the scan area. It is noticed that the overall deformation values of the rejuvenated RAP blends were reduced in all cases. A deformation value of 2.80 nm, 2.93 nm, and 2.99 nm was observed for the WCO-, EBO-, and EVF-modified binder, respectively. However, the deformation of the binders was found to be higher if the corresponding modulus was lower due to the incorporation of rejuvenators.

Table 15. Mechanical Properties of the Rejuvenated RAP1 Binders from S1.

Binder Description	Aging Condition	DMT Modulus (MPa)		Average Deformation (nm)	
		Average	Std. Error	Average	Std. Error
S1PG64-22+RAP1(0)+Rej(0)U	Unaged	132	5.41	11.10	0.59
S1PG64-22+RAP1(25)+WCO(10)U	Unaged	105	4.50	3.77	0.66
S1PG64-22+RAP1(25)+EBO(10)U	Unaged	93	2.67	4.60	0.41
S1PG64-22+RAP1(25)+EVF(10)U	Unaged	77	3.10	7.15	0.66
S1PG70-22+RAP1(0)+Rej(0)U	Unaged	390	8.47	5.97	0.56
S1PG70-22+RAP1(25)+WCO(10)U	Unaged	254	4.13	2.71	0.91
S1PG70-22+RAP1(25)+EBO(10)U	Unaged	205	6.33	1.28	0.62
S1PG70-22+RAP1(25)+EVF(10)U	Unaged	193	6.43	2.04	0.22
S1PG76-22+RAP1(0)+Rej(0)U	Unaged	521	11.57	5.0	0.59
S1PG76-22+RAP1(25)+WCO(10)U	Unaged	406	8.45	2.80	0.71
S1PG76-22+RAP1(25)+EBO(10)U	Unaged	366	10.22	2.93	0.86
S1PG76-22+RAP1(25)+EVF(10)U	Unaged	327	6.74	2.99	0.62

5.4.2. Scanning Electron Microscope (SEM) Test Results

In this study, the SEM tests were conducted on selected rejuvenated binders to observe the effects of rejuvenators in the binders' surface morphology and microstructures. Figure 42 shows the surface morphology image of the base and 10% WCO rejuvenated PG 64-22 S1 binders obtained from the SEM tests. As seen in Figures 42 and 43, the surface of the base binder is not noticeably

changed compared to the WCO-modified binder due to the rejuvenation. Since EBO did not exhibit favorable rheological properties, it was not considered in the SEM study yet. However, the research team intends to conduct additional SEM tests of some other binder blends and report accordingly.

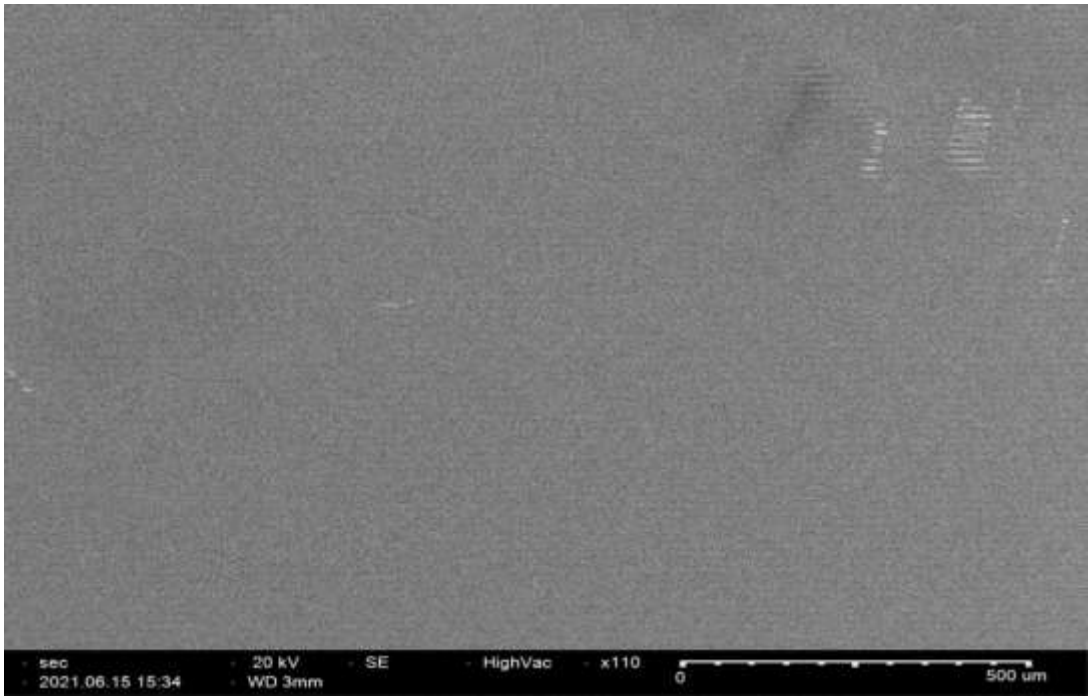

Figure 42. The SEM Image of the Base Binders from S1: PG 64-22.

Figure 43. SEM Image of the WCO-Rejuvenated Asphalt Binder from S1: PG 64-22.

5.5. Mixture Test and Field Performance Evaluations

5.5.1. Texas Boiling Test (TBT) Results

The TBT results of the unrejuvenated and rejuvenated RAP blends from S1 and S1 are shown in Figures 44, and 45, respectively. In this test, the moisture damage potentials of the asphalt mixture were determined based on the percentage of the asphalt retention, through visual observation as per the TTI guidelines.

As seen in Figures 44 and 45, it is found that EBO-modified binders had a lower percentage of asphalt retention, irrespective of binder grades, among all rejuvenated binders used in this study. A similar percentage of asphalt retention was found for PG 64-22 and PG 70-22 binders from S1 in the cases of WCO- and EVF-modified binder blends. For PG 76-22 S1 binders rejuvenated with WCO showed a higher asphalt retention rate (80%) than EVF (70%). Moreover, it is noticed that there is a similar pattern in asphalt binder retention after boiling in the cases of both S1 and S2 binders. Based on the TBT results, it can be concluded that the binders rejuvenated using WCO may have higher resistance against moisture damage potential compared to other rejuvenators. Moreover, the TBT results of WCO-rejuvenated binders are comparable with that of the engineered rejuvenator (EVF), especially for RAP-modified PG 64-22 and PG 70-22 binders from S1.

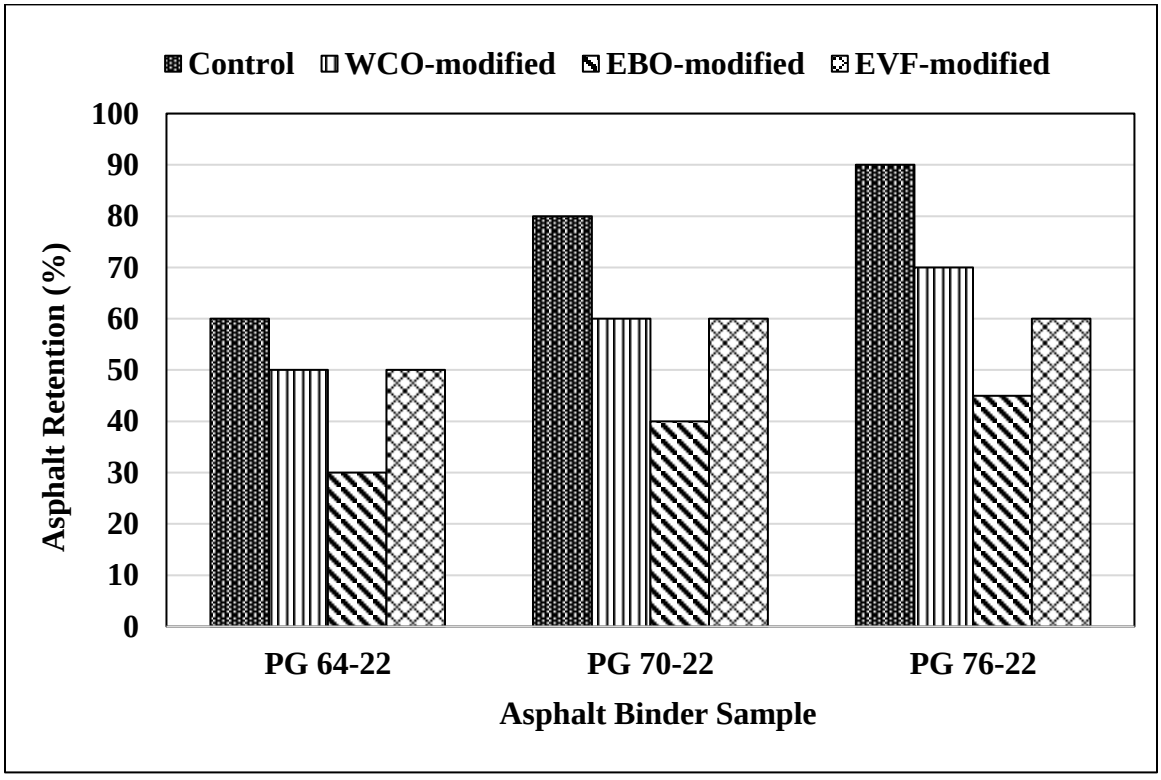

Figure 44. Texas Boiling Test Results of Rejuvenated Binders from S1.

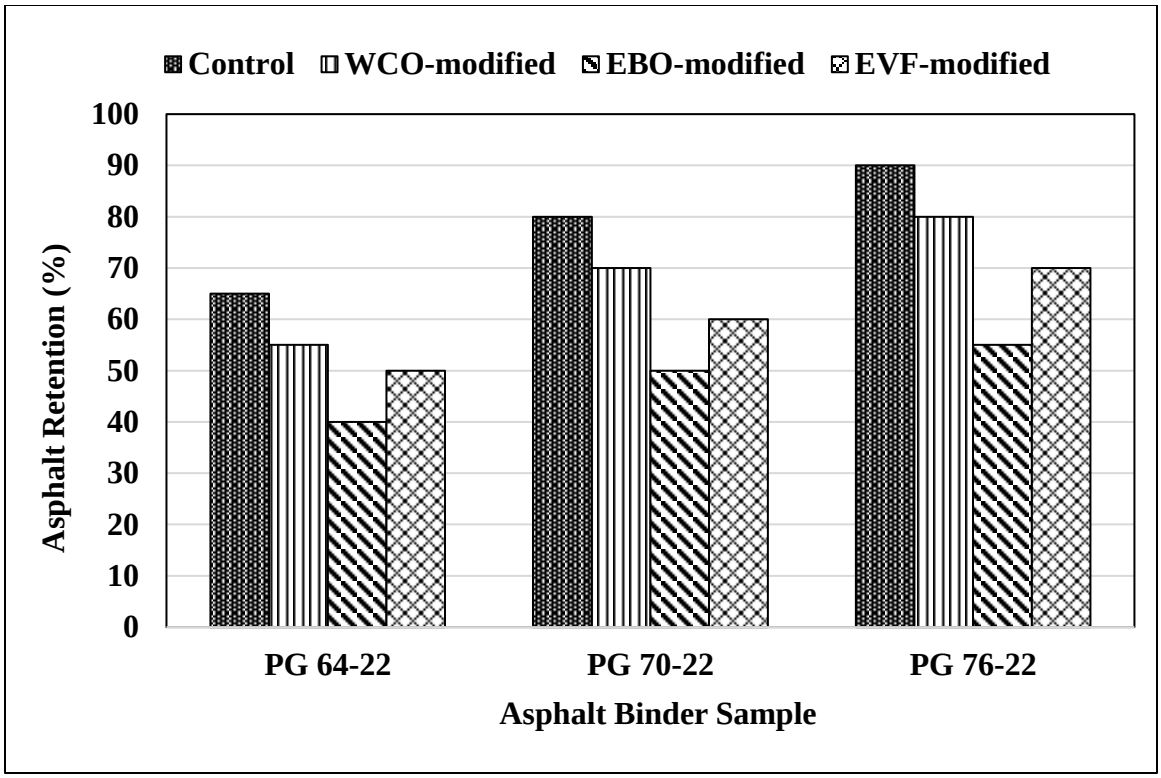

Figure 45. Texas Boiling Test Results of Rejuvenated Binders from S2.

5.5.2. Volumetric Properties and Retained Stability Test Results of Plant Mixes

Two mix designs containing 25% RAP (high RAP) for paving of "12.5 MM ACHM Surface" were collected from a local plant, namely, Delta Asphalt of Arkansas, Inc., located at Paragould, AR. One mix design is identified as WMA019-21 while the other is HMA037-21. From the mix designs, the retained stability of 96.5% and 98.8% were found for the design mix of WMA019-21, and HMA037-21, respectively. Both mixes used 0.25% NovaGrip 975 from Road Science, Division of ArrMaz as an anti-stripping agent. WMA019-21 used a PG 64-22 binder from Heartland Asphalt Materials New Madrid, MO. On the other hand, HMA037-21 used a PG 70-22 binder from Ergon Asphalt and Emulsion, Inc. Memphis, TN.

The plant-produced asphalt mixture samples were collected from the plant sites for laboratory evaluation. Table 16 shows some of the major volumetric properties of mixes such as maximum theoretical specific gravity (Gmm), Bulk specific gravity (Gmb), air content, voids in mineral aggregates (VMA), and voids filled with asphalt (VFA), and retained stability data.

Table 16. Summary of Field Mixture Designs collected from the Local Plant.

Mix Design Number	Mixing Temp. ^{o}C (F)	Compaction Temp. ^{o}C (F)	Asphalt Content (%)	Gmm	Gmb	Va (%)	VMA (%)	VFA (%)	Retained Stability (%)
WMA019-21	137.8 (280)	126.7 (260)	5.2	2.492	2.379	4.0	14.7	72.8	96.5
HMA037-21	160 (320)	146 (295)	5.2	2.495	2.404	4.0	14.8	72.9	98.8

5.5.3. Compressive Strength Test Results

The plant-produced asphalt mixture samples were used to conduct the compressive strength test on the compacted cylindrical asphalt specimens of 6” dia. and 6” height produced by using a Superpave Gyratory compactor. While preparing these test specimens the design number of gyrations (Nd) was used. Table 17 shows the compressive strength test results of the compacted HMA specimens. Figures 46 and 47 show the HMA specimens before and after the tests.

Table 17. Compressive Strength Test Results of the Compacted HMA Specimens.

Mix Design Number	Height at Nd	Height at Nm	Compressive Strength (MPa)
WMA019-21	75	115	5.58
HMA037-21	100	160	6.00

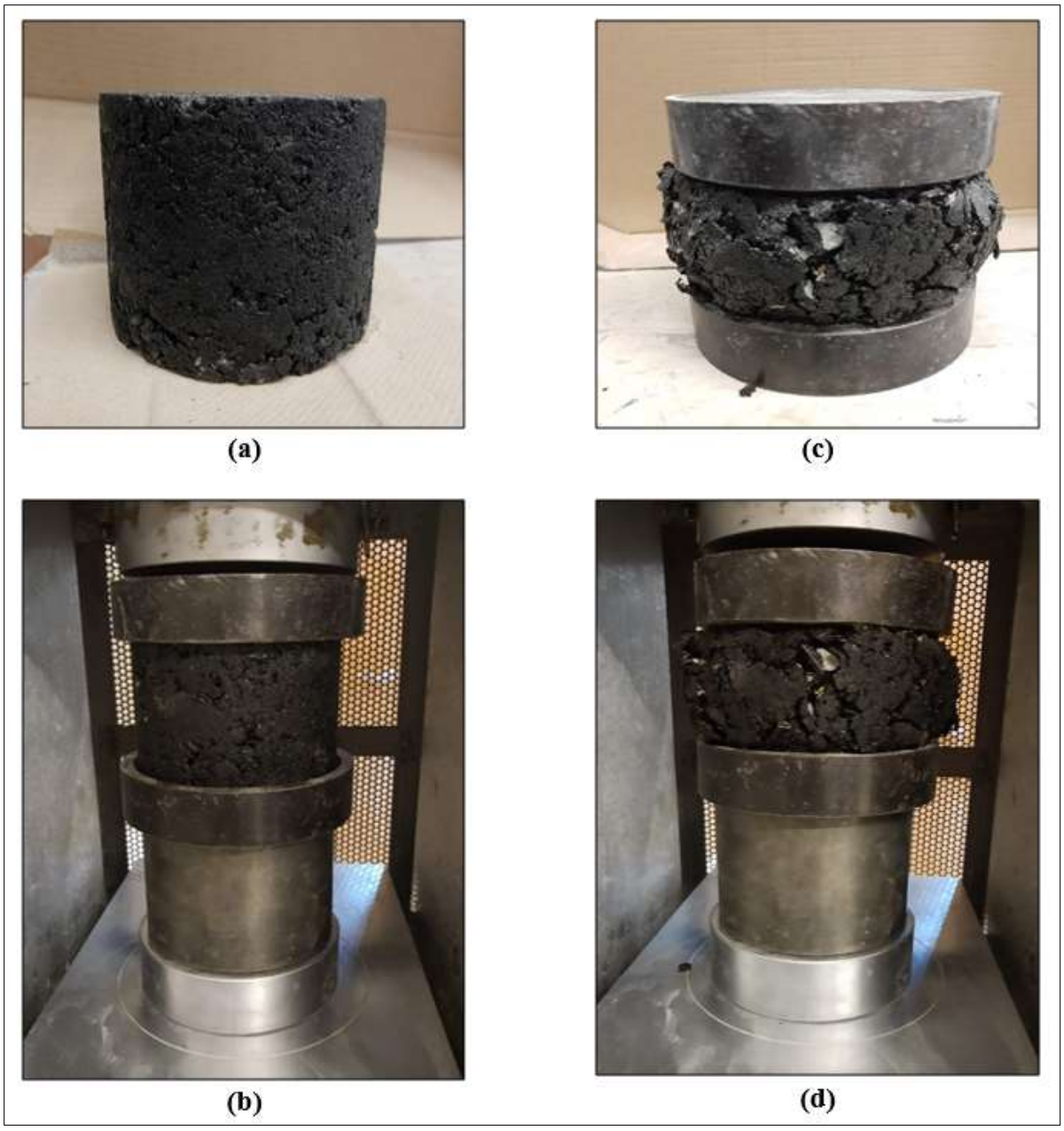

Figure 46. (a)-(b) Before and (c)-(d) After the Compressive Strength Test on Compacted HMA Specimens from Mix Design of WMA019-21

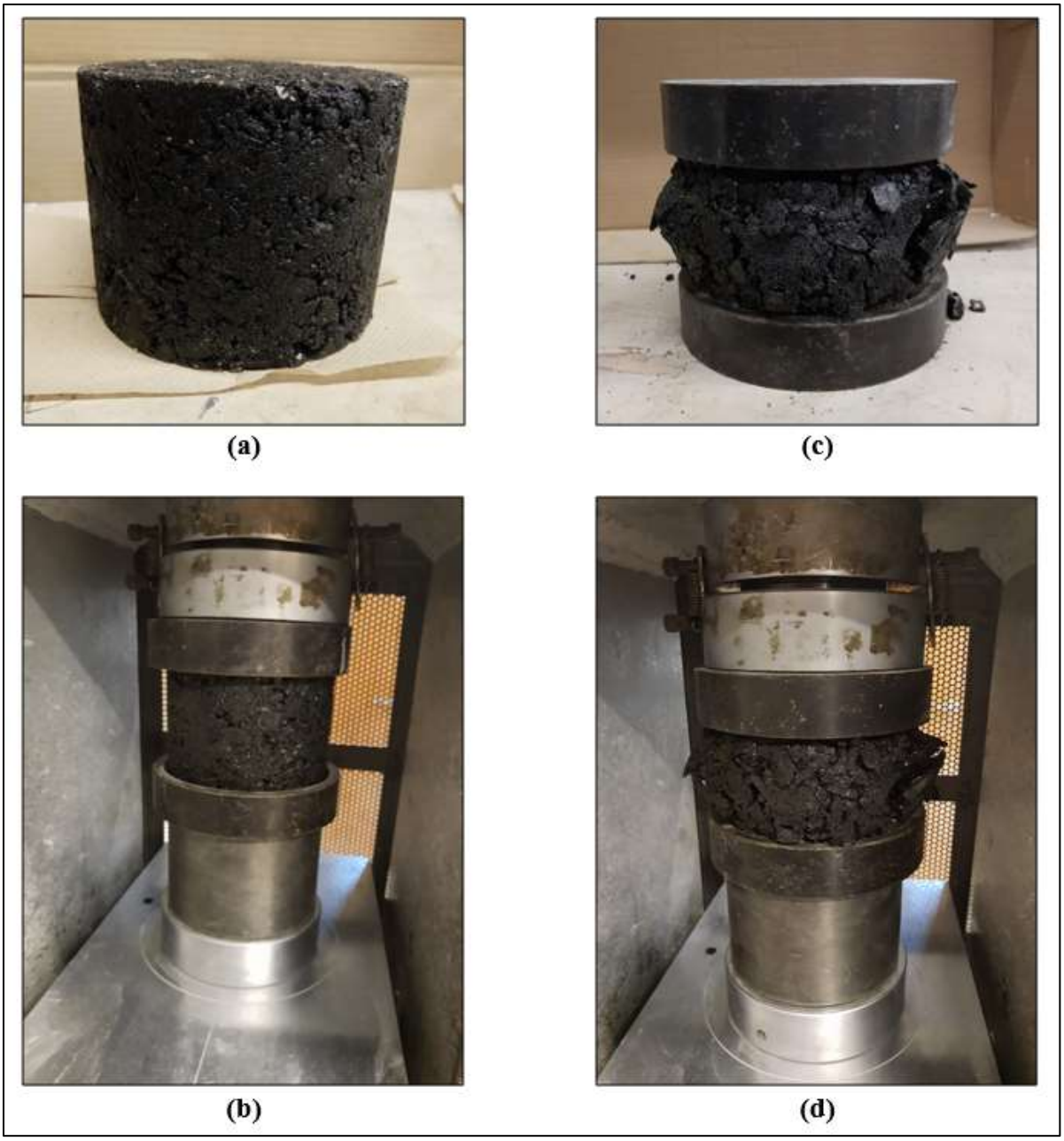

Figure 47. (a)-(b) Before and (c)-(d) After the Compressive Strength Test on Compacted HMA Specimens from Mix Design of HMA037-21.

5.5.3. Field Performance Evaluations

To observe in-service performance, the PI visited the two construction sites on August 7, 2021. where the 12.5 MM ACHM Surface mixes were placed. Visual observations were made at both job sites as shown in Figures 45 and 46. As mentioned earlier, one mix design is identified as HMA037-21 and placed at US 412 in Paragould, AR (the GPS coordinates for the project are-starts at 36.53050 N, 90.506912 W and ends at 36.059969 N, 90.522011 W) on June 02, 2021, and the other mix is known as WMA019-21 and placed at Anchor Packaging Plant driveway and parking lot (2211 N 12th Ave, Paragould, AR 72450) on June 17, 2021. Both mix designs are

designed by Delta Asphalt of Arkansas, Inc. in Paragould, AR. From visual inspections, both pavement sections appear to perform very well. Another inspection of these test sections will be done toward the end of the implementation phase of the project to observe any sign of premature deterioration.

Figure 48. Project Site after Construction of Design Mix of WMA019-21.

Figure 49. Project Site after Construction of Design Mix of HMA037-21.

6. CONCLUSIONS

The main objective of this study is to evaluate the effectiveness of different softening agents in RAP blended binders' rheological and mechanistic properties. To achieve the goal of this study, both laboratory and field tests were performed. Besides the conventional test methods, some fundamental science-based advanced tests were considered to investigate the properties of rejuvenated asphalt binders at the molecular level.

Asphalt binder samples used for this study were collected from two different sources (S1 and S2). The tested binders included unmodified (PG 64-22) and polymer-modified PG 70-22 and PG 76-22 binders. Two RAP samples were collected with the help of a local contractor in Jonesboro, AR, and they were investigated in this study. One RAP sample was originated from a roadway section on Interstate 555 (I-555) between Marked Tree and I-55 while the other RAP sample was obtained from U.S Highway 67 (Hwy 67) between the Lawrence County line and Hwy 62 in Pocahontas, AR. The collected RAP samples were used for binder recovery and the recovered binders were used in different percent with the PG binders, along with softening agents. Three RAP blends (0%, 15%, 25%, 40%, and 60% by weight) were prepared and tested in this study. To find the rejuvenators effects, two waste-based softening agents such as waste cooking oil (WCO) and engine bottom oil (EBO) were used in addition to a commercially produced rejuvenator (EVF).

To fulfill the objectives of this project, a series of laboratory tests were conducted and test data were analyzed to draw meaningful conclusions and provide recommendations for further study. The performance test also called "Superpave tests" such as Rotational Viscometer, Dynamic Shear Rheometer (DSR), Rolling Thin-Film Oven (RTFO), Pressure-Aging Vessel (PAV), Bending Beam Rheometer (BBR), and Multiple Stress Creep Recovery (MSCR) test were performed to evaluate the rheological properties of the tested binder samples. Additionally, two empirical tests such as penetration and pH test were also included to find the qualitative effects of rejuvenators used in this study. To evaluate the moisture resistance of the asphalt mixtures, the Texas Boiling test (TBT) has been conducted on loose mixture samples in this study. An AFM tool was also used to characterize the microscopic morphology (roughness) and micro-mechanical properties (e.g., adhesion, DMT modulus, and deformation) of the asphalt binders at the molecular level. Furthermore, a Scanning Electron Microscope (SEM) was included in this study to examine the effects of rejuvenators in the binders' surface morphology and microstructures. For the chemical analysis of the rejuvenated binders, this study also included the Fourier Transform Infrared Spectroscopy (FTIR) test to detect the presence of any functional group due to the rejuvenation.

Based on the test results, the following conclusions can be drawn:

1. The penetration test results showed that the increment of rejuvenators increased the penetration values of all blends compared to their corresponding base binders regardless of binder grade and crude source. This result suggested that the rejuvenated binders become softer after rejuvenations.
2. From the pH test results, the acidity level of the rejuvenated binders can be compared and the changes in the pH values in the rejuvenated binders due to their modification can be identified. Based on the pH measurement, the presence of acid, and degree of rejuvenation can be understood tentatively.
3. The dynamic viscosity of the RAP blends reduced significantly due to the addition of the softening agents. Thus, the mixing and compaction temperatures were found to be reduced due to the addition of the rejuvenators. Among three selected softening agents (WCO, EBO, and

EVF), the lowest reduction of mixing (up to 4 ^{o}C) and compaction (up to 12 ^{o}C) temperatures are expected for EBO.

4. As expected, the DSR test results suggest that the rejuvenated binders possess lower rutting factors at a higher testing temperature. Thus, the high PG temperatures of rejuvenated blends are slightly lower than the unrejuvenated counterparts, but they maintain their marketed high PG.
5. The BBR test results showed that the EBO showed the highest stiffness value among all the rejuvenated binders, but the stiffness values are well below the Superpave limit. The m-value data suggest that the rate of stress relaxation is significantly higher for rejuvenated asphalt binders with 25% RAP binder. Thus, the low PG temperatures of these RAP blends would also be slightly lowered when any of the softening agents are used to modify the binder blends.
6. The MSCR test results showed that the percent recovery values were higher for unrejuvenated and rejuvenated PG 76-22 and PG 70-22 binders compared to PG 64-22 binders. The percent recovery values were found to be decreased while increasing the non-recoverable creep compliance values due to the rejuvenation.
7. Based on FTIR test results, EBO increased the three indices significantly compared to WCO and EBO among all rejuvenated binders. The WCO increased the carbonyl index only for the PG 76-22 binder from Source 1.
8. The Atomic Force Microscope (AFM) test results agreed with the Superpave test data. The AFM-based maps showed that the addition of rejuvenators changed the morphologies and nanomechanical properties of the control binders. The AFM-based modulus and deformation values decreased for all rejuvenated binder blends, however, there is no similarity in their decreasing trend.
9. The SEM test results revealed that there is a minor change in binders' surface morphology and microstructures due to the rejuvenation.
10. Based on the Texas Boiling test (TBT), the highest asphalt retention was observed for WCO-modified PG 76-22 binder, whereas EBO showed the least percentage of retention of asphalt binder among all rejuvenators regardless of the binders' grade.
11. An amount of 10% WCO or EBO was found to be effective in RAP-blended binders up to 25% RAP in surface mixes. However, WCO produced more favorable rheological and performance test results than EBO. The test results of the WCO-modified RAP-binder were more comparable with an engineered rejuvenator (EVF).
12. Compared to all tests considered in this study, the TBT is simple, quick, and easy to execute to find the moisture damage potential of the asphalt binders qualitatively. On the other hand, the AFM tool is found to be useful for investigating the rejuvenated asphalt binders' micromorphology and micromechanical properties at the atomic scale qualitatively and quantitatively.

REFERENCES

1. Giustozzi F, Crispino M, Toraldo E, Mariani E. Mix design of polymer-modified and fiber-reinforced warm-mix asphalts with high amount of reclaimed asphalt pavement: achieving sustainable and high-performing pavements. Transportation Research Record. 2015 Jan;2523(1):3-10.
2. Copeland A. Reclaimed asphalt pavement in asphalt mixtures: State of the practice. United States. Federal Highway Administration. Office of Research, Development, and Technology; 2011 Apr 1.
3. Wright Jr F. FHWA recycled materials policy. Federal Highway. 2001.
4. Cavalli MC, Partl MN, Poulikakos LD. Effect of ageing on the microstructure of reclaimed asphalt binder with bio-based rejuvenators. Road Materials and Pavement Design. 2019 Oct 3;20(7):1683-94.
5. Cavalli MC, Partl MN, Poulikakos LD. Measuring the binder film residues on black rock in mixtures with high amounts of reclaimed asphalt. Journal of Cleaner Production. 2017 Apr 15;149:665-72.
6. AHTD. Standard Specifications for Highway Construction, Arkansas State Highway and Transportation Department, 2014 Edition, Little Rock, AR.
7. Ma T, Wang H, Huang X, Wang Z, Xiao F. Laboratory performance characteristics of high modulus asphalt mixture with high-content RAP. Construction and Building Materials. 2015 Dec 30;101:975-82.
8. Mangiafico S, Di Benedetto H, Sauzéat C, Olard F, Pouget S, Planque L. Relations between linear ViscoElastic behaviour of bituminous mixtures containing reclaimed asphalt pavement and colloidal structure of corresponding binder blends. Procedia engineering. 2016 Jan 1;143:138-45.
9. Tang S, Williams RC, Cascione AA. Reconsideration of the fatigue tests for asphalt mixtures and binders containing high percentage RAP. International Journal of Pavement Engineering. 2017 May 4;18(5):443-9.
10. Stimilli A, Virgili A, Canestrari F. Warm recycling of flexible pavements: Effectiveness of Warm Mix Asphalt additives on modified bitumen and mixture performance. Journal of Cleaner Production. 2017 Jul 10;156:911-22.
11. Taylor NH. Life expectancy of recycled asphalt paving. InRecycling of bituminous pavements 1978 Jan. ASTM International.
12. Reyes-Ortiz O, Berardinelli E, Alvarez AE, Carvajal-Muñoz J, Fuentes LG. Evaluation of hot mix asphalt mixtures with replacement of aggregates by reclaimed asphalt pavement (RAP) material. Procedia-Social and Behavioral Sciences. 2012 Oct 3;53:379-88.
13. Zaumanis M, Mallick RB, Frank R. Evaluation of rejuvenator's effectiveness with conventional mix testing for 100% reclaimed Asphalt pavement mixtures. Transportation research record. 2013 Jan;2370(1):17-25.
14. Hugener M, Partl MN, Morant M. Cold asphalt recycling with 100% reclaimed asphalt pavement and vegetable oil-based rejuvenators. Road materials and pavement design. 2014 Apr 3;15(2):239-58.
15. Zaumanis, M., Mallick, R. B., Poulikakos, L., & Frank, R. (2014). Influence of six rejuvenators on the performance properties of Reclaimed Asphalt Pavement (RAP) binder and 100% recycled asphalt mixtures. Construction and Building Materials, 71, 538-550.

16. Shen J, Amirkhanian S, Tang B. Effects of rejuvenator on performance-based properties of rejuvenated asphalt binder and mixtures. Construction and building materials. 2007 May 1;21(5):958-64.
17. Dony A, Colin J, Bruneau D, Drouadaine I, Navaro J. Reclaimed asphalt concretes with high recycling rates: Changes in reclaimed binder properties according to rejuvenating agent. Construction and Building Materials. 2013 Apr 1;41:175-81.
18. Romera R, Santamaría A, Peña JJ, Muñoz ME, Barral M, García E, Jañez V. Rheological aspects of the rejuvenation of aged bitumen. Rheologica acta. 2006 Apr;45(4):474-8.
19. Chen M, Xiao F, Putman B, Leng B, Wu S. High temperature properties of rejuvenating recovered binder with rejuvenator, waste cooking and cotton seed oils. Construction and Building Materials. 2014 May 30;59:10-6.
20. Sun D, Sun G, Du Y, Zhu X, Lu T, Pang Q, Shi S, Dai Z. Evaluation of optimized bio-asphalt containing high content waste cooking oil residues. Fuel. 2017 Aug 15;202:529-40.
21. Majidifard H, Tabatabaee N, Buttlar W. Investigating short-term and long-term binder performance of high-RAP mixtures containing waste cooking oil. Journal of Traffic and Transportation Engineering (English Edition). 2019 Aug 1;6(4):396-406.
22. Cavalli MC, Zaumanis M, Mazza E, Partl MN, Poulikakos LD. Aging effect on rheology and cracking behaviour of reclaimed binder with bio-based rejuvenators. Journal of Cleaner Production. 2018 Jul 10;189:88-97.
23. Loise V, Caputo P, Porto M, Calandra P, Angelico R, Oliviero Rossi C. A review on Bitumen Rejuvenation: Mechanisms, materials, methods and perspectives. Applied Sciences. 2019 Jan;9(20):4316.
24. Król JB, Kowalski KJ, Niczke Ł, Radziszewski P. Effect of bitumen fluxing using a bio-origin additive. Construction and Building Materials. 2016 Jul 1;114:194-203.
25. Somé C, Pavoine A, Chailleux E, Andrieux L, DeMarco L, Da Silva Philippe BS. Rheological behavior of vegetable oil-modified asphaltite binders and mixes. InProceedings of the 6th Eurasphalt & Eurobitume Congress, Prague, Czech Republic 2016 Jun 3 (pp. 1-3).
26. Zargar M, Ahmadinia E, Asli H, Karim MR. Investigation of the possibility of using waste cooking oil as a rejuvenating agent for aged bitumen. Journal of hazardous materials. 2012 Sep 30;233:254-8.
27. Elkashef M, Williams RC, Cochran E. Thermal stability and evolved gas analysis of rejuvenated reclaimed asphalt pavement (RAP) bitumen using thermogravimetric analysis–Fourier transform infrared (TG–FTIR). Journal of Thermal Analysis and Calorimetry. 2018 Feb;131(2):865-71.
28. Zhu H, Xu G, Gong M, Yang J. Recycling long-term-aged asphalts using bio-binder/plasticizer-based rejuvenator. Construction and building materials. 2017 Aug 30;147:117-29.
29. Mokhtari A, Lee HD, Williams RC, Guymon CA, Scholte JP, Schram S. A novel approach to evaluate fracture surfaces of aged and rejuvenator-restored asphalt using cryo-SEM and image analysis techniques. Construction and Building Materials. 2017 Feb 15;133:301-13.
30. Yu X, Zaumanis M, Dos Santos S, Poulikakos LD. Rheological, microscopic, and chemical characterization of the rejuvenating effect on asphalt binders. Fuel. 2014 Nov 1;135:162-71.
31. Kuang D, Yu J, Chen H, Feng Z, Li R, Yang H. Effect of rejuvenators on performance and microstructure of aged asphalt. Journal of Wuhan University of Technology-Mater. Sci. Ed.. 2014 Apr 1;29(2):341-5.

32. Nahar SN, Schmets AJ, Schitter G, Scarpas A. Quantitative nanomechanical property mapping of bitumen micro-phases by peak-force atomic force microscopy. In12th ISAP Conference on 2014 (Vol. 30).
33. Zhang J, Zhang X, Liang M, Jiang H, Wei J, Yao Z. Influence of different rejuvenating agents on rheological behavior and dynamic response of recycled asphalt mixtures incorporating 60% RAP dosage. Construction and Building Materials. 2020 Mar 30;238:117778.
34. Mamun AA, Al-Abdul Wahhab HI. Comparative laboratory evaluation of waste cooking oil rejuvenated asphalt concrete mixtures for high contents of reclaimed asphalt pavement. International Journal of Pavement Engineering. 2020 Sep 18;21(11):1297-308.
35. McGraw J, Iverson D, Schmidt G, Olson J. Selection of an alternative asphalt extraction solvent. 2001 Aug.
36. Hossain Z, Lewis S, Zaman M, Buddhala A, O'Rear E. Evaluation for warm-mix additive-modified asphalt binders using spectroscopy techniques. Journal of Materials in Civil Engineering. 2013 Feb 1;25(2):149-59.
37. Hossain Z, Roy S, Rashid F. Microscopic examination of rejuvenated binders with high reclaimed asphalts. Construction and Building Materials. 2020 Oct 10;257:119490.
38. Alam S, Hossain Z. Changes in fractional compositions of PPA and SBS modified asphalt binders. Construction and building materials. 2017 Oct 15;152:386-93.
39. Roberts FL, Kandhal PS, Brown ER, Lee DY, Kennedy TW. Hot mix asphalt materials, mixture design and construction.
40. McGennis RB, Shuler S, Bahia HU. BACKGROUND OF SUPERPAVE ASPHALT BINDER TEST METHODS. FINAL REPORT. 1994 Jan.
41. Bagchi T, Hossain Z, Rahaman MZ, Baumgardner G. Comparing Micro-and Macro-level Rheological Properties of Polymeric and RAP modified Asphalt Binders. 2021.
42. Hossain Z, Rashid F, Mahmud I, Rahaman MZ. Morphological and nanomechanical characterization of industrial and agricultural waste–modified asphalt binders. International Journal of Geomechanics. 2017 Mar 1;17(3):04016084.
43. Hossain Z, Roy S, Rashid F. Microscopic examination of rejuvenated binders with high reclaimed asphalts. Construction and Building Materials. 2020 Oct 10;257:119490.
44. Rashid F, Hossain Z, Bhasin A. Nanomechanistic properties of reclaimed asphalt pavement modified asphalt binders using an atomic force microscope. International Journal of Pavement Engineering. 2019 Mar 4;20(3):357-65.
45. Roy S, Hossain Z. Nanoscale quantification of moisture susceptibility of paving asphalts. InMATEC Web of Conferences 2019 (Vol. 271, p. 03005). EDP Sciences.
46. Roy S, Hossain Z. Use of molecular-level dissipated energy of asphalt binders to predict moisture effects on pavements. International Journal of Pavement Engineering. 2021 Sep 19;22(11):1351-62.
47. Tarefder RA, Zaman AM. Nanoscale evaluation of moisture damage in polymer modified asphalts. Journal of Materials in Civil Engineering. 2010 Jul;22(7):714-25.
48. Dourado ER, Simao RA, Leite LF. Mechanical properties of asphalt binders evaluated by atomic force microscopy. Journal of microscopy. 2012 Feb;245(2):119-28.
49. Jahangir R, Little D, Bhasin A. Evolution of asphalt binder microstructure due to tensile loading determined using AFM and image analysis techniques. International Journal of Pavement Engineering. 2015 Apr 21;16(4):337-49.
50. Masson JF, Leblond V, Margeson J. Bitumen morphologies by phase-detection atomic force microscopy. Journal of microscopy. 2006 Jan;221(1):17-29.

51. Nahar SN, Mohajeri M, Schmets AJ, Scarpas A, Van de Ven MF, Schitter G. First observation of blending-zone morphology at interface of reclaimed asphalt binder and virgin bitumen. Transportation research record. 2013 Jan;2370(1):1-9.
52. Hossain Ph D Z, Elsayed Ph D A, Bagchi T, Roy S. Assessment of Compatibility of Mineral Aggregates and Binders Used In Highway Construction and Maintenance Projects.
53. Bagchi T, Hossain Z, Rahaman MZ, Baumgardner G. Comparing Micro-and Macro-level Rheological Properties of Polymeric and RAP modified Asphalt Binders. 2021.
54. Mazumder M, Ahmed R, Ali AW, Lee SJ. SEM and ESEM techniques used for analysis of asphalt binder and mixture: A state of the art review. Construction and Building Materials. 2018 Oct 20;186:313-29.
55. Fazaeli H, Amini AA, Nejad FM, Behbahani H. Rheological properties of bitumen modified with a combination of FT paraffin wax (sasobit®) and other additives. Journal of civil Engineering and management. 2016 Feb 17;22(2):135-45.
56. Shirzad S, Hassan MM, Aguirre MA, Mohammad LN, Daly WH. Evaluation of sunflower oil as a rejuvenator and its microencapsulation as a healing agent. Journal of Materials in Civil Engineering. 2016 Nov 1;28(11):04016116.
57. Yildirim Y. Polymer modified asphalt binders. Construction and Building Materials. 2007 Jan 1;21(1):66-72.
58. Pavia DL, Lampman GM, Kriz GS, Vyvyan JA. Introduction to spectroscopy: cengage learning. Ainara López Maestresalas. 2008;153:752.
59. Liu S, Peng A, Wu J, Zhou SB. Waste engine oil influences on chemical and rheological properties of different asphalt binders. Construction and Building Materials. 2018 Dec 10;191:1210-20.
60. Al Alam MS. Chemical Variations and Engineering Implications of Reclaimed Asphalt Pavement and Chemically Modified Asphalt Binders. Arkansas State University; 2017.
61. Kennedy TW, Roberts FL, Lee KW. Evaluation of moisture susceptibility of asphalt mixtures using the Texas Freeze-Thaw Pedestal Test. In Association of Asphalt Paving Technologists Proceedings 1982 (Vol. 51).

APPENDIX A: Rotational Viscosity (mPa.s) Test Results

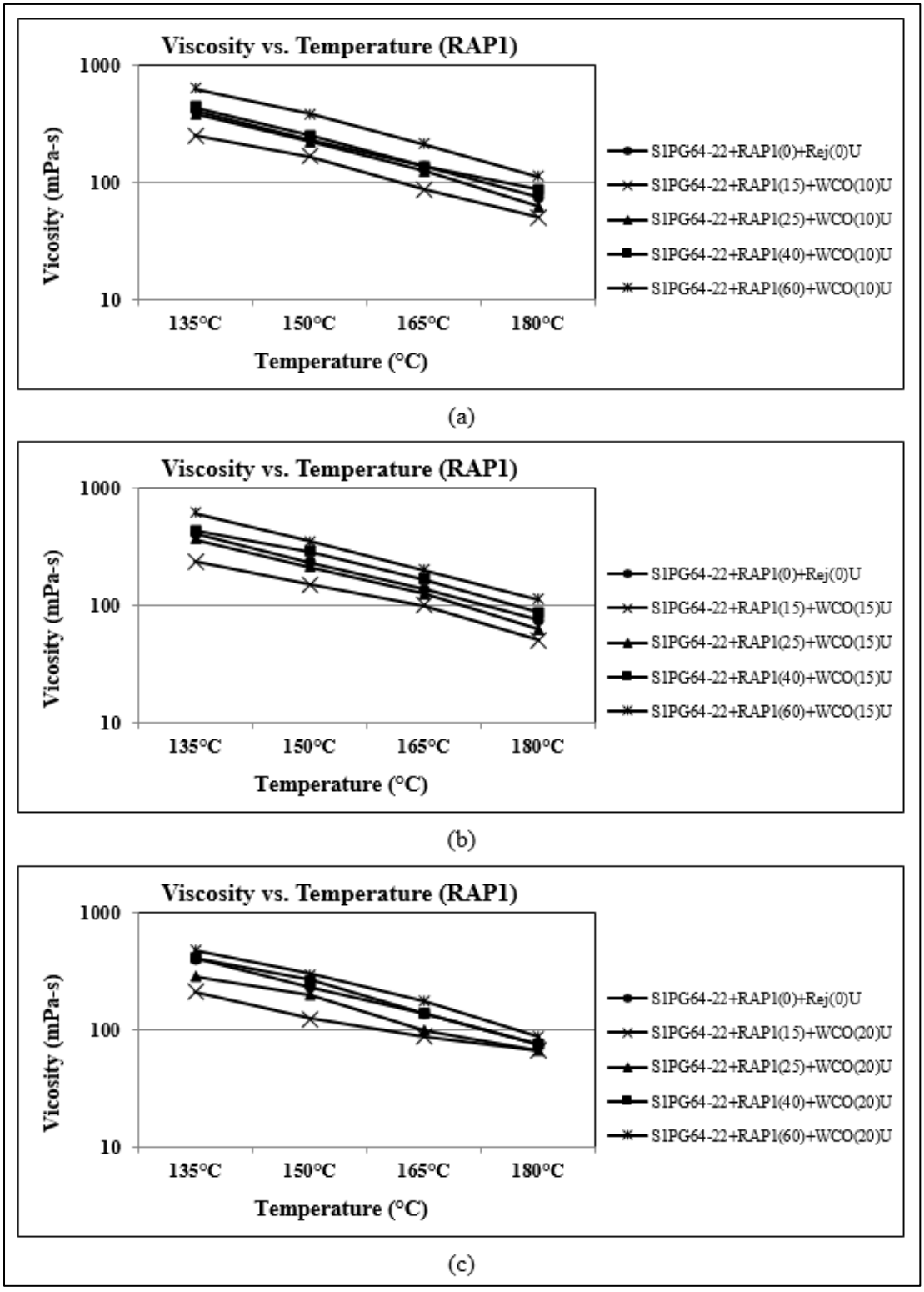

A_Figure 1. Rotational Viscosity (mPa.s) of WCO-Rejuvenated RAP1+PG 64-22 Binders from S1.

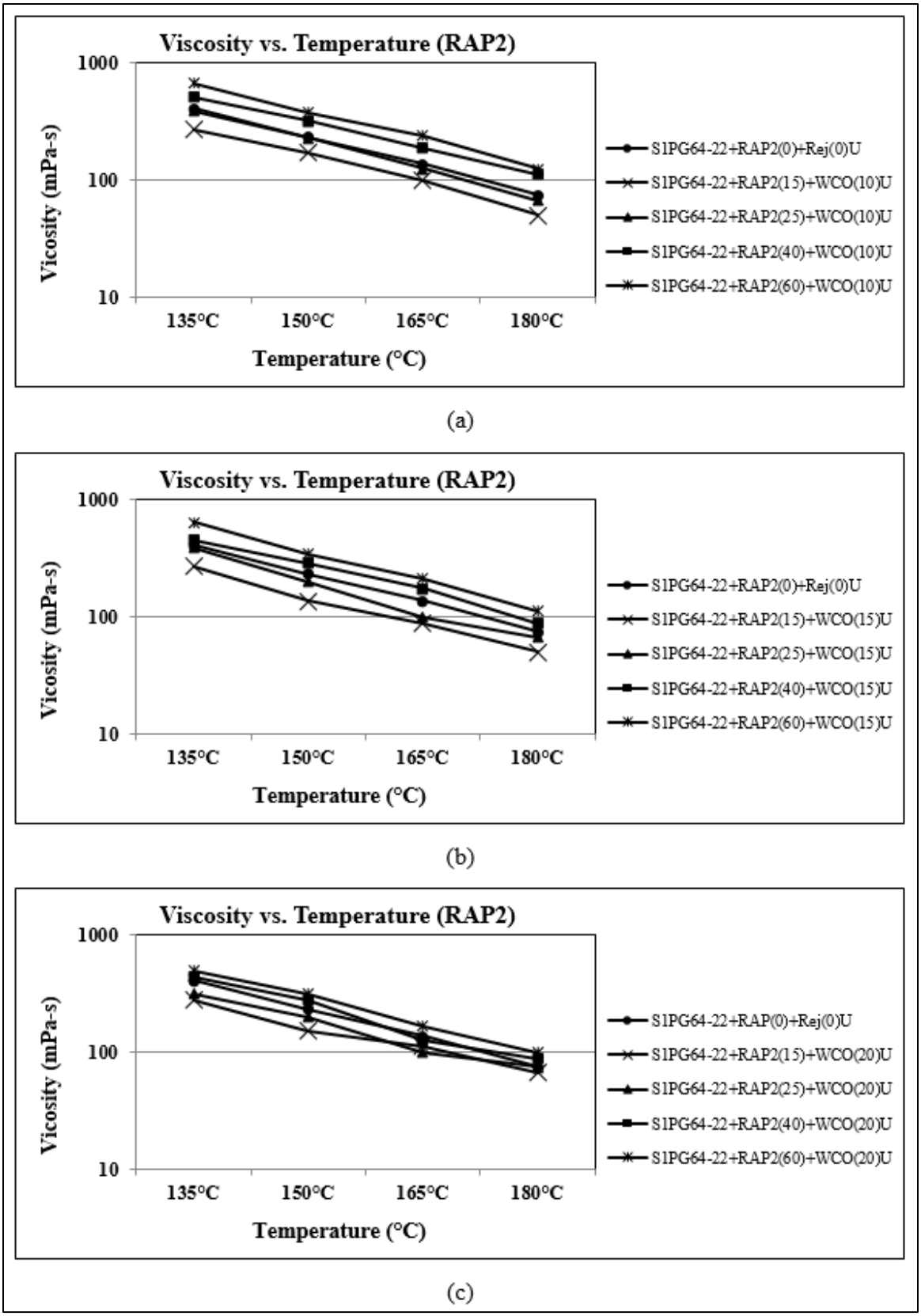

A_Figure 2. Rotational Viscosity (mPa.s) of WCO-Rejuvenated RAP2+PG 64-22 Binders from S1.

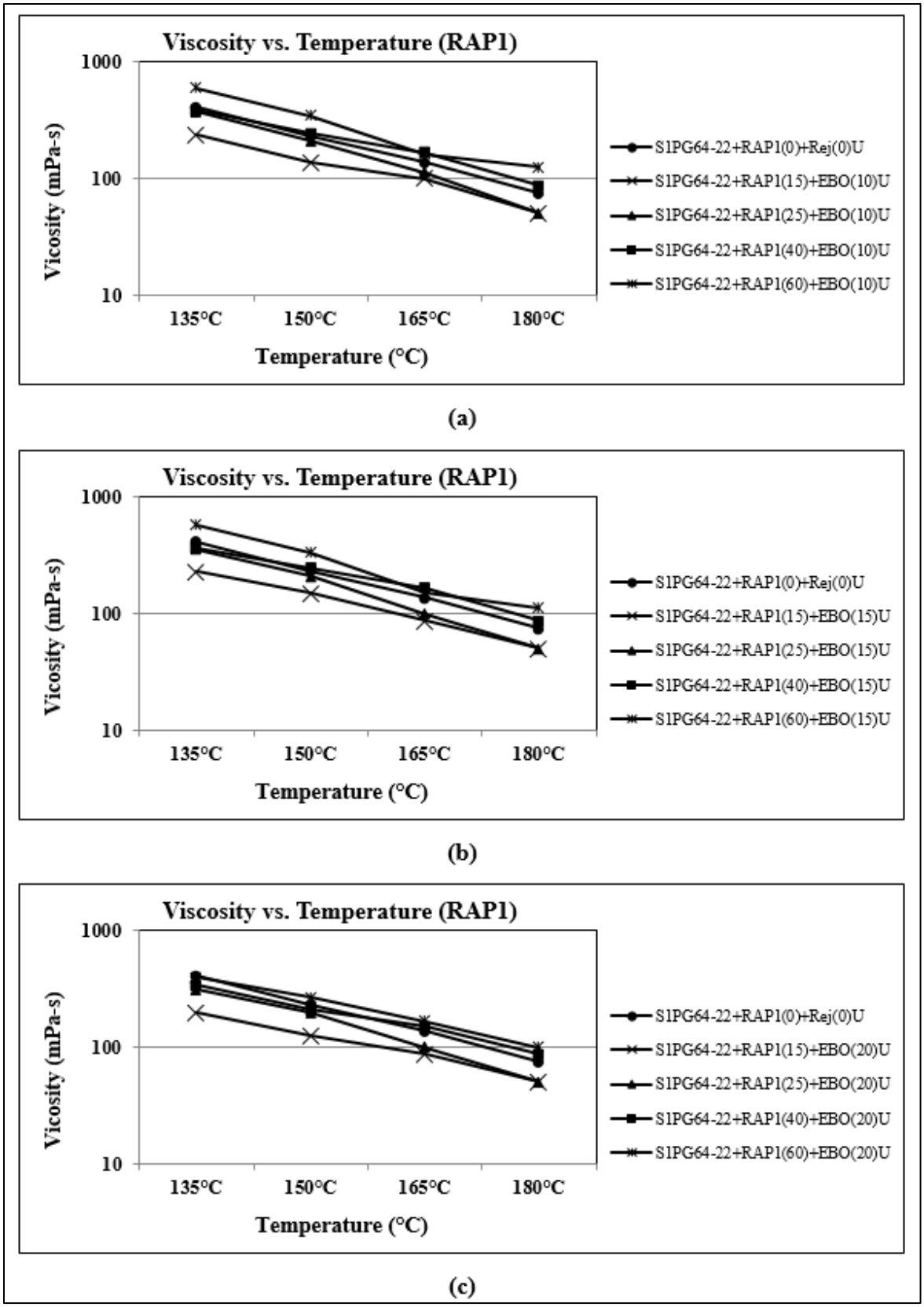

A_Figure 3. Rotational Viscosity (mPa.s) of EBO-Rejuvenated RAP1+PG 64-22 Binders from S1.

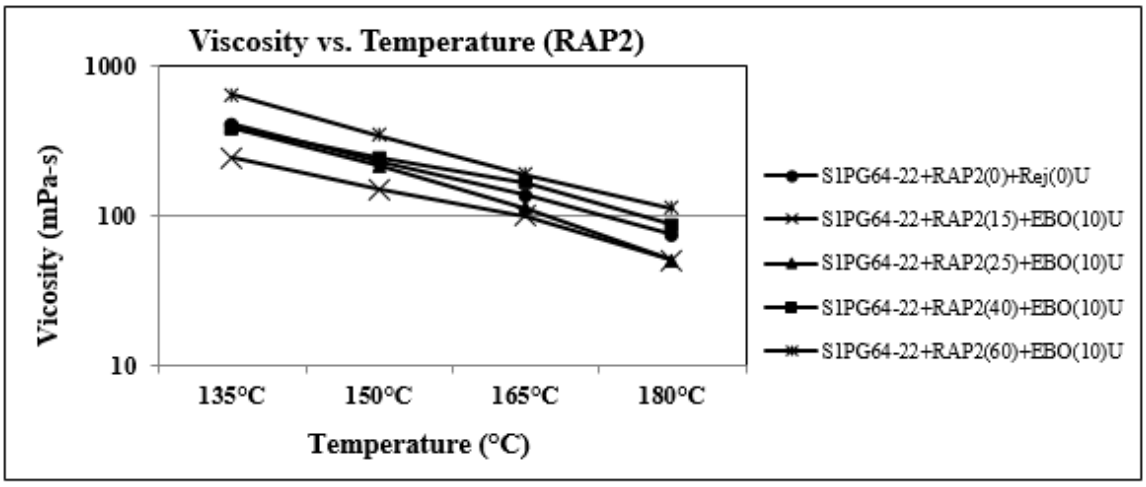

(a)

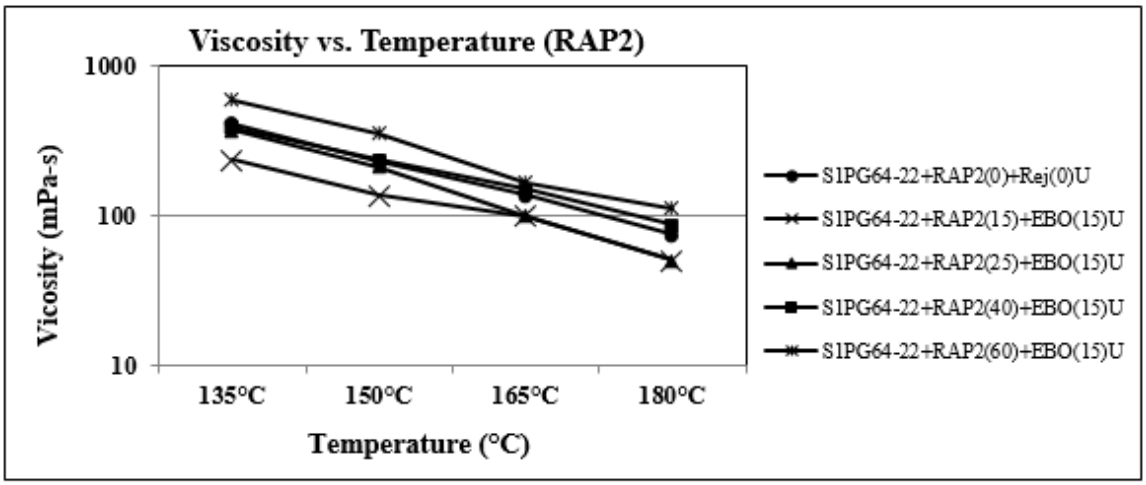

(b)

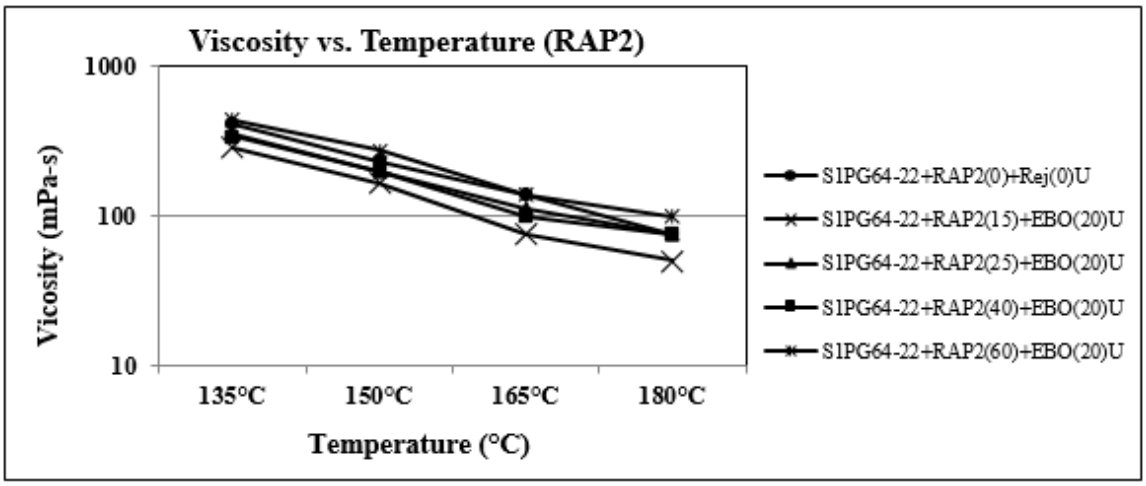

(c)

A_Figure 4. Rotational Viscosity (mPa.s) of EBO-Rejuvenated RAP2+PG 64-22 Binders from S1.

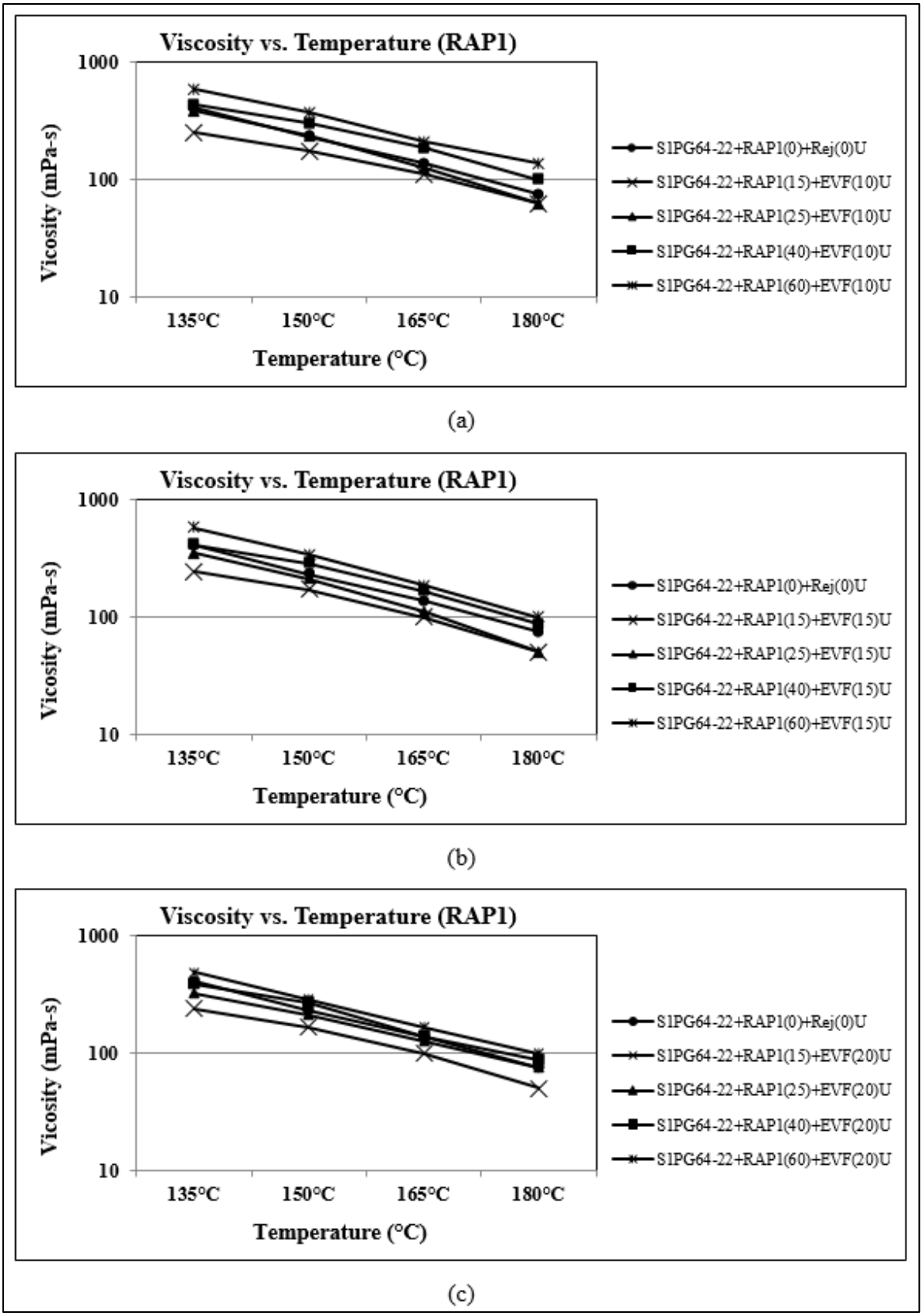

A_Figure 5. Rotational Viscosity (mPa.s) of EVF-Rejuvenated RAP1+PG 64-22 Binders from S1.

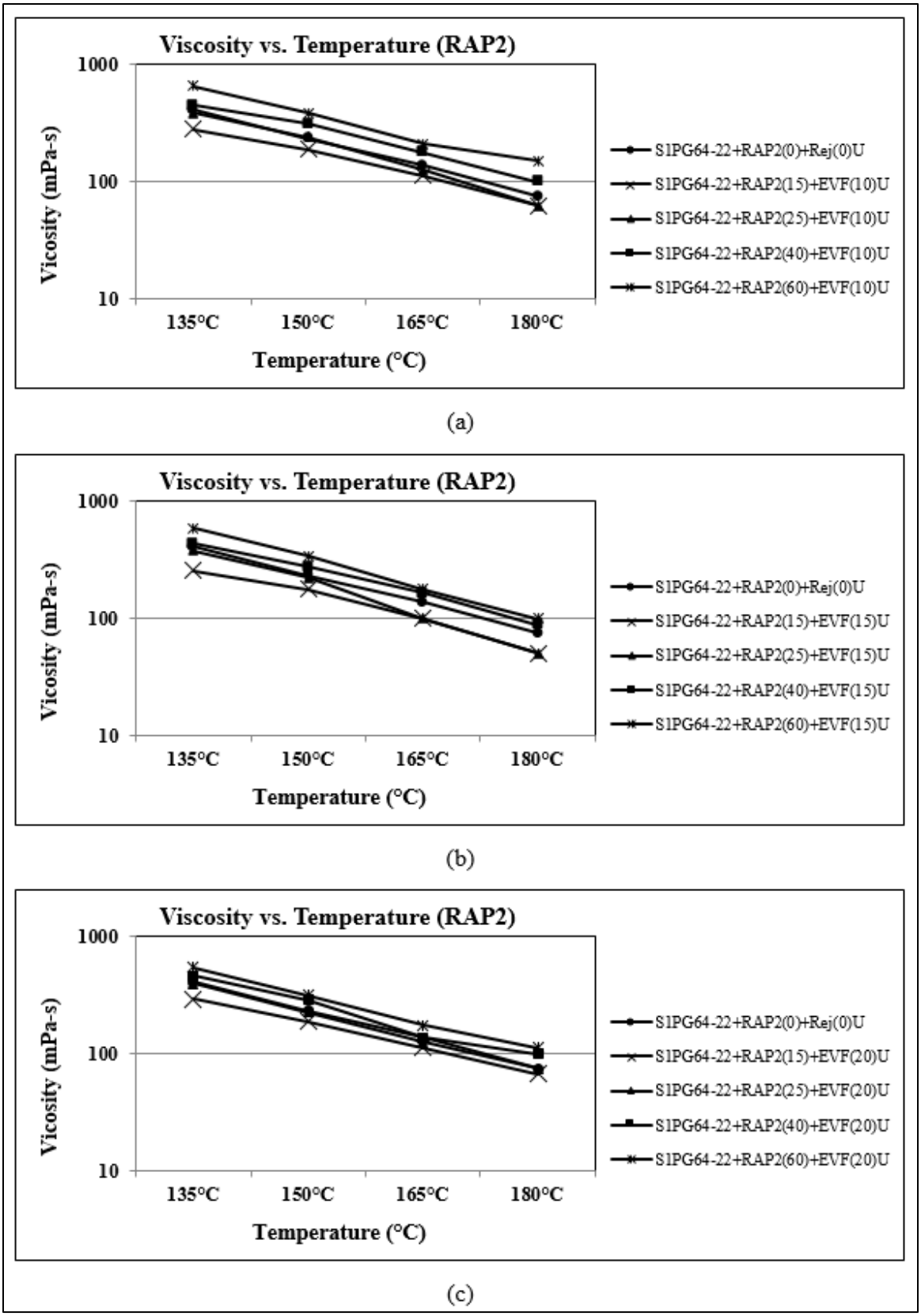

A_Figure 6. Rotational Viscosity (mPa.s) of EVF-Rejuvenated RAP2+PG 64-22 Binders from S1.

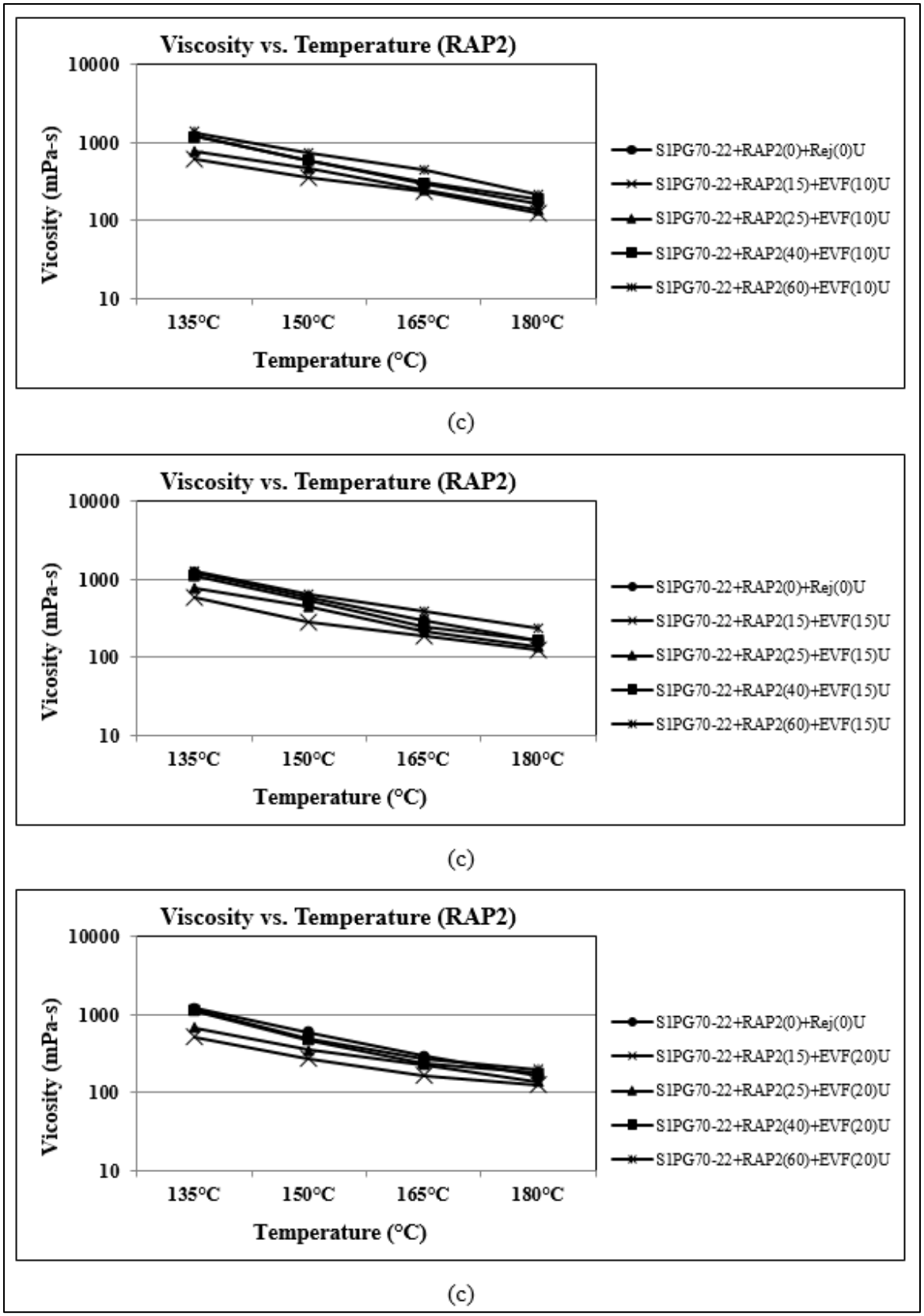

A_Figure 7. Rotational Viscosity (mPa.s) of EVF-Rejuvenated RAP2+PG 70-22 Binders from S1.

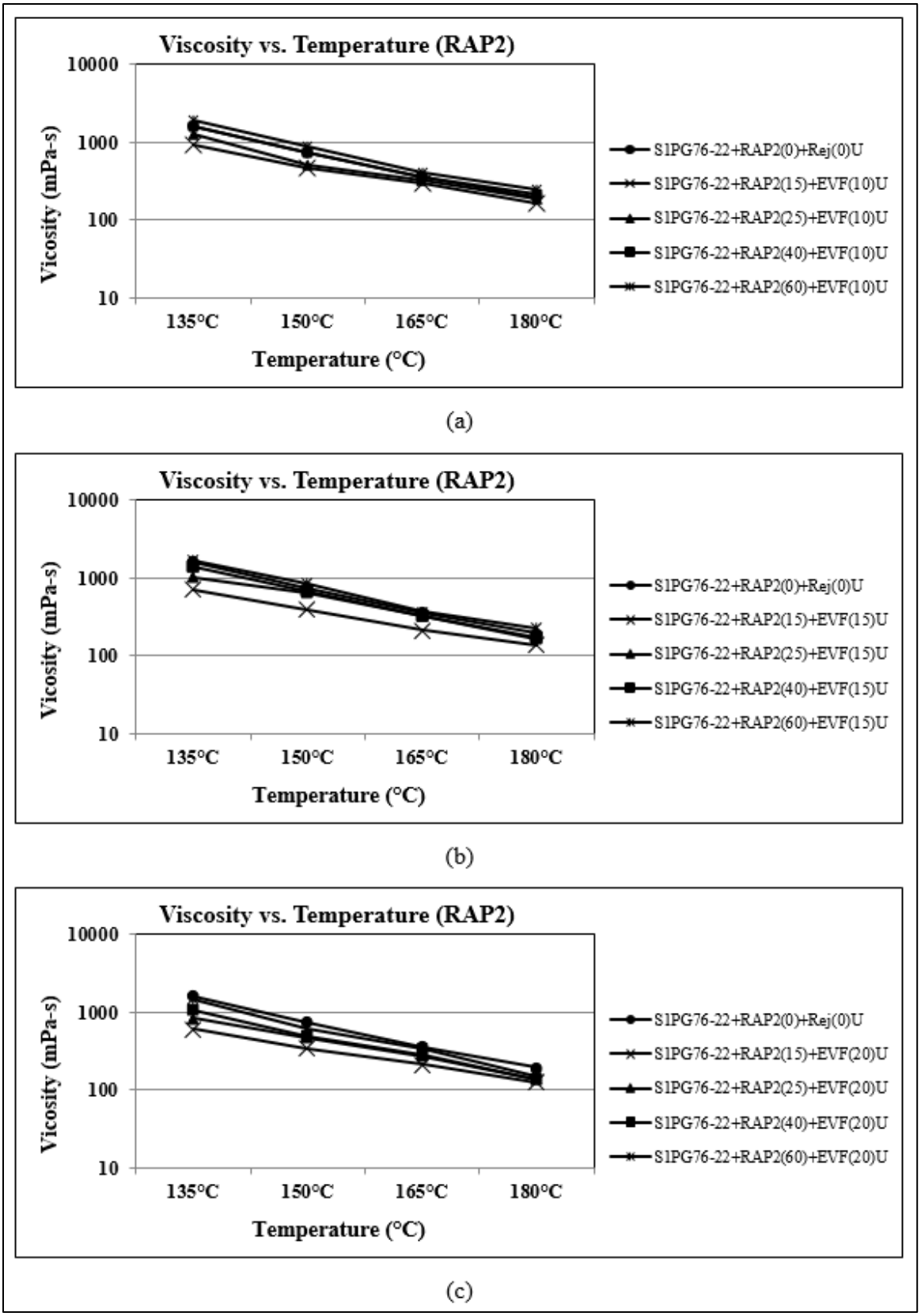

A_Figure 8. Rotational Viscosity (mPa.s) of EVF-Rejuvenated RAP2+PG 76-22 Binders from S1.